# Damage Assessment of Shear Structures Based on Autoregressive Models and Substructure Approach

**Keio University**

**Graduate School of Science and Technology**

**Directed by Professor Akira Mita**

**March 2011**

**Zhenhua Xing**

# Abstract

Structural Health Monitoring (SHM) can be defined as the process of implementing damage detection and characterization strategy for engineering structures. In the past decades, many damage detection methods were proposed. The vibration data used to detect the structural damage include frequency response functions, natural frequencies, mode shapes, mode shape curvatures, modal flexibility, modal strain energy, etc. This thesis is devoted to improve on the distance measures that have been studied so far and propose an effective damage detection scheme with as fewer sensors as possible, especially for the large scale structures.

Firstly, the improvements on the damage assessment method based on autoregressive (AR) models are proposed, which has rarely been applied to civil engineering structures. To improve the noise immunity of this method, the distance measure of low-order AR models is used as a damage indicator since its advantages in computational efficiency, emphasis of high-energy frequency range, and less sensitivity to spectral peaks caused by noise. In addition, adaptive component weighting is introduced to relieve the noise effect further. Moreover, a method to choose the optimum AR order for distance measures is proposed to solve the problem that the order of the AR models determined by Akaike Information Criterion or Bayesian Information Criteria is not the optimum AR order for the distance measure. The effect of varying the data length, number of parameters, and other factors are also carefully studied.

Secondly, a substructure approach to local damage detection is proposed. Every substructure is confined to one DOF, which can satisfy the identifiability of substructure easily. By cutting substructure with overlaps, ARMAX models can be directly used to determine the modal information and detect the damage. Substructure approach is to divide a complete structure into several substructures in order to significantly reduce the number of unknown parameters for each substructure so that damage detection processes can be independently conducted on each substructure. This method doesn't need the vibration measurements at all degrees of freedom.

Moreover, the identifiability of substructures for civil engineering structures is investigated, and a structure division method is proposed to make the substructure identifiable when it is not strongly system identifiable (SSI). To clarify the identifiability of the substructures, the substructures are classified into three types. The structure is divided by using the proposed structure division method, and then the support vector machine (SVM) is applied for each substructure to detect the local damages.

Finally, the conclusion is given. The damage assessment based on autoregressive models and substructure approach is proposed, and it can detect and localize the damage accurately. The using of the substructure approach makes this method work efficiently in identification of large scale structures, and moreover the damage detection processes can be independently conducted on each substructure. Thus, it is also suitable for use in a parallel and distributed damage detection system.

# Acknowledgements

My deepest gratitude goes first and foremost to Professor Akira Mita, my supervisor, for his constant encouragement and professional instructions during these years. He has walked me through all the stages of the writing of this thesis. Without his insightful suggestion and expert guidance, the completion of this thesis would not have been possible.

I would like to express my heartfelt gratitude to Professor Ohmori, Professor Oguni and Professor Takahashi for reviewing this thesis and giving me instructive advice and useful suggestions.

I am extremely grateful to Professor Songtao Xue at Tongji University, for his great kindness and unwavering support.

In particular, I would like to thank all the students of Mita Laboratory and all my friends in Keio University for their kind help in my research and life.

Finally, my thanks would go to my parents, my wife and my son for their love, faith and support.

# Contents

# Figures

# Tables

# *CHAPTER 1*
# Introduction

## 1.1 Structural Health Monitoring

The process of implementing a damage detection and characterization strategy for engineering structures is referred to as Structural Health Monitoring (SHM) (Mita 2003). The SHM process involves the observation of a structure over time using periodically sampled measurements from an array of sensors, the extraction of damage-sensitive features from these measurements, and the statistical analysis of these features to determine the current state of structural health. For long term SHM, the output of this process is periodically updated information regarding the ability of the structure to perform its intended functions in light of the inevitable aging and degradation resulting from operational environments. After extreme events, such as earthquakes or blast loading, SHM is used for rapid condition screening and aims to provide, in near real time, reliable information regarding the integrity of the structure (Cempel 1980; Hou, Noori et al. 2000; Auweraer and Peeters 2003; Farrar and Worden 2007).

The SHM problem is fundamentally one of a statistical pattern recognition paradigm

(Sohn and Laboratory 2004; Hayton, Utete et al. 2007). The paradigm can be divided into four parts:

1) Operational Evaluation,
2) Data Acquisition, Fusion, and Cleansing,
3) Feature Extraction and Information Condensation,
4) Statistical Model Development for Feature Discrimination.

## 1.2 Definition of Damage

Damage is defined as changes to the material or geometric properties of a structural system, including changes to the boundary conditions and system connectivity, which adversely affect the system's performance. According to the amount of information provided regarding the damage state, the damage identification can be classified into four levels (Rytter 1993):

Level 1: Damage Existence. Is there damage in the system?

Level 2: Location. Where is the damage in the system?

Level 3: Extent. How severe is the damage?

Level 4: Prognosis. How much useful life remains?

Answers to these questions in order represent increasing knowledge of the damage state. When applied in an unsupervised learning mode, statistical models are typically used to answer questions regarding the existence and location of damage. When applied in a supervised learning mode and coupled with analytical models, the statistical procedures can be used to better determine the type of damage, the extent of damage and remaining useful life of the structure. The statistical models are also used

to minimize false indications of damage (Farrar and Worden 2007).

False indications of damage fall into two categories:

1) False-positive damage indication (indication of damage when none is present),

2) False-negative damage indication (no indication of damage when damage is present).

Errors of the first type are undesirable, as they will cause unnecessary downtime and consequent loss of revenue as well as loss of confidence in the monitoring system. More importantly, there are clear safety issues if misclassifications of the second type occur. Many pattern recognition algorithms allow one to weigh one type of error above the other; this weighting may be one of the factors decided at the operational evaluation stage (Hayton, Utete et al. 2007; Sohn 2007).

## 1.3 Damage Detection Methods

The main parts of the SHM in civil engineering are damage detection and localization, which are essential monitoring zones for structures after major events such as earthquakes (Ljung 1999; Mita 2003).

*Using Natural Frequency* Generally, there are two types of frequency analysis, the forward identification and the inverse identification that can be used for damage identification (Hearn and Testa 1991; Ljung 1999; Vestroni and Capecchi 2000; Peeters, Maeck et al. 2001; Kessler, Spearing et al. 2002; Kim, Ryu et al. 2003). Both methods assume that natural frequency of a structure shifts when the damage occurs. Cawley and Adams (1979) used frequency shifts to detect damage in composite materials. It assumes that natural frequency shifts when the physical properties change.

Rytter and Kirkegaard (1997) performed a vibration test of a full-scale four-story reinforced concrete building at the European Laboratory for Structural Assessment (ELSA). The relative changes in the modal parameters are used as inputs of the networks to detect the bending stiffness changes of the system at the output layer. Williams and Messina (1999) formulated a correlation coefficient that compares changes in a structure's resonant frequencies with predictions based on a frequency-sensitivity model derived from a finite element model.

*Using Mode Shape* West (1986) and Wolff and Richardson (1989) suggested the use of the modal assurance criterion (MAC) to detect the existence and the location of structural faults. MAC is a scale quantity ranging from 0 to 1.0, representing that the degree of correlation between two sets of modal vectors is uncorrelated at all or perfectly correlated respectively. The method is based on the assumption that changes in modal vectors at the degrees of freedom near the damage are relatively larger than others located far from the damage. As the MAC only uses one pair of modes for damage localization, the problem of how to choose appropriate modes for MAC calculation induces the similar COMAC methods for damage localization, which stands for Coordinate Modal Assurance (Lieven and Ewins 1988). The location where a COMAC value is close to zero is the possible damage location. Salawu and Williams (1995) conducted modal tests of a full-scale bridge before and after rehabilitation and concluded that the natural frequencies of the bridge did not change much as a result of structural repairs whilst both MAC and COMAC performed good to indicate the location of the repairs. The limitation of this method is that it is only sensitive in the case that the measurement point is close to node points for a particular mode.

*Using Curvature/Strain Mode* Compared with the method using mode shape, this method is feasible for damage localization and higher derivatives of mode shapes are more sensitive to damage. Pandey et al. (1991) demonstrated that mode shape

curvature could be a useful indicator to damage detection of beam structures. Chance et al. (1994) investigated the measured strain mode shape and found it was much feasible for damage localization. Wang et al. (2000) presented a numerical study of damage detection of Tsing Ma Bridge in Hong Kong SAR by utilizing the changes of the mode shape curvatures. Qiao et al. (2007) used the experimental and numerical curvature mode shapes to detect the presence, location, and size of the delamination.

*Using Modal Strain Energy* Stubbs et al. (1992) presented the pioneer work on using Modal Strain Energy (MSE) for damage localization. Stubbs and Kim (1996) and Shi et al. (1998) improved the method by using modal strain energy to localize the damage and estimated the damage size without baseline modal properties.

*Using Dynamic Flexibility* As the fact that higher modes contribute more to the system stiffness matrix than lower modes (Berman and Flannelly 1971), a large number of dynamic modes are needed to obtain good stiffness matrix estimation or its changes. However, measuring the higher frequency response is very difficult due to practical limitations. To avoid the problem, a method using dynamically measured flexibility matrix is proposed to estimate the changes in structural stiffness. Bernal (2002) set up a numerical example of a 39-DOF truss and obtained the accurate results of identifying the modes. He concluded that changes in the flexibility matrix were desirable to monitor than the changes in stiffness matrix. Gao and Spencer (2006) discussed the issues relating to the synthesis of modal flexibility matrix from ambient and forced vibration data and implemented damage locating vector (DLV) method for online damage localization.

*Artificial Neural Network* An artificial neural network (ANN), usually called neural network (NN), is a mathematical model or computational model that is inspired by the structure and/or functional aspects of biological neural networks. A neural network consists of an interconnected group of artificial neurons, and it processes information

using a connectionist approach to computation. The advantage of this method is that there is no need to know the physical relationships between the structural properties and damage occurrence. This approach relies on the use of vibration measurements from a healthy system to train a neural network for identification purposes. Subsequently, the trained network is fed comparable vibration measurements from the same structure under different episodes of response in order to monitor the health of the structure (Berman and Flannelly 1971; Cawley and Adams 1979; Cempel 1980; Qian and Mita 2008). However, by using this method, large training sample is needed for accurate detection.

*Wavelet Method* Wavelets can decompose any signal, and signal transferred by Wavelets method can be shown to be more sensitive to local changes in structural properties. It can be also viewed as an extension of the traditional Fourier transform with adjustable window location and size. Hou et al. (2000) proposed a wavelet-based approach for structural damage detection and health monitoring. The methodology was applied to simulation data generated from a simple structural model subjected to a harmonic excitation. Results show the great promise of the wavelet approach for damage detection and structural health monitoring.

*Distance Measures of AR Models* Distance measures have been widely used in speech recognition (Tohkura 1986; Itakura and Umezaki 1987). Basseville (1989) presented some general tools for measuring distances either between two statistical models or between a parametric model and a signal. The question of spectral distances between processes is investigated based on the autoregressive (AR) models and autoregressive moving average (ARMA) models. Martin (2000) discussed a metric defined on ARMA models, and gave a natural measure of the "distance" between two ARMA processes. Dhiral (2001) introduced a distance measure for measuring the dissimilarity and the similarity between different autoregressive integrated moving average (ARIMA) models. Zheng et al. (2007; 2008; 2009) introduced the distance

measures of AR models into civil engineering by proposing a novel damage indicator based on the distance measure between AR models. However, there are still some problems unsolved. The main challenges are that how to choose the optimal order for distance measures and reduce the noise effect on this method, which will be studied in Chapter 2.

*Substructure Method* Most of damage detection methods need complete information of the structure, which means many sensors are required to be installed into a building. It may be feasible for small systems. However, it is impossible for large-scale civil structures. For large systems, data measurement and identification are not easy tasks. The computation time required for convergence increases dramatically with the increase in the number of the degrees of freedom (DOFs) due to the nature of the inverse analysis. To overcome these problems, some researchers have been using the substructure method for large-scale structures. Koh et al. (1991) proposed substructure system identification and used the Extended Kalman Filter (EKF) (Hoshiya and Saito 1984; Ljung 2002) as the numerical tool to identify unknown structural parameters. Park et al. (1998) offered structural damage detection methods based on the relative changes in localized flexibility properties. The localized flexibility matrices are obtained either by applying a decomposition procedure to an experimentally determined global flexibility matrix or by processing the output signals of a vibration test in a substructure-by-substructure manner. However the structure division and the identifiability of substructure have rarely been studied. These problems will be discussed in Chapter 3 and Chapter 4.

## 1.4 Objectives

System identification techniques based on dynamic responses of structures have been used for structural identification for decades, and many non-destructive methods of

damage detection for structural identification were proposed which also have been shown the feasibility. However, most of them need complete information of the structure, which means many sensors are required to be installed into a building. It may be feasible for small systems, but impossible for large-scale civil structures, since the large number of sensors results in long setup time, high equipment costs as well as enormous efforts needed for wiring and designing. Complicated and expensive SHM systems are by no means practical for most civil structures. The main objective of this thesis is to develop a damage assessment with as fewer sensors as possible. Moreover, this thesis aims to solve the problem caused by large systems which is that data measurement and computation time increase dramatically with the increase in the number of the degrees of freedom (DOFs), and to make the damage detection method work more efficiently.

## 1.5 Organization of Thesis

This thesis is divided into six chapters as illustrated in Figure 1.1.

Chapter 1 gives a brief introduction of SHM and damage detection.

Chapter 2 presents the improvements on the distance measures of AR model. To strengthen the noise immunity of this method, the distance measure of low-order AR models is used as a damage indicator since its advantages in computational efficiency, emphasis of high-energy frequency range, and less sensitivity to spectral peaks caused by noise. In addition, adaptive component weighting (ACW) is introduced to relieve the noise effect further. A method to choose the optimum AR order for distance measures is proposed, because it is shown that the sensitivity of the distance measure is strongly affected by the order of the AR models and the order determined by Akaike information criterion or Bayesian Information Criteria is not the optimum AR order

for the distance measure. Moreover, the effect of varying the data length, number of parameters, and other factors are carefully studied in this Chapter.

Chapter 3 proposes a substructure approach to local damage detection. Every substructure is confined to one DOF, which can satisfy the identifiability of substructure easily. By cutting substructure with overlaps, ARMAX models can be directly used to determine the modal information and detect the damage. Here, substructure approach is to divide a complete structure into several substructures in order to significantly reduce the number of unknown parameters for each substructure.

Chapter 4 investigates the identifiability of substructures for civil engineering structures, and a structure division method is proposed to make the substructure identifiable when it is not strongly system identifiable (SSI). To clarify the identifiability of the substructures, the substructures are classified into three types. It should be noted that a substructure is a feedback system as it has feedback forces from the remainder of the structure. It is not true that the substructure can have as many DOFs as we want. Under certain conditions, the identification may fail due to the closed-loop nature of the system.

Chapter 5 introduces the support vector machine (SVM) for each substructure to detect the local damages. The proposed structure division method is used to divide the structure, and then the support vector machine (SVM) is applied for each substructure because multiple modal frequency changes provide information on the location of damaged stories.

Chapter 6 summarizes contributions of this thesis, and points out the direction for future works.

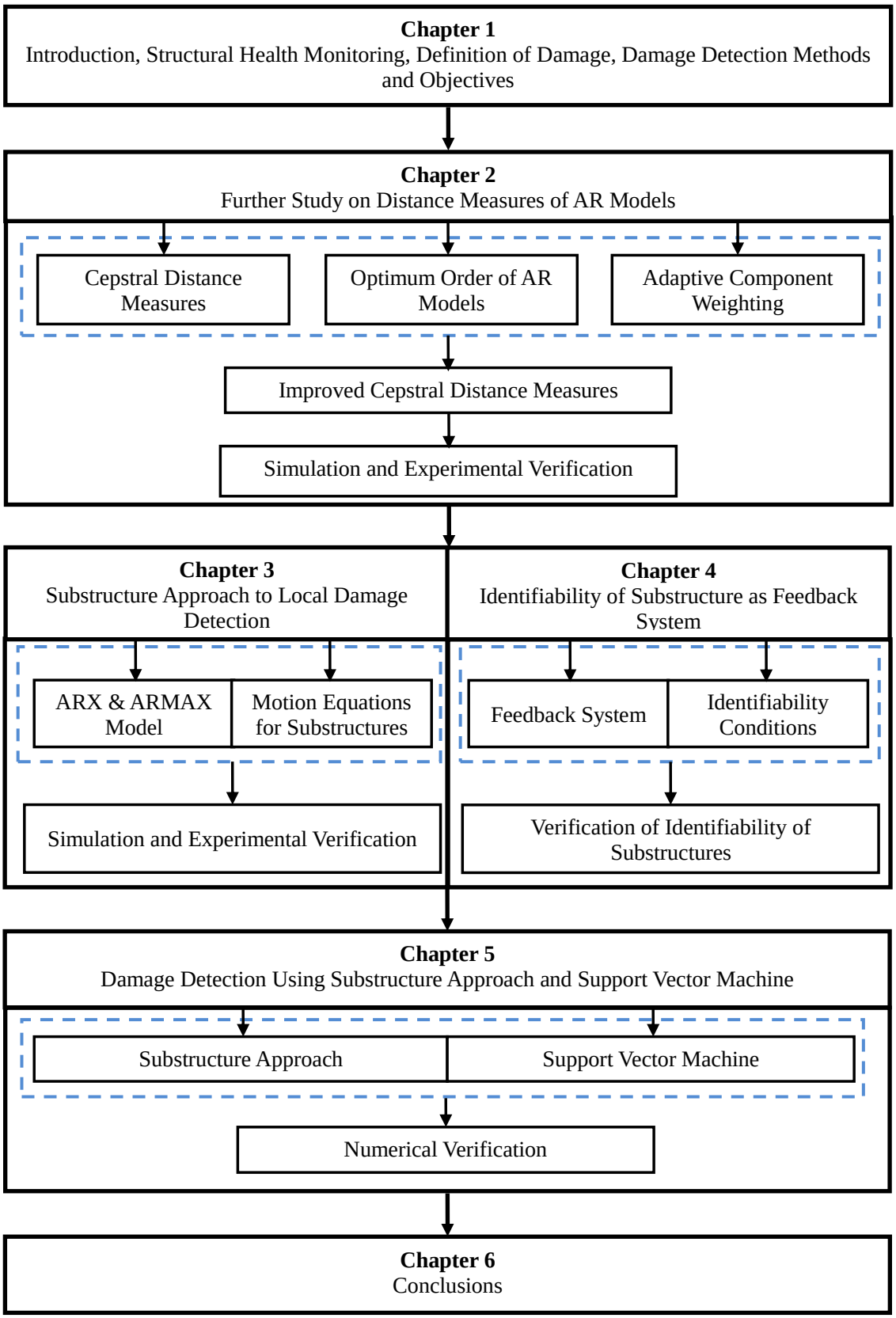


Figure 1.1. Organization of thesis

# *CHAPTER 2*

# Further Study on Distance Measures of AR Models

## 2.1 Introduction

Most damage detection methods based on the assumption that damage will alter the stiffness, mass, or energy dissipation properties of a system, which in turn alter the measured dynamic response of the system (Mayes 1991; Fox 1992; Ljung and Glad 1994; Zhang, Quiong et al. 1998; Goldenfeld and Kadanoff 1999; Ljung 1999; Roeck 2003; Lynch 2005). Although the basis for damage detection appears very easy, its actual application poses many significant challenges. The most fundamental challenge is that damage is typically a local phenomenon and may not significantly influence the lower-frequency global response of a structure that is normally measured during vibration tests.

In this chapter, improvements on the distance measures of autoregressive (AR) models are proposed. To improve the noise immunity of this method, the distance measure of low-order AR models is chosen as a damage indicator. In addition,

adaptive component weighting (ACW) (Assaleh and Mammone 1994) is introduced, which can significantly reduce noise. A method to choose the optimum AR order for distance measures is proposed, because it is shown that the sensitivity of the distance measure is strongly affected by the order of the AR models and the order determined by Akaike Information Criterion or Bayesian Information Criteria is not the optimum AR order for the distance measure. Moreover, the effect of varying the data length, number of parameters, and other factors are carefully studied.

## 2.2 Cepstral Distance Measures

Zheng and Mita (2007) used cepstral distance measures based on the AR models for the purpose of damage detection in civil engineering. AR models are used to fit the vibration response of the structure. The AR models are obtained for the undamaged state and unknown states, and then the cepstral distance between the reference model and the new model can be calculated. The cepstral distance can reveal the difference between two models, a big value of cepstral distance means a big difference. Thus the damage can be identified according to the cepstral distance.

### 2.2.1 Autoregressive Model

In statistics and signal processing, AR model is a type of random process which is often used to model and predict various types of time series. In the filter design, it is known as an infinite impulse response filter (IIR) or an all pole filter, and is sometimes known as a maximum entropy model in physics applications. It can also be regarded as one of a group of linear prediction formulas that attempt to predict an output of a system based on the previous outputs and inputs. An AR model can be written as

$$y(t) = \sum_{i=1}^{p} a_i y(t-i) + e(t) \tag{2.1}$$

where $a_i$ are the AR coefficients to be estimated, $y(t)$ is the time series under investigation, $p$ is the order of the AR model which is generally very much less than the length of the time series, and $e(t)$ is the prediction error term or noise, which is almost always assumed to be Gaussian white noise.

### 2.2.2 Cepstral Distance

The cepstrum of a signal is defined as the inverse Fourier transform of the log magnitude spectrum, and it was originally used for detecting echoes (Bogert, Healy et al. 1963). First, the cepstral metric for the AR model is introduced, as proposed by Martin (2000),

$$D(\mathrm{M}^{(1)}, \mathrm{M}^{(2)}) = \left[ \sum_{n=1}^{\infty} n \left| c_n^{(1)} - c_n^{(2)} \right|^2 \right]^{1/2} \tag{2.2}$$

where $c_n^{(1)}$ and $c_n^{(2)}$ are the cepstral coefficients of AR models $\mathrm{M}^{(1)}$ and $\mathrm{M}^{(2)}$, and $D$ is cepstral distance between the two AR models. Then combining Equation (2.2) with Equation (2.3) (Oppenheim and Schafer 1989),

$$c_n = \begin{cases} \dfrac{1}{|n|} \left[ \sum_{i=1}^{p} \alpha_i^{|n|} - \sum_{i=1}^{q} \beta_i^{|n|} \right], & n \neq 0 \\ \log \sigma^2, & n = 0 \end{cases} \tag{2.3}$$

where $\alpha_i$ and $\beta_i$ mean the poles and zeros of the model, $p$ and $q$ are the numbers of the poles and zeros of the model respectively, $c_n$ is the cepstral coefficient, and $\sigma$ is the variance of the white noise input, and then by using the identity,

$$\sum_{n}^{\infty}\alpha^{n} \equiv -\log(1-\alpha) \qquad (|\alpha|<1) \tag{2.4}$$

the cepstral distance between pole-zero models can be obtained as follows:

$$D\left(\mathrm{M}^{(1)},\mathrm{M}^{(2)}\right)^{2} = \log\frac{\prod_{i=1}^{p^{(1)}+p^{(2)}}\prod_{j=1}^{p^{(1)}+p^{(2)}}\left(1-\varphi_i^{(1)}\overline{\varphi}_j^{(2)}\right)\prod_{i=1}^{p^{(1)}+p^{(2)}}\prod_{j=1}^{p^{(1)}+p^{(2)}}\left(1-\varphi_i^{(2)}\overline{\varphi}_j^{(1)}\right)}{\prod_{i=1}^{p^{(1)}+p^{(2)}}\prod_{j=1}^{p^{(1)}+p^{(1)}}\left(1-\varphi_i^{(1)}\overline{\varphi}_j^{(1)}\right)\prod_{i=1}^{p^{(1)}+p^{(2)}}\prod_{j=1}^{p^{(2)}+p^{(2)}}\left(1-\varphi_i^{(2)}\overline{\varphi}_j^{(2)}\right)} \tag{2.5}$$

where $D$ means the cepstral distance between models $\mathrm{M}^{(1)}$ and $\mathrm{M}^{(2)}$, $\boldsymbol{\varphi}^{(1)} = \left[\boldsymbol{\alpha}^{(1)}, \boldsymbol{\beta}^{(2)}\right]$, $\boldsymbol{\varphi}^{(2)} = \left[\boldsymbol{\alpha}^{(2)}, \boldsymbol{\beta}^{(1)}\right]$, $\alpha_i$ and $\beta_i$ are the poles and zeros of the models, and $p^{(1)}$ and $p^{(2)}$ are the orders of the models $\mathrm{M}^{(1)}$ and $\mathrm{M}^{(2)}$, respectively.

## 2.3 Improved Cepstral Distance Measures

As an improvement to the cepstral distance method introduced by Zheng and Mita (2007), the distance measure of low-order AR models is proposed as a damage indicator to strengthen the noise immunity of this method. Low-order AR models have advantages in terms of computational efficiency, emphasis of high-energy frequency range, and less sensitivity to spectral peaks caused by noise. Adaptive component weighting (ACW) is introduced to improve further the ability of this method in noise resistance. Moreover, a method to choose the optimum AR order for distance measures is proposed, because it is shown that the sensitivity of the distance measure is strongly affected by the order of the AR models and the order determined by Akaike information criterion (Akaike 1974) or Bayesian Information Criteria (Schwarz 1978) is not the optimum AR order for the distance measure.

### 2.3.1 Optimum Order of AR Models

The previous study (Zheng and Mita 2007) in which autoregressive (AR) models are used to get the cepstral distance, however, how to choose the optimal order for distance measures is still a problem unsolved. Here, a method is proposed to solve this problem. Figure 2.1 shows a simplified structure model. The mass of every floor and the lateral stiffness is assumed to be 100 kg and 1 MN/m, respectively. 3% is chosen as the damping ratio of all modes. Data sampling frequency is 200 Hz. The Gaussian white noise is used to simulate the input such as earthquakes and ambient vibration. The stiffness reduction is regarded as the damage to the structure. To get the optimum AR order for the distance measure, AR models are examined with different orders (3-19) for different multiple degrees of freedom (MDOF) systems (3-19-DOF) with different damage severities (8%, 16%, 24%, 32% and 40% lateral stiffness reduction) in different damage locations ($1^{st}$, $2^{nd}$... $n^{th}$ story). Because the number of results is very huge, only those of AR model orders (3, 4, 5, 6, 9 and 13) for 3, 5, 7 and 13-DOF systems with 8% damage severity in the $2^{nd}$ story are listed in Table 2.1.

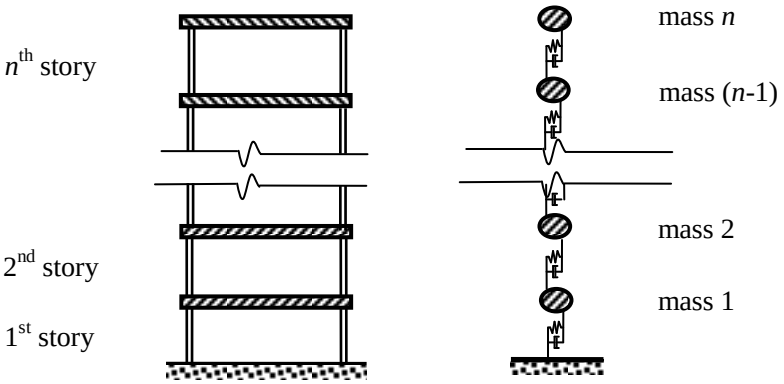


Figure 2.1. Simplified structural model with n DOFs

Table 2.1. Cepstral distance (8% stiffness reduction in the 2nd story, double underlined values: largest cepstral distance, single underlined values: second largest cepstral distance)

| AR Order | 3 | 4 | 5 | 6 | 9 | 13 |
|---|---|---|---|---|---|---|
| | 3 DOF (1st natural frequency: 7.1 Hz) | | | | | |
| 1-mass | 0.0663 | 0.1095 | 0.1508 | 0.1667 | 0.1042 | 0.2351 |
| 2-mass | 0.0838 | 0.1125 | 0.1956 | 0.2399 | 0.5514 | 0.5131 |
| 3-mass | 0.0350 | 0.0175 | 0.0069 | 0.0440 | 0.0519 | 0.1911 |
| | 5 DOF (1st natural frequency: 4.5 Hz) | | | | | |
| 1-mass | 0.0615 | 0.0910 | 0.1161 | 0.1210 | 0.1250 | 0.1223 |
| 2-mass | 0.0946 | 0.1317 | 0.1370 | 0.1408 | 0.2525 | 0.2496 |
| 3-mass | 0.0528 | 0.0137 | 0.0275 | 0.0133 | 0.0774 | 0.0809 |
| 4-mass | 0.0242 | 0.0222 | 0.0569 | 0.0587 | 0.0821 | 0.0713 |
| 5-mass | 0.0124 | 0.0056 | 0.8430 | 0.0164 | 0.0222 | 0.0600 |
| | 7 DOF (1st natural frequency: 3.3 Hz) | | | | | |
| 1-mass | 0.0416 | 0.0781 | 0.1192 | 0.1270 | 0.1290 | 0.1174 |
| 2-mass | 0.1137 | 0.1295 | 0.1445 | 0.1203 | 0.2143 | 0.1895 |
| 3-mass | 0.0469 | 0.0134 | 0.0269 | 0.0803 | 0.0259 | 0.1149 |
| 4-mass | 0.0215 | 0.0196 | 0.0325 | 0.0318 | 0.0516 | 0.0829 |
| 5-mass | 0.0080 | 0.0121 | 0.0024 | 0.0162 | 0.0114 | 0.0164 |
| 6-mass | 0.0116 | 0.0238 | 0.0249 | 0.0135 | 0.0223 | 0.0447 |
| 7-mass | 0.0068 | 0.0072 | 0.0060 | 0.0013 | 0.0147 | 0.0191 |
| | 13 DOF (1st natural frequency: 1.9 Hz) | | | | | |
| 1-mass | 0.0542 | 0.0969 | 0.1206 | 0.1141 | 0.1333 | 0.1269 |
| 2-mass | 0.1078 | 0.1326 | 0.1500 | 0.1363 | 0.2049 | 0.1775 |
| 3-mass | 0.0368 | 0.0182 | 0.0253 | 0.0797 | 0.0608 | 0.1118 |
| 4-mass | 0.0260 | 0.0182 | 0.0309 | 0.0315 | 0.0482 | 0.0691 |
| 5-mass | 0.0072 | 0.0085 | 0.0067 | 0.0104 | 0.0217 | 0.0244 |
| 6-mass | 0.0019 | 0.0043 | 0.0055 | 0.0087 | 0.0159 | 0.0351 |
| 7-mass | 0.0033 | 0.0089 | 0.0037 | 0.0133 | 0.0158 | 0.0169 |
| 8-mass | 0.0016 | 0.0059 | 0.0032 | 0.0087 | 0.0144 | 0.0109 |
| 9-mass | 0.0046 | 0.0146 | 0.0060 | 0.0194 | 0.0194 | 0.0135 |
| 10-mass | 0.0052 | 0.0095 | 0.0044 | 0.0139 | 0.0150 | 0.0206 |
| 11-mass | 0.0032 | 0.0039 | 0.0037 | 0.0065 | 0.0107 | 0.0158 |
| 12-mass | 0.0195 | 0.0359 | 0.0190 | 0.0288 | 0.0230 | 0.0274 |
| 13-mass | 0.0024 | 0.0103 | 0.0038 | 0.0100 | 0.0266 | 0.0137 |

The cepstral distance was chosen as the damage indicator because it increases as the difference between two models increases. After damage occurs in the 2nd story, the acceleration response of the 1st and 2nd mass is affected more than the others and is shown as an increase in the cepstral distance of the 1st and 2nd mass. Thus, the cepstral distance of the 1st and 2nd mass should be much larger than the cepstral distances of the other masses when damage occurs in the 2nd story. Table 2.1 lists the cepstral distances of masses for different AR orders. The double and single underlined values mean the largest and second largest cepstral distances, respectively. If the cepstral distances of the 1st and 2nd masses are not much larger than the others, it indicates that the damage can't be shown clearly and the corresponding AR order is not the optimum one. If the cepstral distances of the 1st and 2nd masses are smaller than the others, it means that the result gives the wrong damage location, and thus the order of the AR model is wrong.

The acceleration of masses closer to the damage will be the most affected. In the current case, damage to the 2nd story, let's consider the ratios of the cepstral distance of the 3rd mass to the 1st mass and the cepstral distance of the 3rd mass to the 2nd mass, Equation (2.6) and Equation (2.7), as the index for choosing the proper AR order.

$$R1 = \frac{D_{3^{rd}\ mass}}{D_{1^{st}\ mass}} \tag{2.6}$$

$$R2 = \frac{D_{3^{rd}\ mass}}{D_{2^{nd}\ mass}} \tag{2.7}$$

The smaller $R1$ and $R2$ are, the better the recognition results mean. If $R1$ and $R2$ are larger than 1, it means that the AR order is wrong. Figures 2.2~2.5 show that increasing the AR order doesn't improve the recognition results. AR orders of 4 and 5 are more stable than others. The results for cases in which different stories suffered damage of different severities (not listed here) also indicate that 4 and 5 are the most

stable AR orders. Taller structures were also tested, and similar results were obtained. So in this study, low-order AR models of order 4 are used.

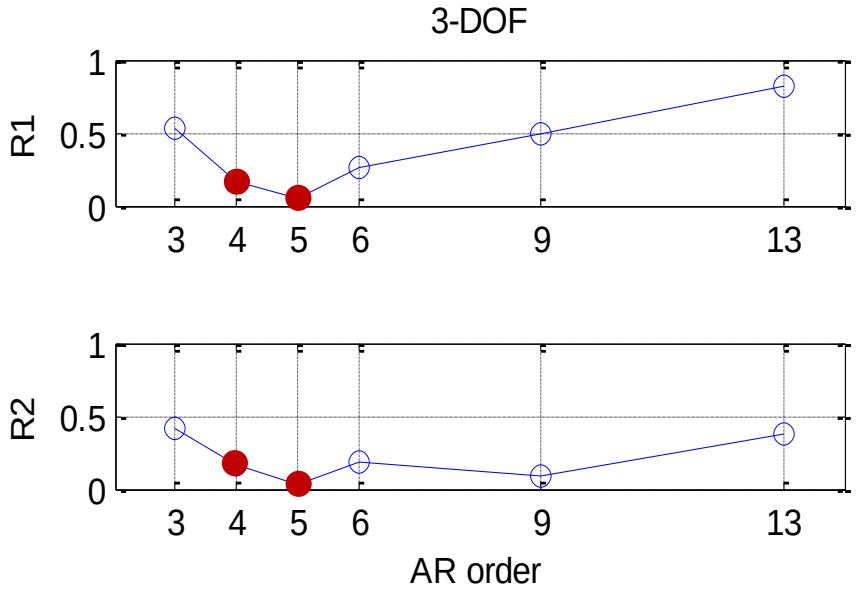


Figure 2.2. Ratio of cepstral distance (3-DOF)

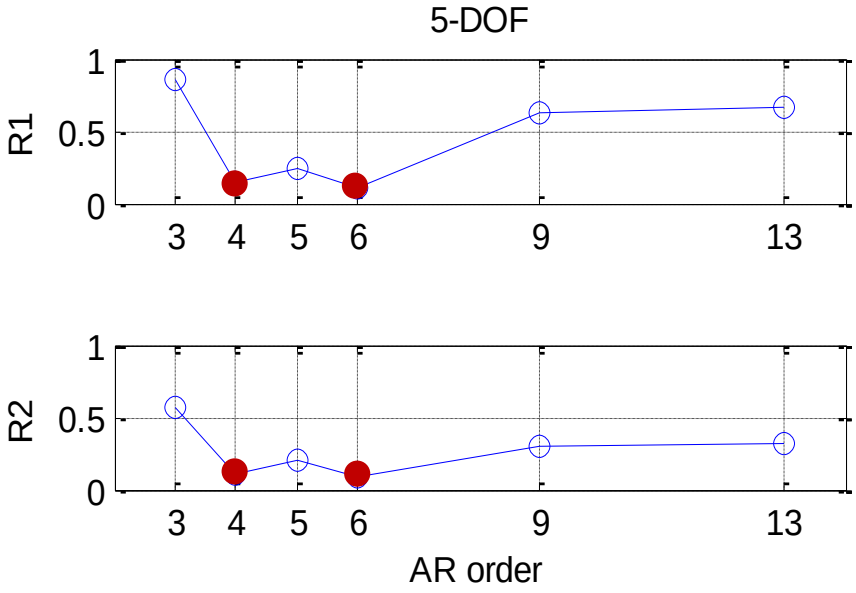


Figure 2.3. Ratio of cepstral distance (5-DOF)

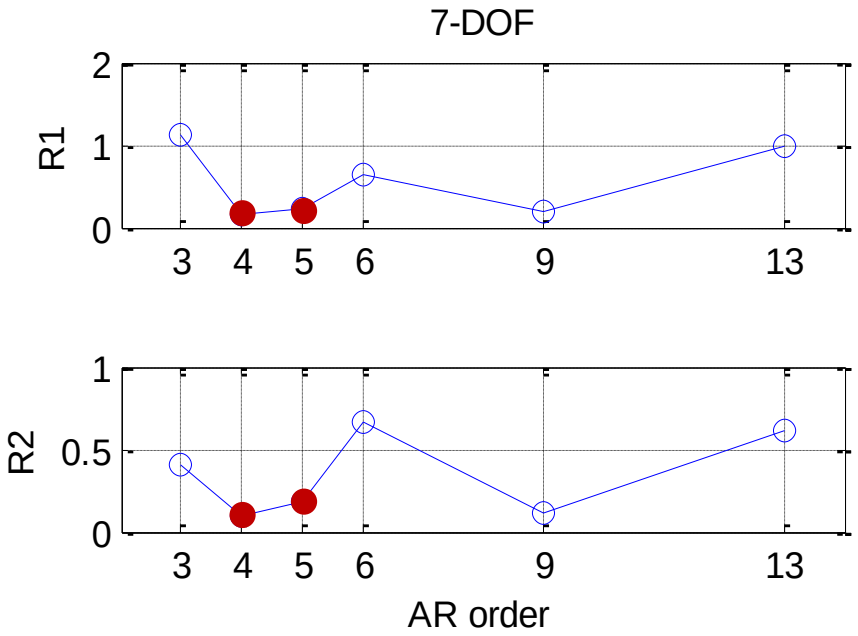


Figure 2.4. Ratio of cepstral distance (7-DOF)

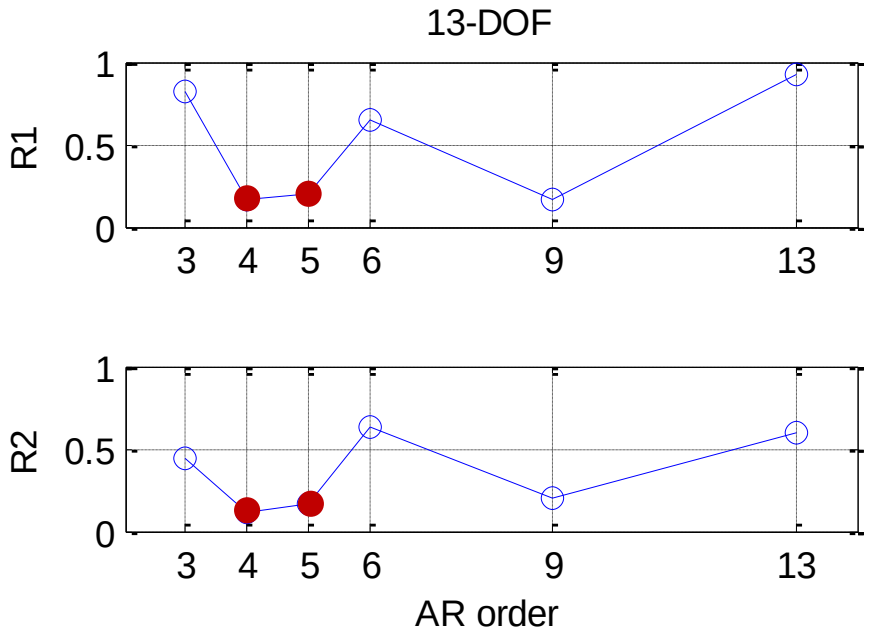


Figure 2.5. Ratio of cepstral distance (13-DOF)

### 2.3.2 Adaptive Component Weighting (ACW)

AR models are susceptible to noise. To reduce the effect of noise, adaptive component weighting (ACW) is used, as is done in speaker identification (Assaleh and Mammone 1994). ACW modified the linear prediction (LP) spectrum so as to emphasize the formant structure. The ACW spectrum introduces zeros into the usual all-pole LP spectrum. This is equivalent to applying a finite impulse response (FIR) filter that normalizes the narrow-band modes of the spectrum. Unlike existing fixed cepstral weighting schemes, the ACW cepstrum provides an adaptively weighted version of the LP cepstrum.

$$\frac{1}{A(z)} = \frac{1}{1-\sum_{k=1}^{p}\alpha_k z^{-k}} = \frac{1}{\prod_{k=1}^{p}(1-f_k z^{-1})} = \sum_{k=1}^{p}\frac{r_k}{1-f_k z^{-1}} \tag{2.8}$$

where $f_k$ for $1 \le k \le p$ represent the poles of the AR model, and $r_k$ are the residues of the poles. It has been shown that the sensitivity of a pole to noise in the LP coefficients is proportional to the residues $r_k$ (Assaleh and Mammone 1994) and the variation caused by the residues $r_k$ can be removed by setting all residues equal to a given constant such as unity.

Hence, the ACW spectrum is given by

$$H(z) = \sum_{k=1}^{p}\frac{1}{1-f_k z^{-1}} = \frac{N(z)}{A(z)} = \frac{N(z)}{1-\sum_{k=1}^{p}\alpha_k z^{-k}} \tag{2.9}$$

where

$$N(z) = \sum_{k=1}^{p}\prod_{\substack{i=1\\ i\neq k}}^{p}(1-f_i z^{-1}) = p(1-\sum_{k=1}^{p-1}b_k z^{-k}) \tag{2.10}$$

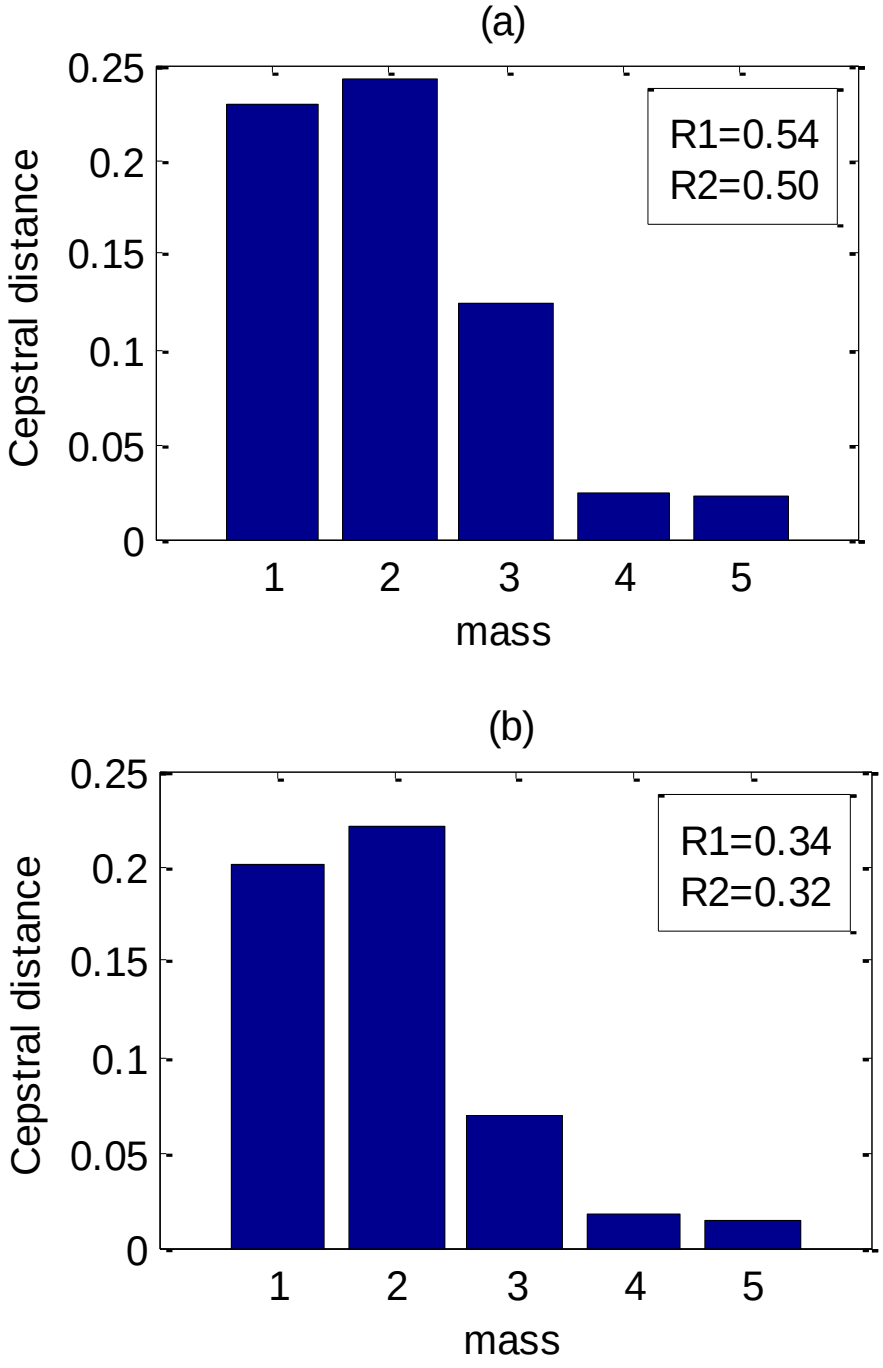


Figure 2.6. 5-DOF system with 24% stiffness reduction in the 2nd story (data length=9000, SNR=10): (a) Without ACW, (b) With ACW

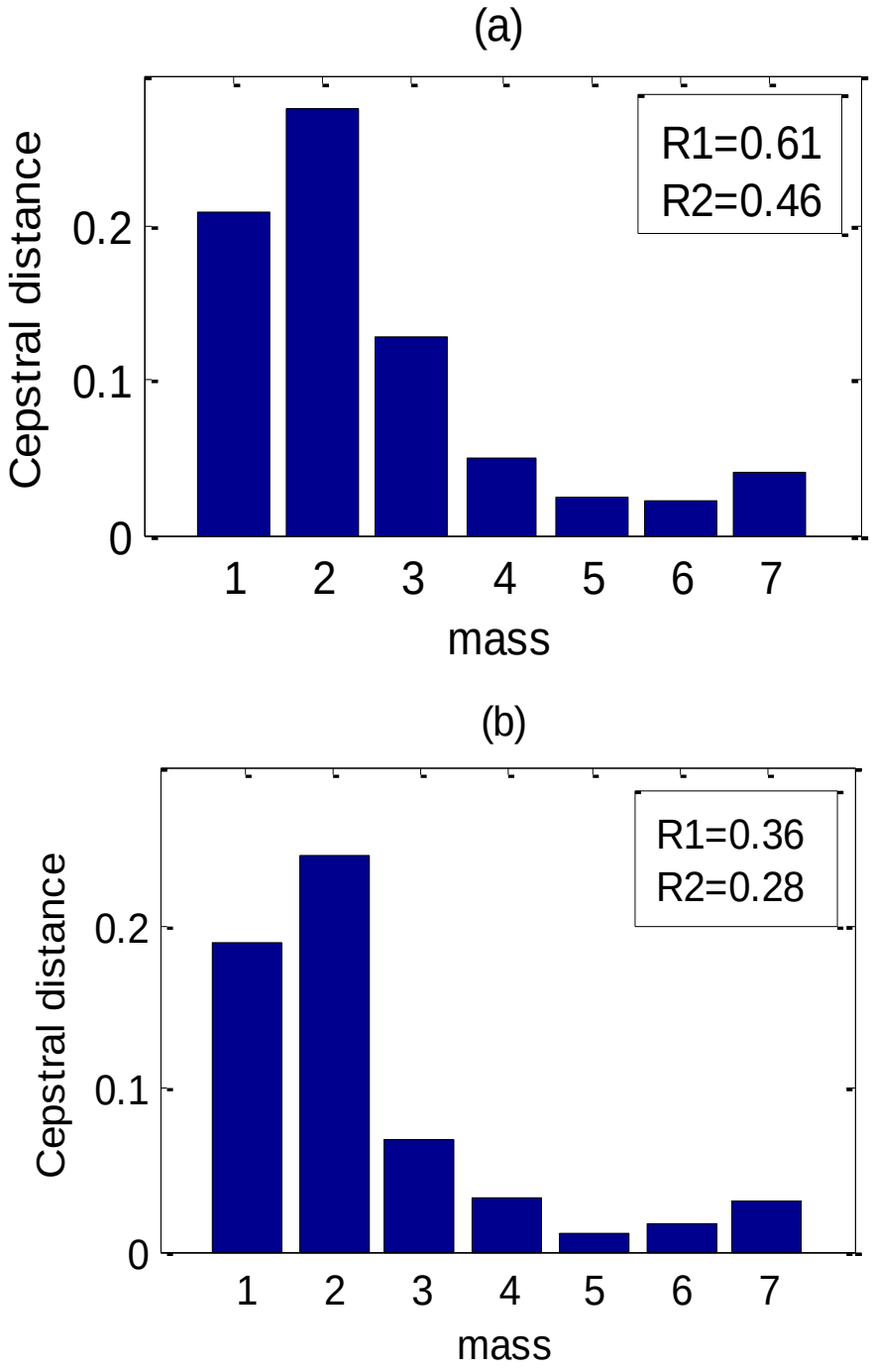


Figure 2.7. 7-DOF system with 24% stiffness reduction in the 2nd story (data length=9000, SNR=10): (a) Without ACW, (b) With ACW

As mentioned in the previous section, AR models of order 4 were adopted to examine whether ACW can reduce the effects of noise on the recognition results. ACW was applied to different MDOF structure systems (3-19-DOF) with damage of different severities (8%, 16%, 24%, 32% and 40% lateral stiffness reduction) and in different locations ($1^{st}$, $2^{nd}$... $n^{th}$ story).

Here, only the results for the 5-DOF and 7-DOF structures with 24% stiffness reduction in the $2^{nd}$ story (Figure 2.6 and Figure 2.7). $R1$ means the ratio of cepstral distance of the $3^{rd}$ mass to the $1^{st}$ mass, and $R2$ means the cepstral distance of the $3^{rd}$ mass to the $2^{nd}$ mass. $R1$ and $R2$ are computed from Equation (2.6) and Equation (2.7), respectively, and smaller values mean better recognition results.

## 2.4 Performance Verification by Simulation

A simulation of a five-story shear building model was performed to show the feasibility of the proposed scheme for damage detection. The building was simplified into a 5-DOF structural system (Figure 2.8).

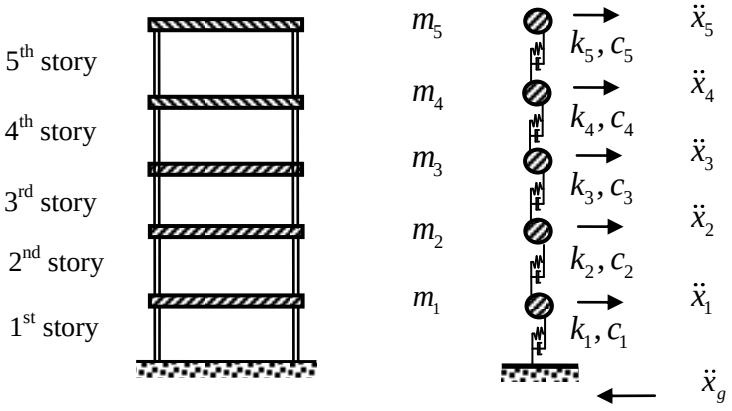


Figure 2.8. 5-story shear building

The mass of every floor and the lateral stiffness were assumed to be 100 kg and 1 MN/m respectively. 3% was chosen as the damping ratio of all modes. The data sampling frequency is 200 Hz. The undamaged natural frequencies of the structure are 4.5 Hz, 13.2 Hz, 20.8 Hz, 28.6 Hz, and 30.5 Hz for the 1st mode, 2nd mode, 3rd mode, 4th mode, and 5th mode, respectively. The 5-DOF system was assumed to be excited by the Gaussian white noise, which is used to simulate the input such as earthquakes and ambient vibration, and 10% noise was added to the acceleration responses of the structure. The story stiffness reduction was regarded to be damage to the structure. Five damage cases (damage in the 1st story, 2nd story, 3rd story, 4th story, or 5th story) with five different damage severities (8%, 16%, 24%, 32% and 40% lateral stiffness reduction) were studied. Hence, there are 25 different damage scenarios in total.

To deal with the strong mutual correlation in the acceleration data, a pre-whitening filter (Zheng and Mita 2007) was used to whiten the 5-dimensional signals. Then the AR models of order 4 were constructed to fit the acceleration responses of the structure in the 25 different scenarios. Burg's method was used to obtain the AR model because of its high frequency resolution and resulting stable AR model. The AR models were arranged in pairs (reference model and new model), and adaptive component weighting (ACW) was used to reduce the effect of noise by transforming the all-pole models (AR model) to pole-zero models. Finally, Equation (2.5) was used to get the cepstral distance between every pair of models. The cepstral distance can reveal the difference between two models, a big value of cepstral distance means a big difference. Thus the damage can be judge according to the cepstral distance. A large cepstral distance means that the structure is damaged, and a small distance means that the structure is undamaged.

Figures 2.9-2.11 show the recognition results for different data lengths. In order to show the damage more clearly, the cepstral distance on the x axis is squared. It is clear that the change in the recognition results between these figures is related to the data

length. In Figure 2.9, for which the data length is 6000, the recognition result when damage occurs in the 1st story is not as good as the results for other damage to other stories. However, it can be improved by increasing the data length (Figure 2.10 and Figure 2.11).

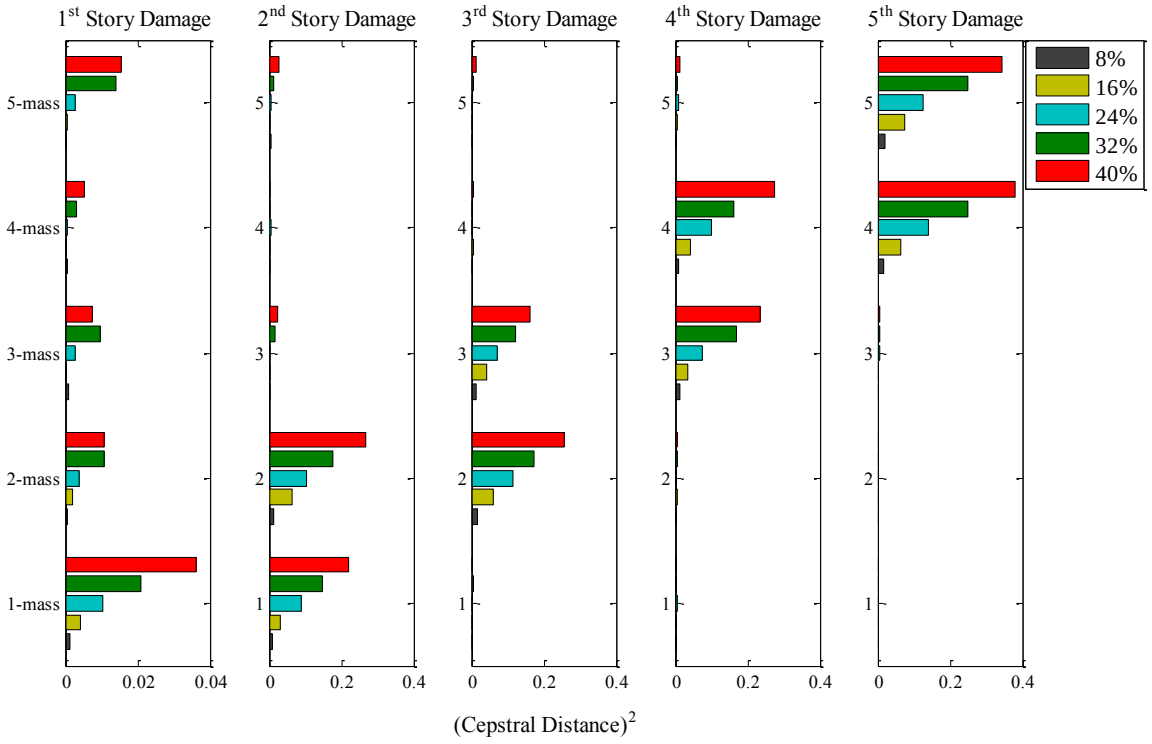


Figure 2.9. Cepstral distance based on the pole-zero models (data length=6000)

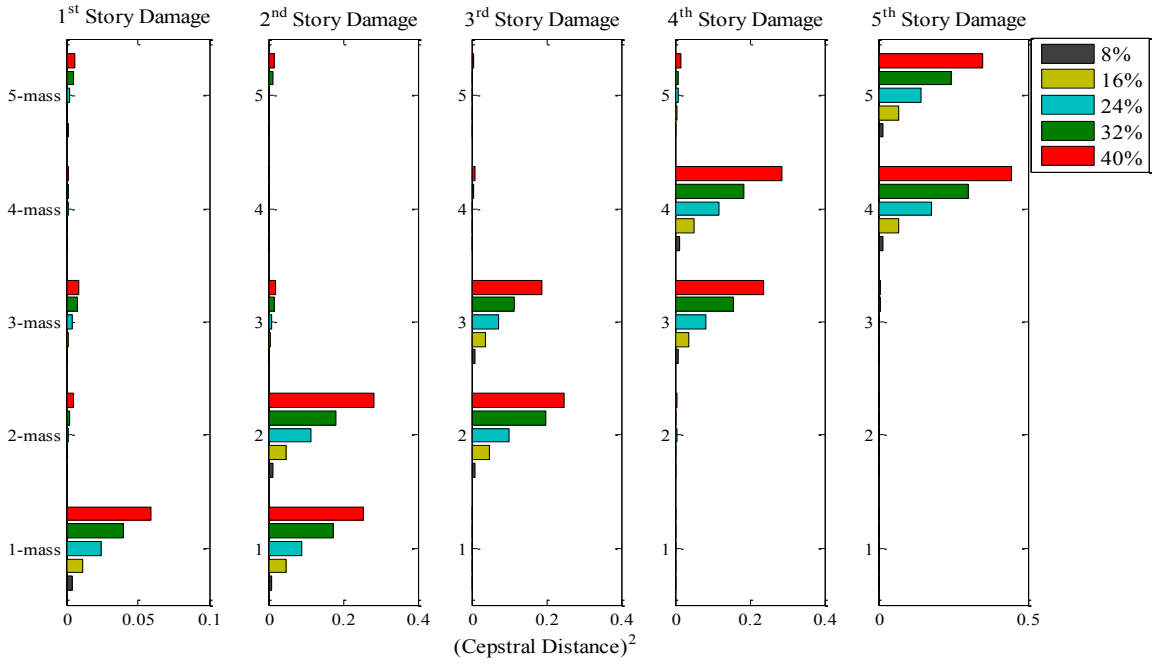


Figure 2.10. Cepstral distance based on the pole-zero models (data length=9000)

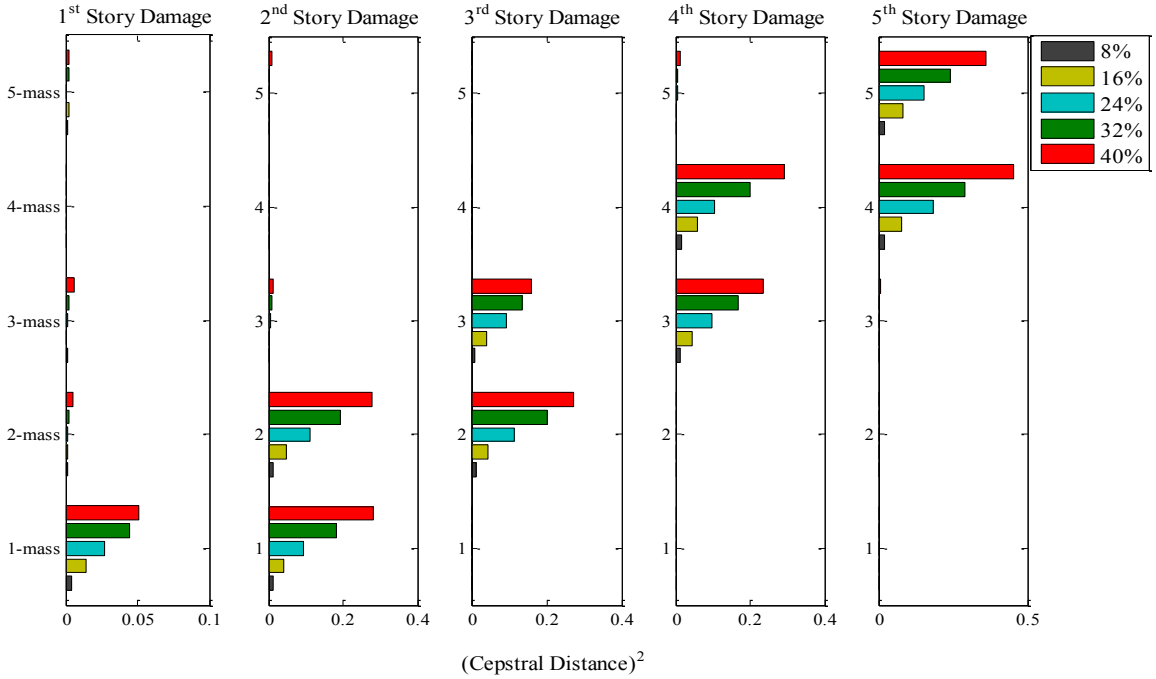


Figure 2.11. Cepstral distance based on the pole-zero models (data length=11000)

This phenomenon is mainly caused by the standard deviations of the AR coefficients, which are determined by the model covariance matrix (Ljung and Ljung 1987), and thus, it is related to the data length. Another reason is that the damage indicators in this case are much smaller than those of the other damage cases and not very big compared with the standard deviations of the AR coefficients. Thus, the damage indicator for the 1st story suffers more from the standard deviations of the AR coefficients than those of the other cases. However, the standard deviations of the AR coefficients can be decreased by increasing the data length, and this in turn reduces the effect on the damage indicators and improves recognition results.

Next, the standard deviations of the AR coefficients are examined when the structure has suffered damage in different locations and with different severities (undamaged, 8%, 16%, 24%, 32% and 40% lateral stiffness reduction). Only the standard deviations of the AR coefficients are listed in Tables 2.2-2.4 when the 1st story suffered no damage, and 8% and 40% lateral stiffness reductions, where $a_i$ means the AR coefficient. From Tables 2.2-2.4, it is clear that increasing the data length reduced the standard deviations, but changing the damage severity had almost no effect on them. Moreover, varying the damage location hardly affected the standard deviations. It is clear that the accuracy of the recognition result depends on the standard deviations of AR coefficients, especially when the standard deviation is not small enough compared with the damage indicator.

Table 2.2. Standard deviations of AR coefficients (undamaged)

| | 1st floor | 2nd floor | 3rd floor | 4th floor | 5th floor |
|---|---|---|---|---|---|
| | Data length 6000 | | | | |
| $a_1$ | 0.0128 | 0.0126 | 0.0128 | 0.0119 | 0.0129 |
| $a_2$ | 0.0125 | 0.0160 | 0.0150 | 0.0153 | 0.0162 |
| $a_3$ | 0.0125 | 0.0160 | 0.0150 | 0.0153 | 0.0162 |

| | | | | | |
|---|---|---|---|---|---|
| $a_4$ | 0.0128 | 0.0126 | 0.0128 | 0.0119 | 0.0129 |
| | Data length 9000 | | | | |
| $a_1$ | 0.0104 | 0.0103 | 0.0104 | 0.0097 | 0.0105 |
| $a_2$ | 0.0102 | 0.0129 | 0.0122 | 0.0126 | 0.0134 |
| $a_3$ | 0.0102 | 0.0129 | 0.0122 | 0.0126 | 0.0134 |
| $a_4$ | 0.0104 | 0.0103 | 0.0104 | 0.0097 | 0.0105 |
| | Data length 11000 | | | | |
| $a_1$ | 0.0094 | 0.0093 | 0.0095 | 0.0088 | 0.0095 |
| $a_2$ | 0.0093 | 0.0117 | 0.0112 | 0.0114 | 0.0120 |
| $a_3$ | 0.0093 | 0.0117 | 0.0112 | 0.0114 | 0.0120 |
| $a_4$ | 0.0094 | 0.0093 | 0.0095 | 0.0088 | 0.0095 |

Table 2.3. Standard deviations of AR coefficients (8% lateral stiffness reduction, damage in the 1st story)

| | 1st floor | 2nd floor | 3rd floor | 4th floor | 5th floor |
|---|---|---|---|---|---|
| | Data length 6000 | | | | |
| $a_1$ | 0.0128 | 0.0126 | 0.0128 | 0.0120 | 0.0129 |
| $a_2$ | 0.0126 | 0.0157 | 0.0150 | 0.0154 | 0.0163 |
| $a_3$ | 0.0126 | 0.0157 | 0.0150 | 0.0154 | 0.0163 |
| $a_4$ | 0.0128 | 0.0126 | 0.0128 | 0.0120 | 0.0129 |
| | Data length 9000 | | | | |
| $a_1$ | 0.0104 | 0.0103 | 0.0104 | 0.0097 | 0.0105 |
| $a_2$ | 0.0102 | 0.0131 | 0.0123 | 0.0125 | 0.0133 |
| $a_3$ | 0.0103 | 0.0131 | 0.0123 | 0.0125 | 0.0133 |
| $a_4$ | 0.0104 | 0.0103 | 0.0104 | 0.0097 | 0.0105 |
| | Data length 11000 | | | | |
| $a_1$ | 0.0095 | 0.0093 | 0.0095 | 0.0088 | 0.0095 |

| | | | | | |
|---|---|---|---|---|---|
| $a_2$ | 0.0093 | 0.0119 | 0.0111 | 0.0114 | 0.0119 |
| $a_3$ | 0.0093 | 0.0119 | 0.0111 | 0.0114 | 0.0119 |
| $a_4$ | 0.0095 | 0.0093 | 0.0095 | 0.0088 | 0.0095 |

Table 2.4. Standard deviations of AR coefficients (40% lateral stiffness reduction, damage in the 1st story)

| | 1st floor | 2nd floor | 3rd floor | 4th floor | 5th floor |
|---|---|---|---|---|---|
| | Data length 6000 | | | | |
| $a_1$ | 0.0128 | 0.0124 | 0.0127 | 0.0117 | 0.0129 |
| $a_2$ | 0.0128 | 0.0163 | 0.0152 | 0.0157 | 0.0166 |
| $a_3$ | 0.0128 | 0.0163 | 0.0152 | 0.0157 | 0.0166 |
| $a_4$ | 0.0128 | 0.0124 | 0.0127 | 0.0117 | 0.0129 |
| | Data length 9000 | | | | |
| $a_1$ | 0.0105 | 0.0102 | 0.0104 | 0.0095 | 0.0105 |
| $a_2$ | 0.0105 | 0.0135 | 0.0126 | 0.0127 | 0.0136 |
| $a_3$ | 0.0105 | 0.0135 | 0.0126 | 0.0127 | 0.0136 |
| $a_4$ | 0.0105 | 0.0102 | 0.0104 | 0.0095 | 0.0105 |
| | Data length 11000 | | | | |
| $a_1$ | 0.0095 | 0.0092 | 0.0094 | 0.0087 | 0.0095 |
| $a_2$ | 0.0095 | 0.0122 | 0.0113 | 0.0115 | 0.0123 |
| $a_3$ | 0.0095 | 0.0122 | 0.0113 | 0.0115 | 0.0123 |
| $a_4$ | 0.0095 | 0.0092 | 0.0094 | 0.0087 | 0.0095 |

In addition to the single damage cases shown as above, multiple damage cases are also studied. Similar to the single damage cases, different multiple degrees of freedom (MDOF) systems (3-19-DOF) with different damage severities (8%, 16%, 24%, 32% and 40% lateral stiffness reduction) in different multiple damage locations were

studied. The data length is 9000 and the order of AR model is 4. Results also show that this method is available to the multiple damage cases. Because of the huge number of results, only the results of a 5-DOF system are listed when the damage with different damage severities (8%, 16%, 24%, 32% and 40% lateral stiffness reduction) in the 1st and 5th story. In Figure 2.12, the damage is localized correctly. The effect on the accuracy of identification results in multiple damage cases, which caused by the data length, the damage severities, damage locations and the standard deviations of AR coefficients, is similar to that in the single damage cases.

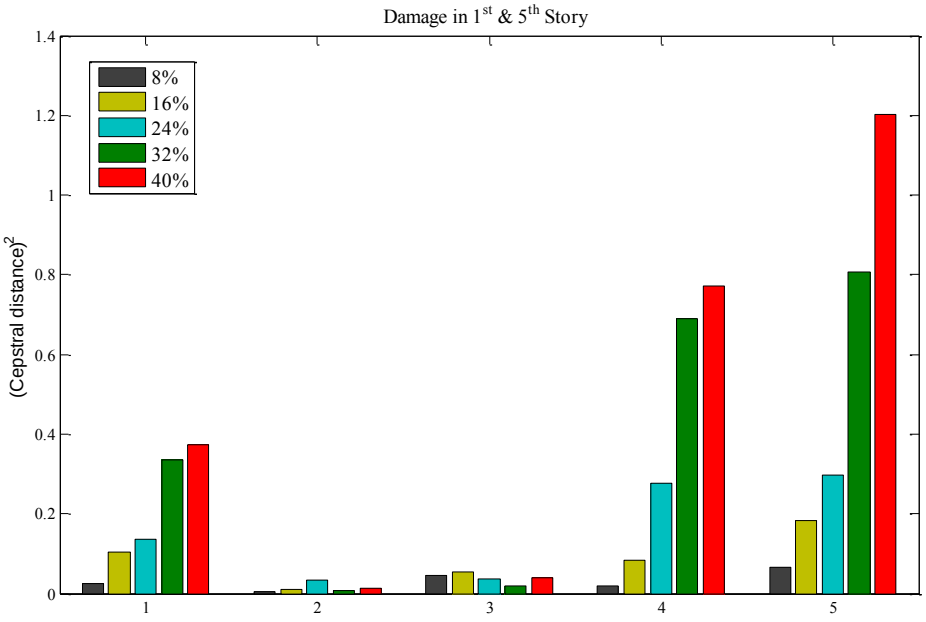


Figure 2.12. Cepstral distance for the multiple damage case (data length=9000)

## 2.5 Experimental Verification

Actual data from a shake table test (Yoshimoto, Mita et al. 2002) were used to evaluate the proposed methodology. A five-story steel structure was tested (Figure 2.13). The long side of every story had removable central columns and braces. The

weight of every story is 2.57 tons, and the story height is 1 m. The lengths of the long and short sides are 3 m and 2 m, respectively. The excitation signal is white noise with bandwidth of 0–200 Hz, in the long side's direction. Accelerometers were mounted on both long sides of every story. The acceleration time histories were recorded with a 0.005 s sampling period. Damage to the building was simulated by removing the central columns and braces; the central columns on the first, third and fifth story were removed as shown in Figure 2.14, and the braces on the first, third and fifth story were removed as shown in Figure 2.16.

Figure 2.15 and Figure 2.17 are the recognition results, and they clearly show the damage locations. The length of data is 6000. Table 2.5 and Table 2.6 list the standard deviations of the AR coefficients when the central columns and the braces on the first story are removed (the standard deviations for the other experimental conditions are similar). The damage indicators are very large compared with the standard deviations, which means that they are not influenced by the standard deviations very much. Thus good recognition results can be obtained, as shown in Figure 2.15 and Figure 2.17.

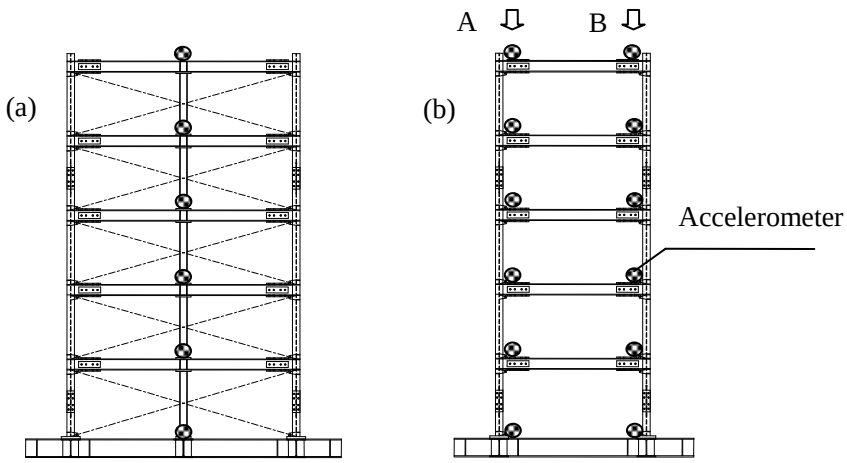


Figure 2.13. Tested building model: (a) long-side and (b) short-side

Table 2.5. Standard deviations of AR coefficients (the central columns on the first story were removed)

| Data length 6000 | 1st floor | 2nd floor | 3rd floor | 4th floor | 5th floor |
|---|---|---|---|---|---|
| $a_1$ | 0.0089 | 0.0078 | 0.0072 | 0.0087 | 0.0079 |
| $a_2$ | 0.0212 | 0.0176 | 0.0162 | 0.0200 | 0.0196 |
| $a_3$ | 0.0212 | 0.0176 | 0.0162 | 0.0200 | 0.0196 |
| $a_4$ | 0.0089 | 0.0077 | 0.0072 | 0.0087 | 0.0079 |

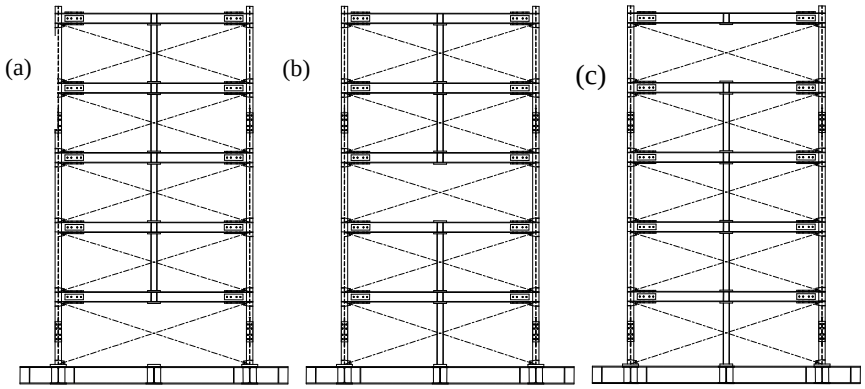


Figure 2.14. Damage case: removing central column on the (a) first, (b) third, and (c) fifth floor

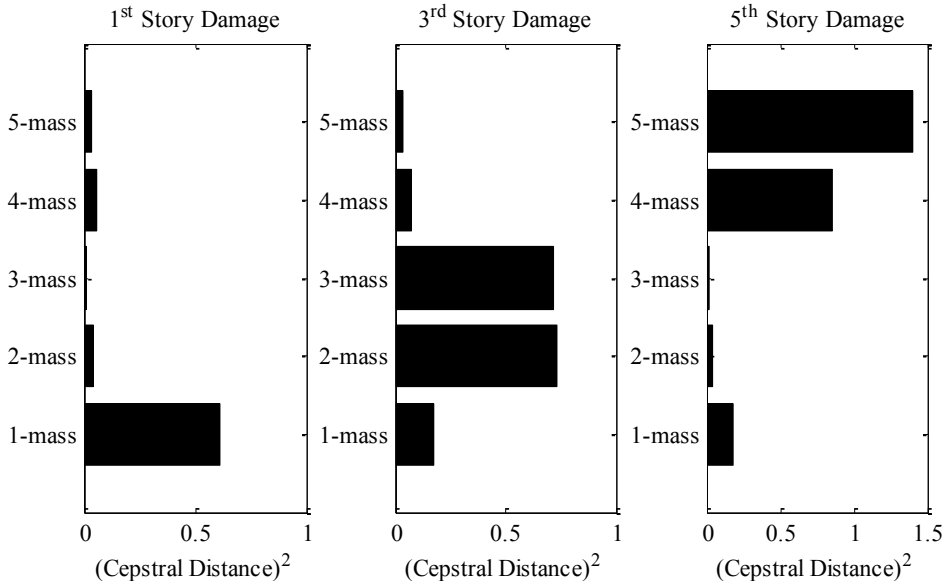


Figure 2.15. Cepstral distances (the central columns were removed, data length=6000)

Table 2.6. Standard deviations of AR coefficients (the braces on the first story were removed)

| Data length 6000 | 1st floor | 2nd floor | 3rd floor | 4th floor | 5th floor |
|---|---|---|---|---|---|
| $a_1$ | 0.0092 | 0.0090 | 0.0091 | 0.0095 | 0.0095 |
| $a_2$ | 0.0185 | 0.0160 | 0.0167 | 0.0173 | 0.0202 |
| $a_3$ | 0.0185 | 0.0160 | 0.0167 | 0.0173 | 0.0202 |
| $a_4$ | 0.0092 | 0.0090 | 0.0091 | 0.0095 | 0.0095 |

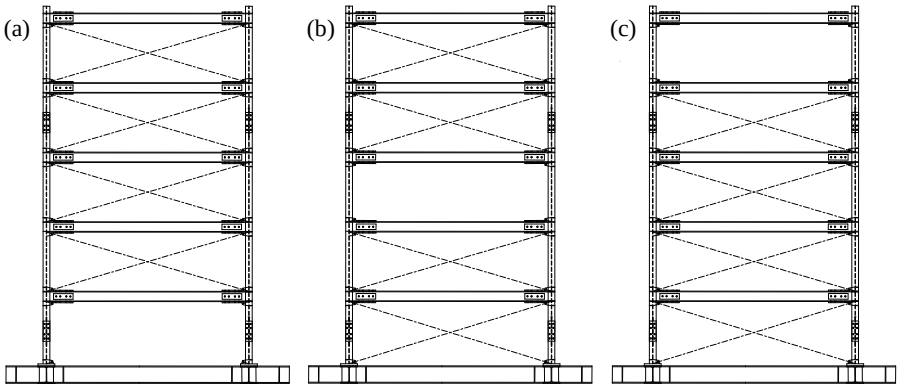


Figure 2.16. Damage case: removing braces on the (a) first, (b) third, and (c) fifth story

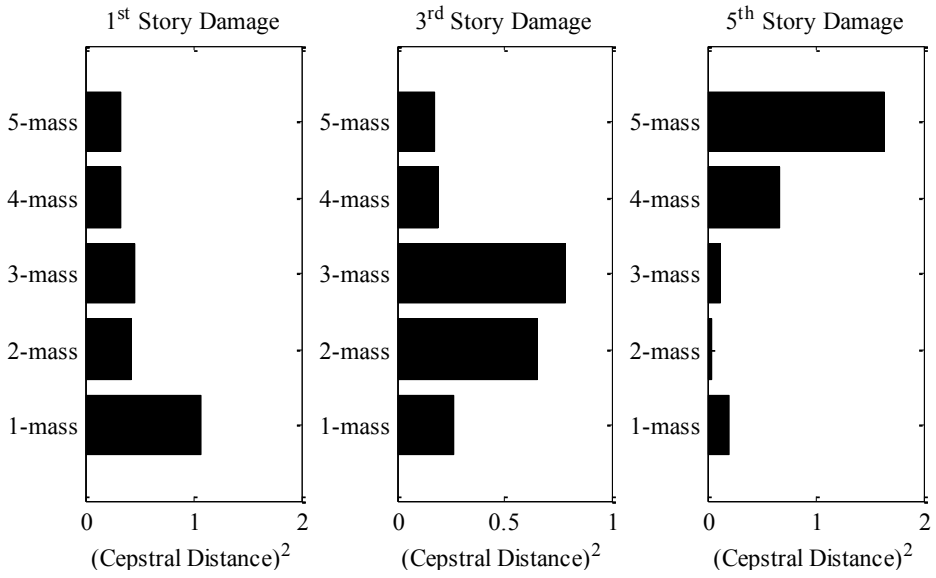


Figure 2.17. Cepstral distances (the braces were removed, data length=6000)

## 2.6 Conclusions

Improvements on distance measures of AR models were proposed. An AR order selection method was proposed to choose the optimum order of the AR model for the distance measures. The combining use of low-order AR models and ACW improves the noise immunity of this method. The standard deviations of the AR coefficients have a significant effect on the accuracy of identification, especially when the standard deviations are not small enough relative to the damage indicators; on the contrary, the severity and location of the damage have little effect on the standard deviations of the AR coefficients. To overcome this problem, the standard deviations of AR coefficients were reduced by increasing the data length. The results of simulations and an experiment show that the scheme is feasible for identifying the damage location. In simulation and experiment, buildings were assumed to be excited by Gaussian white noise. Gaussian white noise can be used to simulate input such as earthquakes and ambient vibration. To apply the method, any excitation including earthquakes or ambient vibration can be used as long as the duration of excitation is long enough. In this study, results with different damage severities show that larger cepstral distance is corresponding to a more serious damage severity and this indicates that there is a relation between the cepstral distance and the damage severity, but so far it is difficult to quantify the damage severity by cepstral distance, and further study is needed.

# *CHAPTER 3*

# Substructure Approach to Local Damage Detection

## 3.1 Introduction

Though many damage detection methods are available for Structural Health Monitoring (SHM), most of them need complete information of the structure, which means many sensors are required to be installed into a building. It may be feasible for small systems. However, it is impossible for large-scale civil structures, since the large number of sensors results in long setup time, high equipment costs as well as enormous efforts needed for wiring and designing (Roeck 2003). Complicated and expensive SHM systems are by no means practical for most civil structures. What we should do is to find a trade-off point between the number of sensors and the accuracy of the damage detection. Another problem for large systems is that data measurement and identification are not easy tasks. The computation time required for convergence increases dramatically with the increase in the number of the degrees of freedom (DOFs) due to the nature of the inverse analysis. The main challenge is the convergence and computation efficiency to achieve reasonable accuracy within

reasonable computation time.

To overcome these problems, some researchers have been using the substructure method for large-scale structures. Koh et al. (1991) proposed substructure system identification and used the Extended Kalman Filter (EKF) (Hoshiya and Saito 1984; Ljung 2002) as the numerical tool to identify unknown structural parameters. Park et al. (1998) offered structural damage detection methods based on relative changes in localized flexibility properties. The localized flexibility matrices are obtained either by applying a decomposition procedure to an experimentally determined global flexibility matrix or by processing the output signals of a vibration test. Zhao et al. (1995) proposed a substructure identification of MDOF structures in the frequency domain.

In this chapter, a substructure algorithm is used to divide a complete structure into substructures. A substructure has a considerably smaller number of degrees of freedom (DOFs) when compared with the entire structure. Much as it appears as a simple idea, it should be known that the substructures are not isolated from the remainder of the structure and it is necessary to consider about the interaction forces at interfaces (Craig and Bampton 1968). To facilitate the handling of interaction forces at substructure interfaces, Koh et al. (2003) used the concept of quasi-static displacement vector, and the damping force was assumed to be negligible. Here, no part of the interaction forces is neglected, and only the accelerations are used for identification. Considering strong flexibility for handling the disturbance modeling, the autoregressive moving average with exogenous inputs (ARMAX) model is adopted to obtain the modal information of the substructures. In the referred papers a little more complicated method is needed to estimate the unknown substructure parameters, e.g. EKF or Genetic Algorithm (GA). Here, each substructure is confined to one DOF and cut substructure with overlaps, thus ARMAX models can be directly used to determine the modal information of each substructure. The extent of damage is

measured by using the squared original frequency and the squared damaged frequency. Each substructure can be treated independently. Three sensors are enough for analyzing a substructure in this method, and for the top substructure, only two sensors are needed.

In many issued papers, the number of DOFs included in a substructure is not highly valued (Saito, Mase et al. 2005; Hou, Jankowski et al. 2010) and they gave us an impression that the substructure can have as many DOFs as we want which is not always true according to the identifiability condition for the feedback system (Schoen 1992; Xie, Mita et al. 2010). It should be noted that a substructure is a feedback system as it has feedback forces from the remainder of the structure. The identifiability of substructures will be discussed in Chapter 4.

## 3.2 ARX Model and ARMAX Model

The autoregressive with exogenous input (ARX) model can be written as

$$y(t)+\sum_{k=1}^{na} a_k y(t-k)=\sum_{k=1}^{nb} b_k u(t-nk-k+1)+e(t) \tag{3.1}$$

where $y(t)$ and $u(t)$ are the output and the input of the structure at sample index $t$, respectively, $a_k$ and $b_k$ are the coefficients to be estimated, $na$ $nb$ and $nk$ are the orders of the ARX model, $nk$ is the number of input samples that occur before the input affects the output, also called the time delay, and $e(t)$ is the prediction error term or residual.

*Advantages:*

1) It is the simplest model incorporating a stimulus signal;

2) The estimation of the ARX model is the most efficient of the polynomial estimation methods because it is the result from solving the linear regression equations in an analytic form;

3) The solution is unique. In other words, the solution always satisfies the global minimum of the loss function.

*Disadvantage:*

ARX model assumes that the transfer function of the deterministic part of the system and the transfer function of the stochastic part of the system have the same set of poles which is unrealistic. The system dynamics and stochastic dynamics of the system do not always share the same set of poles.

The ARMAX model is a generalization of ARX model. The form of ARMAX model is

$$y(t)+\sum_{k=1}^{na} a_k y(t-k)=\sum_{k=1}^{nb} b_k u(t-nk-k+1)+\sum_{k=1}^{nc} c_k e(t-k) \tag{3.2}$$

where $y(t)$ and $u(t)$ are the output and input of the structure at sample index $t$, respectively, $a_k$, $b_k$ and $c_k$ are the coefficients to be estimated, $na$, $nb$, $nc$ and $nk$ are the orders of the ARMAX model, and $e(t-k)$ is the white-noise disturbance value.

Unlike the ARX model, the ARMAX model includes disturbance dynamics. ARMAX models are useful when you have dominating disturbances that enter early on in the process, such as at the input. The ARMAX model has more flexibility for handling the disturbance modeling than the ARX model.

## 3.3 Motion Equations for Substructures

A structure is modeled as a one-dimensional lumped mass shear model, as shown in Figure 3.1. The motion equation for the overall structure is written as

$$\mathbf{M}\ddot{\mathbf{x}} + \mathbf{C}\dot{\mathbf{x}} + \mathbf{K}\mathbf{x} = -\mathbf{M}\mathbf{r}\ddot{x}_g \tag{3.3}$$

where **M**, **K**, and **C** are the mass, stiffness, and damping matrix, respectively. **r** is an $n \times 1$ unit vector ($\mathbf{r} = [1 \cdots 1]^T$), **x** is the displacement relative to the ground, and $\ddot{x}_g$ is the ground acceleration.

$$\mathbf{x} = \begin{bmatrix} x_1 & x_2 & \cdots & x_n \end{bmatrix}^T$$

$$\mathbf{M} = \begin{bmatrix} m_1 & & & 0 \\ & \ddots & & \\ & & m_i & \\ & & & \ddots \\ 0 & & & m_n \end{bmatrix}$$

$$\mathbf{K} = \begin{bmatrix} k_1 + k_2 & -k_2 & & & & 0 \\ -k_2 & k_2 + k_3 & k_3 & & & \\ & & \vdots & & & \\ & & -k_i & k_i + k_{i+1} & -k_{i+1} & \\ & & & & \vdots & \\ 0 & & & & -k_n & k_n \end{bmatrix}$$

$$\mathbf{C} = \begin{bmatrix} c_1 + c_2 & -c_2 & & & & 0 \\ -c_2 & c_2 + c_3 & c_3 & & & \\ & & \vdots & & & \\ & & -c_i & c_i + c_{i+1} & -c_{i+1} & \\ & & & & \vdots & \\ 0 & & & & -c_n & c_n \end{bmatrix}$$

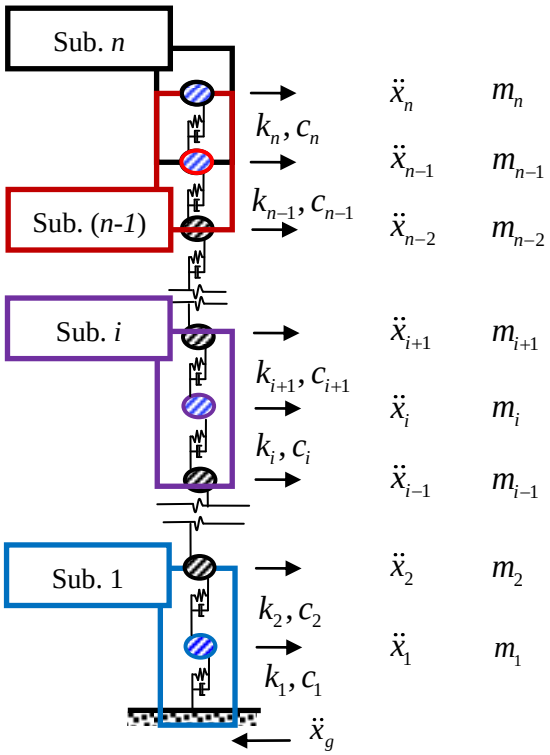


Figure 3.1. Simplified lumped mass shear model

From the motion equation of the whole structure, the motion of the substructure can be obtained as follows:

1) The equation for the substructure $n$ can be formulated by assuming that the substructure behaves as a structure subjected to support excitation ( $\ddot{x}^a_{n-1}$ )

$$m_n\ddot{x}^r_n + c_n\dot{x}^r_n + k_n x^r_n = m_n\ddot{x}^a_{n-1} \tag{3.4}$$

where $x^r_n$ is the displacement of the $n^{\text{th}}$ mass relative to the displacement of the $(n\text{-}1)^{\text{th}}$ mass, $\ddot{x}^a_{n-1}$ is the absolute acceleration of the $(n\text{-}1)^{\text{th}}$ mass, and $c_n$ and $k_n$ mean the damping and stiffness of the $n^{\text{th}}$ story, respectively.

2) The motion equation of substructure (*n*-1) is

$$\begin{aligned} m_{n-1}\ddot{x}_{n-1}^{r} + (c_{n-1}+2c_n)\dot{x}_{n-1}^{r} + (k_{n-1}+2k_n)x_{n-1}^{r} \\ = m_n\ddot{x}_n^{r} + 2c_n\dot{x}_n^{r} + 2k_n x_n^{r} - (m_{n-1}-m_n)\ddot{x}_{n-2}^{a} \end{aligned} \tag{3.5}$$

where $x_{n-1}^{r}$ is the displacement of the ($n$-1)$^{\text{th}}$ mass relative to the displacement of the ($n$-2)$^{\text{th}}$ mass, $x_n^{r}$ is the displacement of the $n^{\text{th}}$ mass relative to the displacement of the ($n$-2)$^{\text{th}}$ mass, and $\ddot{x}_{n-2}^{a}$ is the absolute acceleration of the ($n$-2)$^{\text{th}}$ mass.

3) The motion equation of substructure $i$ $(1 \le i \le n-2)$ using the relative response with respect to the lower response ($\ddot{x}_{i-1}$) is

$$m_i\ddot{x}_i^{r} + (c_i + c_{i+1})\dot{x}_i^{r} + (k_i + k_{i+1})x_i^{r} = -m_i\ddot{x}_{i-1}^{a} + c_{i+1}\dot{x}_{i+1}^{r} + k_{i+1}x_{i+1}^{r} \tag{3.6}$$

where $x_i^{r}$ is the displacement of the $i^{\text{th}}$ mass relative to the displacement of the ($i$-1)$^{\text{th}}$ mass, $x_{i+1}^{r}$ is the displacement of the ($i$+1)$^{\text{th}}$ mass relative to the displacement of the $i^{\text{th}}$ mass, and $\ddot{x}_{i-1}^{a}$ is the absolute acceleration of the ($i$-1)$^{\text{th}}$ mass. Especially, when $i$=0, $\ddot{x}_{i-1}^{a}$, i.e. $\ddot{x}_0^{a}$ means the ground acceleration.

Introducing the difference expression

$$\begin{aligned} \dot{x}_i(t) &= \frac{x_i(t+T) - x_i(t-T)}{2T} \\ \ddot{x}_i(t) &= \frac{x_i(t+T) - 2x_i(t) + x_i(t-T)}{T^2} \end{aligned} \tag{3.7}$$

where $T$ is the sampling interval, into the motion equation of substructure $i$ in Equation (3.6), Equation (3.6) can be transformed as

$$\begin{aligned}\ddot{x}_i^r(t)+a_1\ddot{x}_i^r(t-1)+a_2\ddot{x}_i^r(t-2)=b_{11}\ddot{x}_{i-1}^a(t-1)+b_{12}\ddot{x}_{i-1}^a(t-2)\\ +b_{21}\ddot{x}_{i+1}^r(t-1)+b_{22}\ddot{x}_{i+1}^r(t-2)\\ +c_{31}e(t-1)+c_{32}e(t-1)\end{aligned} \tag{3.8}$$

where $e(t)$ is the prediction error term or residual.

It is clear that Equation (3.6) can be regarded as a two-input and one-output ARMAX model. Similar equations also can be obtained by substituting Equation (3.7) into substructures *n* and (*n*-1) respectively, which are a single-input and single-output ARMAX model for substructure n and a two-input and one-output ARMAX model for substructure (*n*-1).

## 3.4 Performance Verification by Simulation

In this simulation, a five-story shear building model was constructed to show the feasibility of the proposed method. The building is simplified into a 5 DOF structural system, as shown in Figure 3.2.

The mass of every floor and the lateral stiffness were assumed to be 100 kg and 1 MN/m, respectively. Three percent was chosen as the damping ratio for all modes. The data sampling frequency is 200 Hz. The undamaged natural frequencies of the structure are 4.5, 13.2, 20.8, 28.6 and 30.5 Hz for the 1$^{st}$, 2$^{nd}$, 3$^{rd}$, 4$^{th}$ and 5$^{th}$ modes, respectively. The 5-DOF system is assumed to be excited by Gaussian white noise, which is used to simulate an input such as an earthquake, and 5% noise was added to the acceleration responses of the structure. The story stiffness reduction was regarded as damage to the structure. Five cases of damage (damage in the 1$^{st}$, 2$^{nd}$, 3$^{rd}$, 4$^{th}$ or 5$^{th}$ stories) with five different damage severities (10, 20, 30, 40 and 50% lateral stiffness reduction) were studied. Therefore, there are 25 different damage scenarios totally.

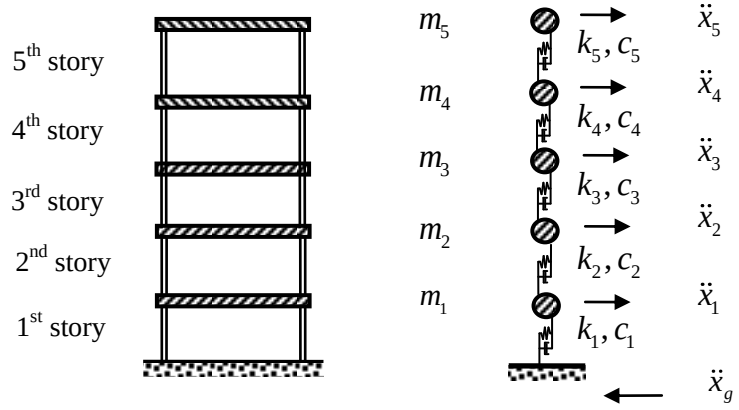


Figure 3.2. Simulation model for a five-story shear building

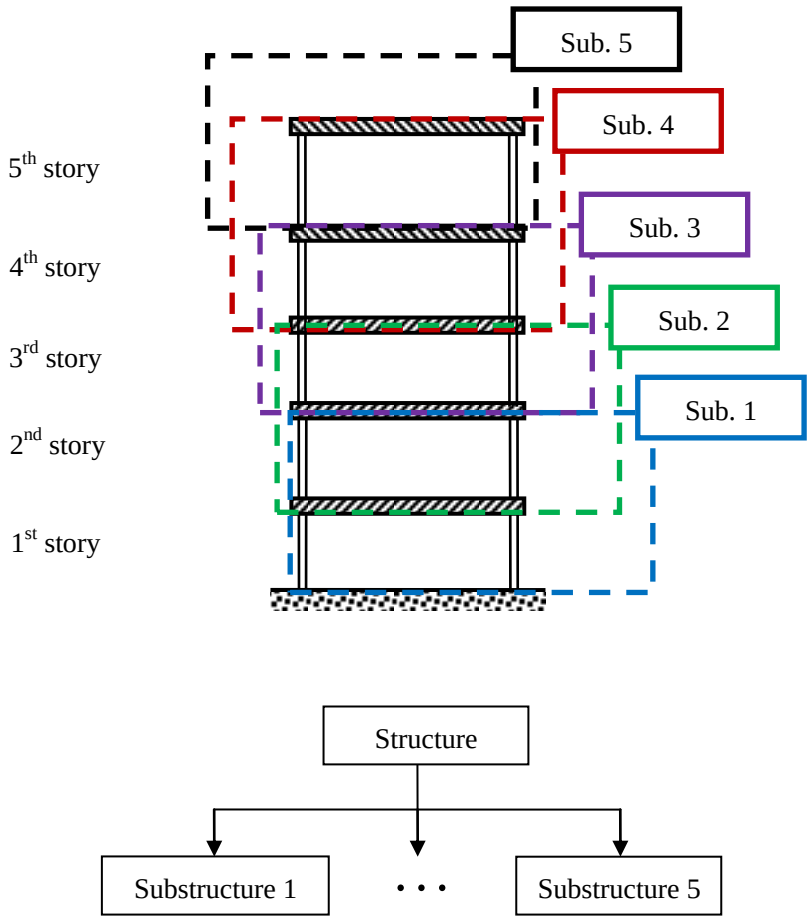


Figure 3.3. Structural division

First, the entire structure is divided into the substructures shown in Figure 3.3.

Then, ARMAX or ARX models are used to model each substructure in the undamaged and unknown states. By using the ARMAX or ARX model, the mode information of a substructure can be obtained easily.

1) *Substructure 5:* The ARMAX or ARX model input of the 5th substructure is the absolute acceleration of the 4th mass ($\ddot{x}_4^a$), and the output is the acceleration of the 5th mass relative to the 4th mass ($\ddot{x}_5^r$). It is a single-input and single-output ARMAX or ARX model.

2) *Substructure 4:* The ARMAX or ARX model inputs of the 4th substructure are the absolute acceleration of the 3rd mass ($\ddot{x}_3^a$) and the acceleration of the 5th mass relative to the 3rd mass ($\ddot{x}_5^r$), and the output is the acceleration of the 4th mass relative to the 3rd mass ($\ddot{x}_4^r$). It is a two-input and single-output ARMAX or ARX model.

3) *Substructure i:* The $i^{th}$ substructure (except the 4th and 5th substructure) can be modeled as a two-input one-output ARMAX or ARX model. The absolute acceleration of the $(i\text{-}1)^{th}$ mass ($\ddot{x}_{i-1}^a$) and the acceleration of the $(i\text{+}1)^{th}$ mass relative to the $(i\text{-}1)^{th}$ mass ($\ddot{x}_{i+1}^r$) are used as the inputs, and the acceleration of the $i^{th}$ mass relative to the $(i\text{-}1)^{th}$ mass ($\ddot{x}_i^r$) is used as the output. Especially, when $i$=0, $\ddot{x}_{i-1}^a = \ddot{x}_0^a = \ddot{x}_g$, where $\ddot{x}_g$ is the ground acceleration.

The extent of damage is measured by using the squared original frequency ($\omega_0^2$) and the squared damaged frequency ($\omega_d^2$). The confidence interval is 95%.

The results show that when no noise is added, the method based on the ARMAX

model doesn't need a lot of data, and only 500 data are enough to obtain results (Figure 3.4). Meanwhile, the method based on the ARX model can also acquire excellent results, and the result is shown in Figure 3.5. The standard deviations in the results are so small that they almost can't be seen in these figures.

When 5% noise is added, the method based on the ARMAX model still obtains a satisfactory result (Figure 3.6) and the standard deviations only slightly increase, which proves the stability of this method. Meanwhile, the method based on the ARX model almost doesn't work (Figure 3.7). As the ARMAX model structure includes disturbance dynamics, the method based on this model has more flexibility in handling the disturbance modeling than the method based on the ARX model.

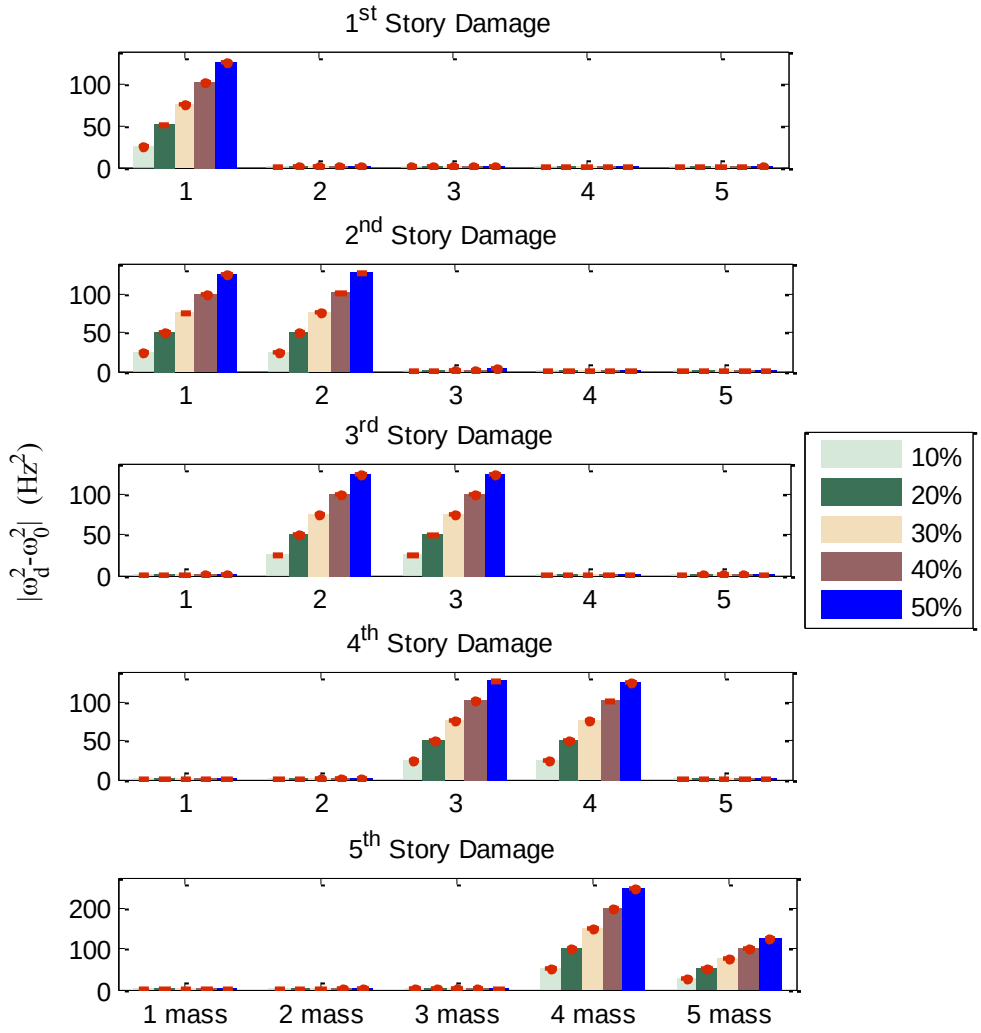


Figure 3.4. Difference between squared original frequency and squared damaged frequency (ARMAX model, no noise, data length=500, $na = 2, nb = 3, nc = 3$, and $nk = 1$)

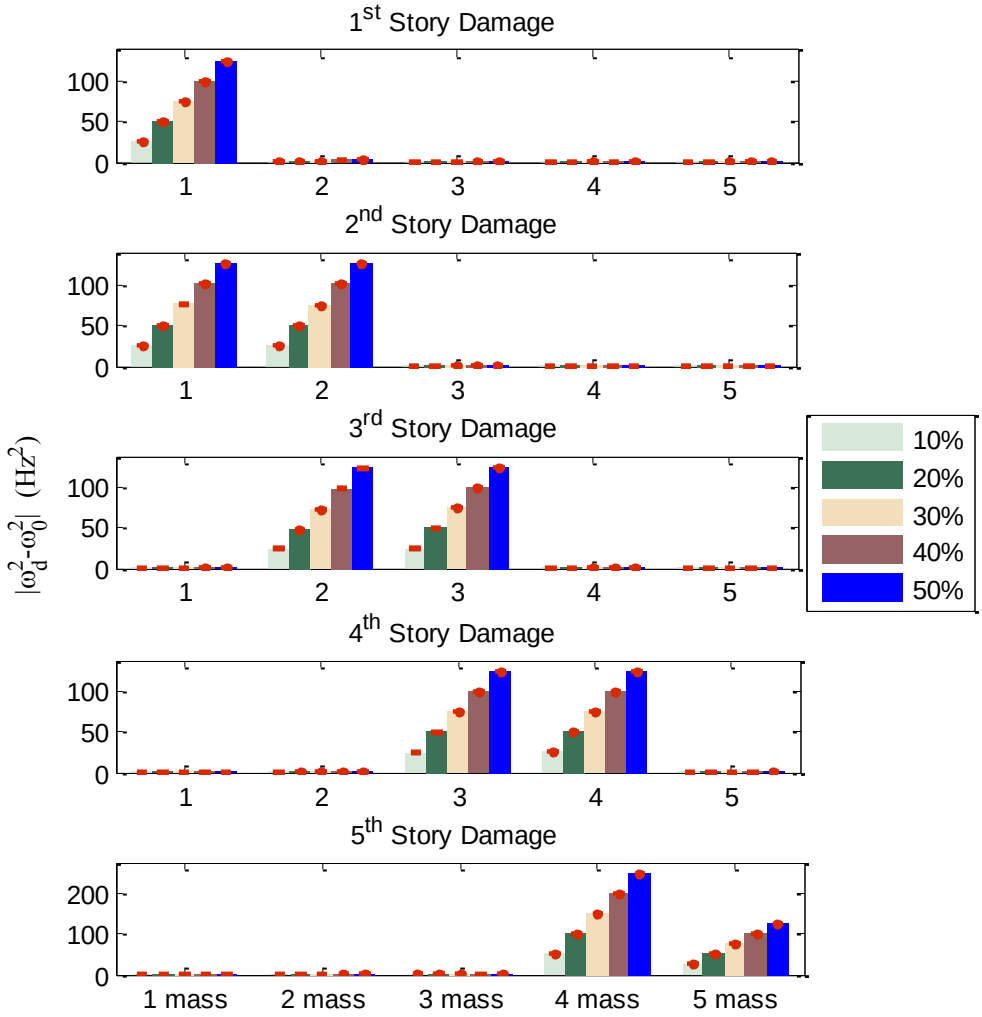


Figure 3.5. Difference between squared original frequency and squared damaged frequency (ARX model, no noise, data length=500, $na = 2, nb = 3$, and $nk = 1$)

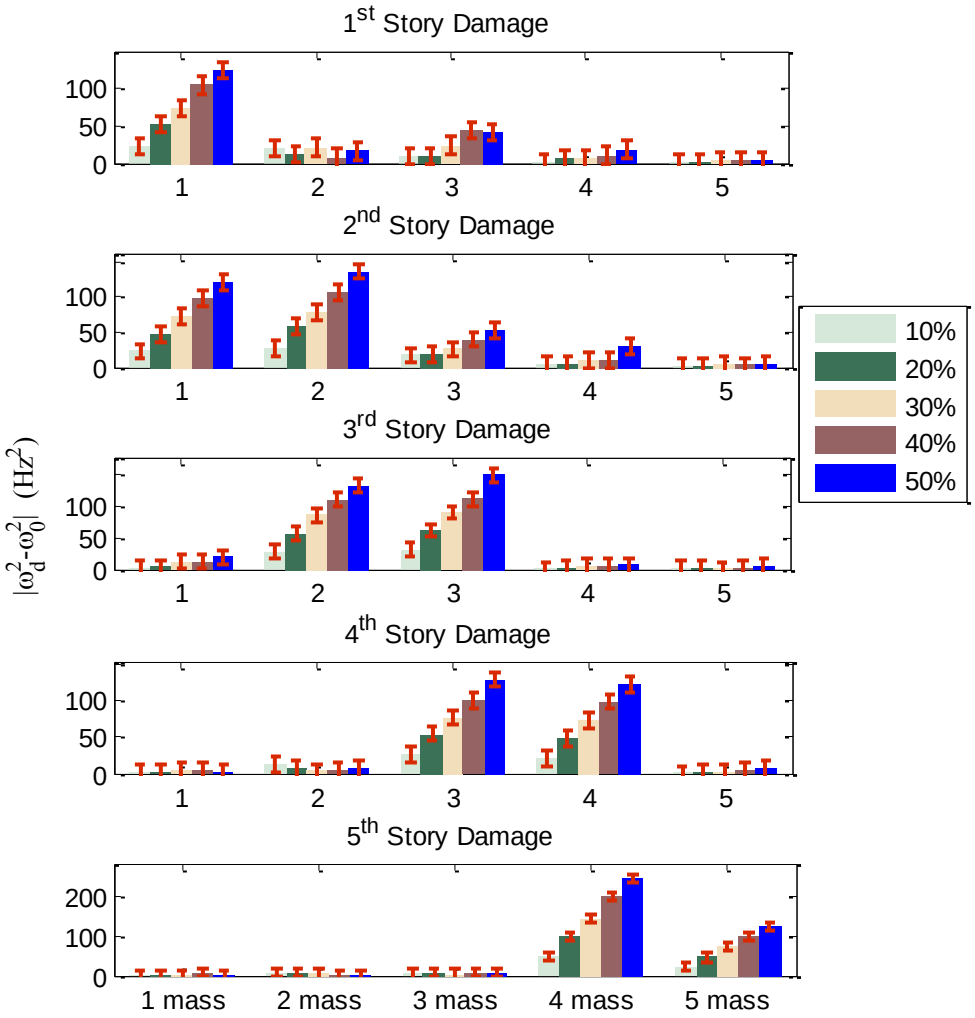


Figure 3.6. Difference between squared original frequency and squared damaged frequency (ARMAX model, 5% noise, data length=500, $na=2, nb=3, nc=3$, and $nk=1$)

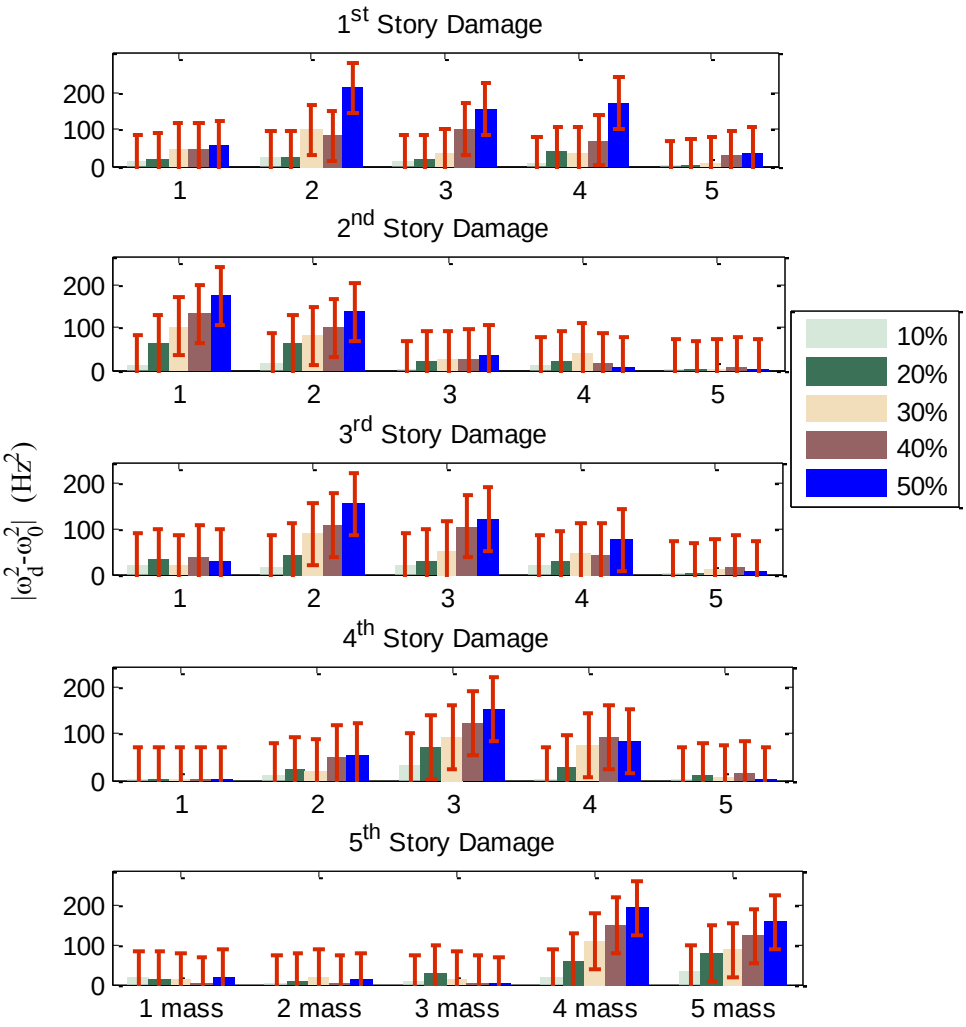


Figure 3.7. Difference between squared original frequency and squared damaged frequency (ARX model, 5% noise, data length=500, $na = 2, nb = 3$, and $nk = 1$)

## 3.5 Experimental Verification

The measured data from a shake table test (Yoshimoto, Mita et al. 2002) was used to verify the methodology. A five-story steel structure was tested (Figure 3.8). The

weight of every story is 2.57 tons, and the story height is 1 m. The lengths of the long and short sides are 3 m and 2 m, respectively. The white noise at a bandwidth range of 0–200 Hz was used as the excitation signal, in the long side direction. Accelerometers were mounted on both long sides of every story. The acceleration time histories were recorded at a 0.005 s sampling period.

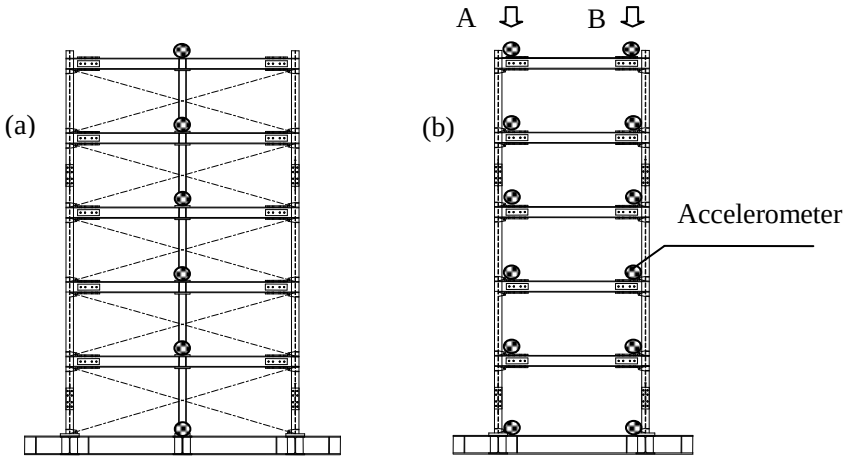


Figure 3.8. Building model: (a) long-side and (b) short-side

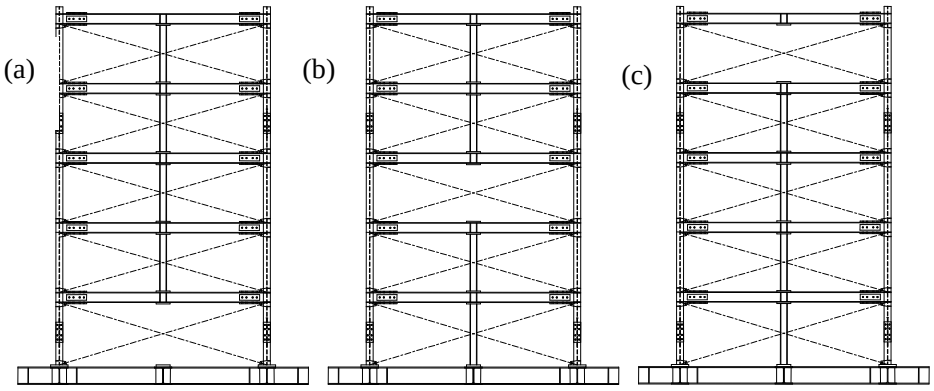


Figure 3.9. Removing central column on (a) first, (b) third, and (c) fifth floors

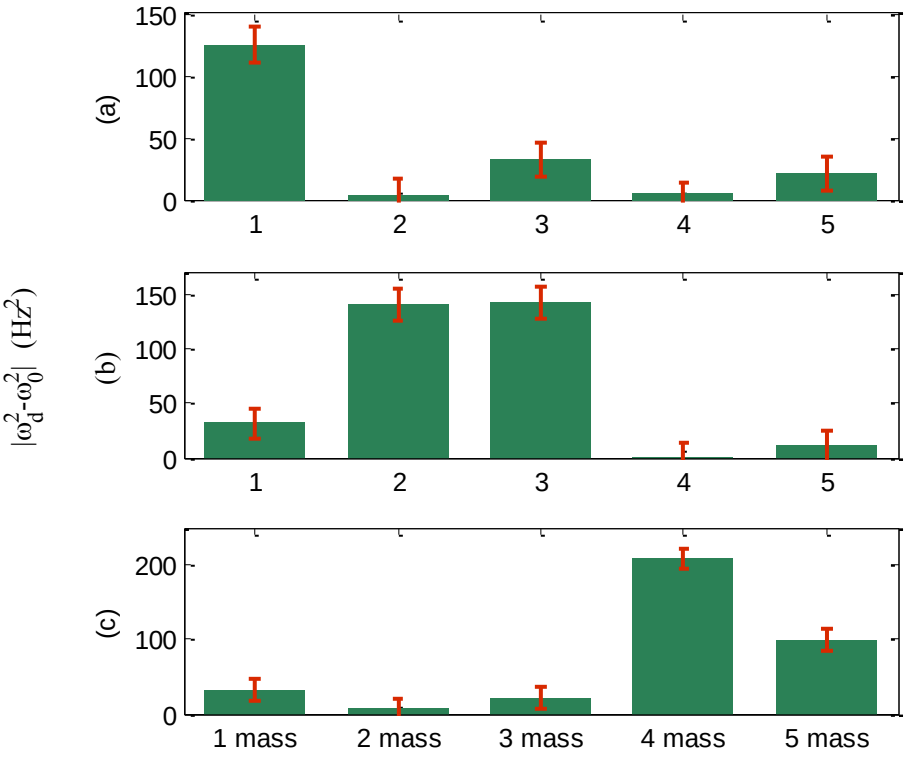


Figure 3.10. Difference between squared original frequency and squared damaged frequency (ARMAX model, data length=1500, $na=2, nb=3, nc=4$, and $nk=1$)

The damage to the building was simulated by removing the central columns; the central columns on the first, third, and fifth stories were removed as shown in Figure 3.9. The confidence interval is 95%. Figure 3.10 shows the recognition results obtained by using the method based on the ARMAX model. From Figure 3.10, we can localize the damage easily which means the proposed method works very well. Moreover, we can find that the standard deviations are small which also confirmed the strong stability of this method.

## 3.6 Conclusions

This chapter presented a new method, based on substructure approach, for the local damage detection of a shear structure. This method requires only three sensors to identify localized damage in any story of a shear structure. As the structure is divided into substructures, which have a considerably smaller number of DOFs, the analysis on each substructure needs fewer data and less computation time. It is not true that the substructure can have as many DOFs as we want. Under certain conditions, the identification may fail due to the closed-loop nature of the system, which will be studied carefully in the next chapter. It should be noted that a substructure is a feedback system as it has feedback forces from the remainder of the structure. Thus every substructure is confined to one DOF, which can satisfy the identifiability condition for the substructure. By cutting substructure with overlaps, ARMAX models can be directly used to determine the modal information of each substructure, instead of using a little more complicated methods, e.g. EKF or Genetic Algorithm (GA). In this way, it simplifies the method significantly. As the damage detection processes can be independently conducted on each substructure, this method is suitable for use in a parallel and distributed damage detection system.

# *CHAPTER 4*
# Identifiability of Substructure as Feedback System

## 4.1 Introduction

In many issued papers, the number of DOFs included in a substructure is not highly valued (Craig and Bampton 1968; Su and Juang 1994; Arikawa, Mitsuhashi et al. 1996; Koh, Hong et al. 2003; Saito, Mase et al. 2005; Yuen and Katafygiotis 2006; Huang and Yang 2008; Hou, Jankowski et al. 2010). They gave us an impression that the substructure can have as many DOFs as we want which is not always true according to the identifiability condition for the feedback system (Schoen 1992; Xie, Mita et al. 2010). It is found that when the engineering structure is divided into substructures, it is more reasonable to carry out the identification of the substructure from the viewpoint of a closed-loop system, which has rarely been investigated in previously published reports, especially when the substructure method is used to identify the engineering structures.

In this chapter, the identifiability of substructures for civil engineering structures is investigated, and a structure division method is proposed to make the substructure

identifiable when the substructure is not strongly system identifiable (SSI). To clarify the identifiability of the substructures, the substructures are classified into three types. It should be noted that a substructure is a feedback system as it has feedback forces from the remainder of the structure. Under certain conditions, the identification may fail due to the closed-loop nature of the system.

## 4.2 Formulation of Substructure System as Feedback System

It is mentioned above that the substructure is a feedback system, as it receives feedback forces from the remainder of the structure. Figure 4.1 shows a closed-loop system. The substructure and the rest of the structure are regarded as the plant and regulator, respectively. It is very important to know whether and how the open-loop system is identified when it is operated under a closed-loop system. Akaike (1967) analyzed the effect of feedback loops in the system on correlation and spectral analysis. The analysis showed that under a feedback system spectral analysis cannot give reasonable results since the correlation between the unmeasurable noise and the input.

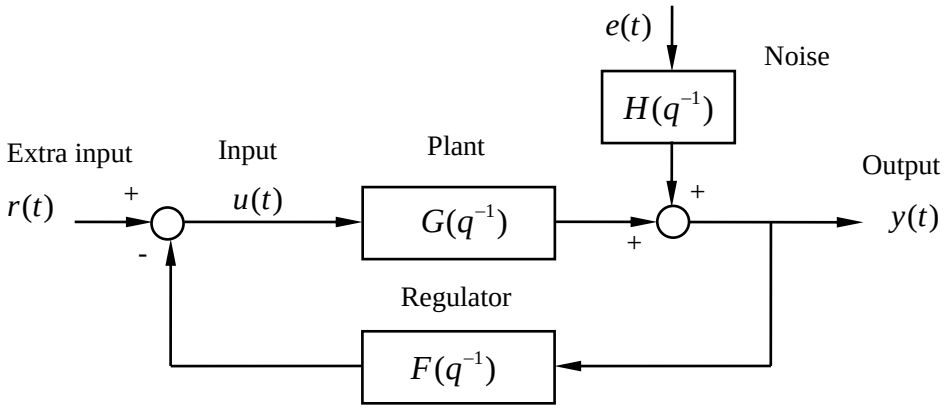


Figure 4.1. A closed-loop system

The open loop system is assumed to be given by

$$y(t) = G(q^{-1})u(t) + H(q^{-1})e(t) \tag{4.1}$$

where the output, $y(t)$, has dimension $n$, and the input, $u(t)$, has dimension $m$, $e(t)$ is a sequence of independent random variables with zero mean value and covariance $Ee(t)e^T(t) = \Lambda$, $q^{-1}$ denotes the backward shift operator, and $G(q^{-1})$ and $H(q^{-1})$ are rational transfer function matrices. The input $u(t)$ is determined by feedback to be

$$u(t) = -F(q^{-1})y(t) + r(t) \tag{4.2}$$

In Equation (4.2) the signal $r(t)$ can be a $q$-dimensional reference value, a set-point, or noise entering the regulator, and it is assumed to be uncorrelated with the noise $e(t)$. The input $u(t)$ to the system given by Equation (4.2) can be chosen freely by the designer, or it can also consist partly of output feedback by a regulator or a given structure.

To determine a model of the system given by Equation (4.1), the functions $G(q^{-1})$ and $H(q^{-1})$ have to be parameterized by a suitable parameter vector $\theta$. A model corresponding to a certain value of $\theta$ is given by

$$y(t) = G_\theta(q^{-1})u(t) + H_\theta(q^{-1})e(t) \tag{4.3}$$

where $e(t)$ is a sequence of independent random variables with zero mean value and covariance $Ee(t)e^T(t) = \Lambda$. When parameter $\theta$ is varied over a reasonable region of values, Equation (4.3) represents a family of models.

Generally, the methods that determine the parameter vector $\theta$ can be summarized as three approaches (Söderström and Stoica 1988):

1) *Direct approach*: Ignore the feedback and identify the open-loop system using measurements of the input and the output. It is clear that the direct approach provides a biased estimate. However, if the bias is acceptable, this approach is very attractive since it is very simple and easy to understand.

2) *Indirect approach:* Identify closed-loop transfer function and determine the open-loop parameters using the knowledge of the regulator. For the indirect approach, knowledge of the regulator is needed. However, the quality of the estimates may be poor due to the possible deterioration of the regulator characteristics or the inclusion of some nonlinearity such as a limiter or dead zone. Moreover, the estimated plant transfer function is of a high order.

3) *Joint input-output approach:* Regard the input and output of the plant as the output from a system driven by some external input, and then determine the open-loop parameters from this system. The advantage of the joint input-output approach is that knowledge of the regulator is not necessary. However, it has the same disadvantage as the indirect approach in that the estimated plant transfer function is of a high order.

## 4.3 Identifiability Conditions

The concept of identifiability has been given with several different definitions. The most common approach is to relate the identifiability properties to the consistency of the parameter estimate $\hat{\theta}$. The true parameter $\theta$ is then said to be identifiable if the sequence of estimates $\hat{\theta}$ converges to $\hat{\theta}$ in some stochastic sense (Astrom and

Bohlin 1966). It has been shown that if there is a time delay in the feedback loop, and if the regulator noise is independent of the system noise, the direct and joint input-output approaches are equivalent for determining identifiability. Furthermore, the indirect approach has no advantage over direct identification in terms of either identifiability or accuracy (Ljung 1999). Thus, the direct identification approach is used.

### 4.3.1 Spectral Analysis

First let us look at the use of spectral analysis in a closed-loop system. For convenience, the signal is introduced:

$$z(t) = F(q^{-1})H(q^{-1})e(t) \tag{4.4}$$

The spectral analysis estimate of $G(e^{-iw})$ is given by

$$\hat{G}(e^{-iw}) = \frac{\phi_{yu}(w)}{\phi_u(w)} = \frac{G(e^{-iw})\phi_r(w) - \phi_z(w)/F(e^{-iw})}{\phi_r(w) + \phi_z(w)} \tag{4.5}$$

where $\phi_u(w)$ and $\phi_{yu}(w)$ are the spectrum of input $u$ and the cross-spectrum between input $u$ and output $y$, respectively. It is assumed that the spectral densities $\phi_u(w)$ and $\phi_{yu}(w)$ can be estimated exactly, which should be true at least asymptotically, as the number of data items tends to be infinite. If there is no disturbance, then $z(t) \equiv 0$, $\phi_z(w) = 0$, and Equation (4.5) can be simplified to $\hat{G}(e^{-iw}) = G(e^{-iw})$, i.e., the true system can be identified. If there is no external input, $\phi_r(w) = 0$, and Equation (4.5) becomes $\hat{G}(e^{-iw}) = -\frac{1}{F(e^{-iw})}$, which is the negative inverse of the feedback. It has been shown that the spectral analysis fails to identify

the open-loop transfer function.

### 4.3.2 Parametric Method

First assume that *r* different feedback laws are used:

$$u(t) = -F_i(q^{-1})y(t) + r(t) \qquad 1 \le i \le r \tag{4.6}$$

The closed-loop system corresponding to the *i*th feedback law is given by:

$$\begin{aligned} y(t) &= (I + GF_i)^{-1}(Gr(t) + He(t)) \\ u &= [I - F_i(I + GF_i)^{-1}G]r(t) - F_i(I + GF_i)^{-1}He(t) \end{aligned} \tag{4.7}$$

Soderstrom (Söderström and Stoica 1988) gave the identifiability condition as follows:

$$r \ge (n_u + n_y)/(n_y + n_r) \tag{4.8}$$

where $r$ is the number of feedback laws, $n_u$ is the number of plant inputs, $n_y$ is the number of plant outputs, and $n_r$ is the number of external signals. This gives a lower bound on the number *r* of different feedback laws that can guarantee the identifiability.

## 4.4 Classification of Substructure Types of Shear Structure

The prediction error method has been widely used as the direct approach to identify the plant of the feedback system. In this study, the autoregressive moving average with exogenous inputs (ARMAX) model is used to identify the substructure, since it includes disturbance dynamics and has more flexibility for handling the disturbance modeling.

$$y(t)+\sum_{k=1}^{na} a_k y(t-k)=\sum_{k=1}^{nb} b_k u(t-nk-k+1)+\sum_{k=1}^{nc} c_k e(t-k) \tag{4.9}$$

where $y(t)$ and $u(t)$ are the output and input of the structure at sample index $t$, respectively, $a_k$, $b_k$, and $c_k$ are the coefficients to be estimated, $na$, $nb$, and $nc$ are the orders of the ARMAX model, $nk$ is the time delay, and $e(t-k)$ is the white-noise disturbance value.

Dividing a structure into substructures is an effective method to overcome the difficulty caused by the increase in the number of DOFs of the structure. Figure 4.2 is a simplified structural model with *n* DOFs. Generally, there are three types of substructures, as shown in Figure 4.2.

*Substructure Type I:* This type of substructure is obtained by cutting the structure from the top. The biggest characteristic of Substructure Type I is that it includes a free end.

*Substructure Type II:* Unlike Substructure Type I, Substructure Type II does not include a free end, but it has two fixed interfaces instead.

*Substructure Type II':* Substructure type II' is a special case of Substructure Type II. Here for clarity, it is regarded as the Substructure Type II'. It is a substructure with two fixed ends: one is the ground, and the other one is the fixed interface.

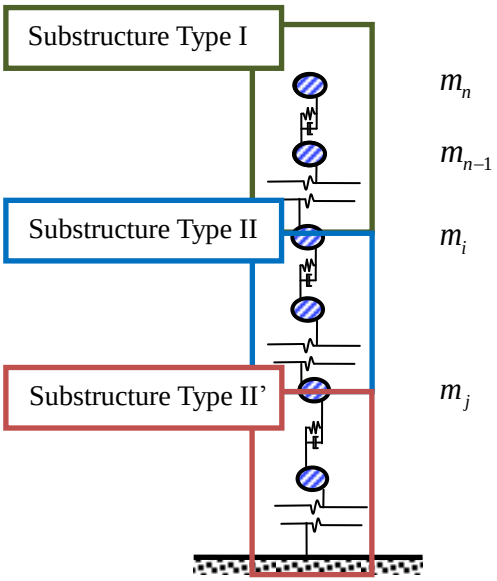


Figure 4.2. Substructure types of shear structure

## 4.5 Verification of Identifiability of Substructures for Types I, II, and II' by Simulation

A twelve-story structure was studied. The structure was assumed to be the shear type and is simplified into a 12-DOF structural system. The mass of every floor and the lateral stiffness were assumed to be 100 kg and 1 MN/m, respectively. A damping ratio of 3% was chosen for all modes. The data sampling frequency is 200 Hz. A 3% noise value was added to the acceleration. The ground acceleration was simulated by Gaussian white noise. Table 4.1 lists the basic information of the simulation, and Table 4.2 lists the modal frequencies of the overall structure.

When the structure is divided, the biggest problem is determining from which mass to which mass can be regarded as a substructure, and of course, it should be identifiable. This problem can be studied in two situations: system with external input and system without external input.

Table 4.1. Basic parameters of the simulation

| Mass of every floor | Lateral stiffness | Damping ratio | Sampling frequency | Noise level | Data length |
|---|---|---|---|---|---|
| 100 kg | 1 MN/m | 3% | 200 Hz | 3% | 2000 data |

Table 4.2. Modal information for the overall structure

| Mode | 1st | 2nd | 3rd | 4th | 5th | 6th |
|---|---|---|---|---|---|---|
| Frequency (Hz) | 1.22 | 3.65 | 6.06 | 8.43 | 10.76 | 13.02 |
| Mode | 7th | 8th | 9th | 10th | 11th | 12th |
| Frequency (Hz) | 22.93 | 24.56 | 26.06 | 27.36 | 28.53 | 29.52 |

### 4.5.1 System with External Input

Figure 4.3 shows the corresponding feedback system of the three types of substructures. The substructure that needs to be identified can be regarded as the plant, and the other part of the structure can be regarded as the regulator. In this study, the regulator was assumed to be time invariant, linear, and noise-free, and thus $r = 1$.

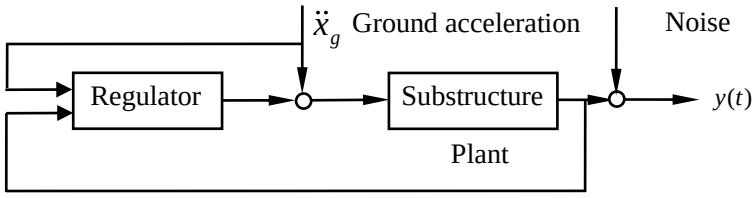


Figure 4.3. Feedback system with external signal

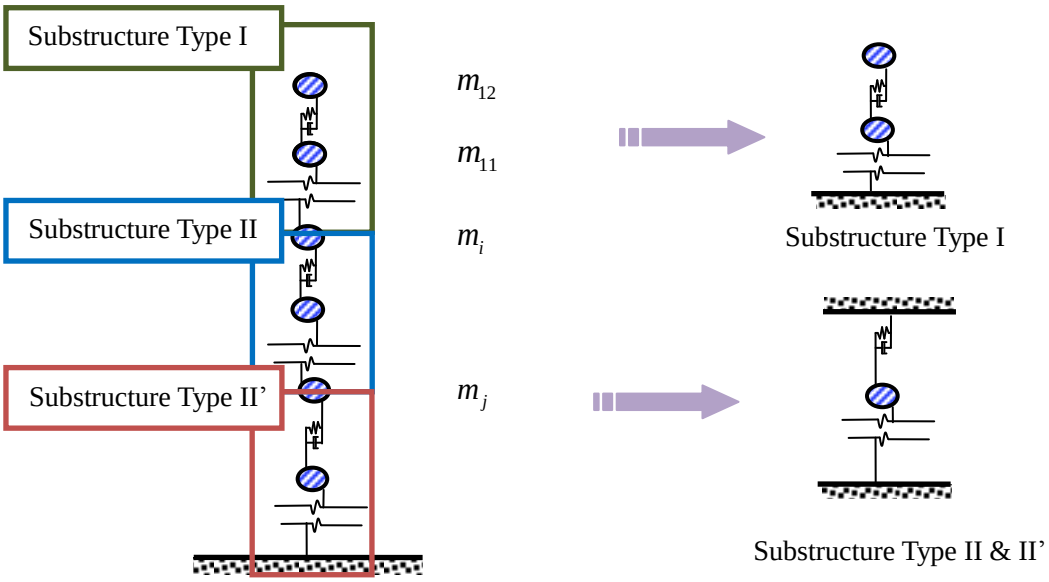


Figure 4.4. Substructure division

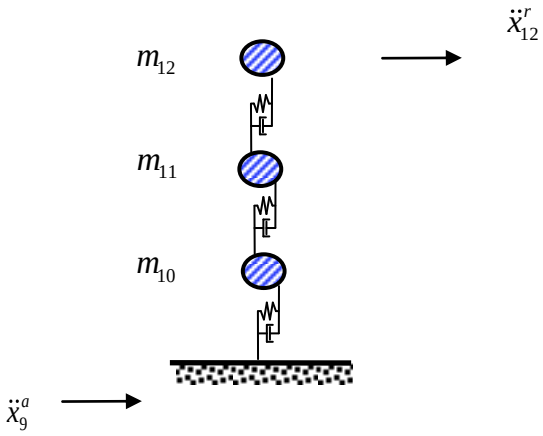


Figure 4.5. Substructure Type I with three DOFs (from 10th mass to 12th mass)

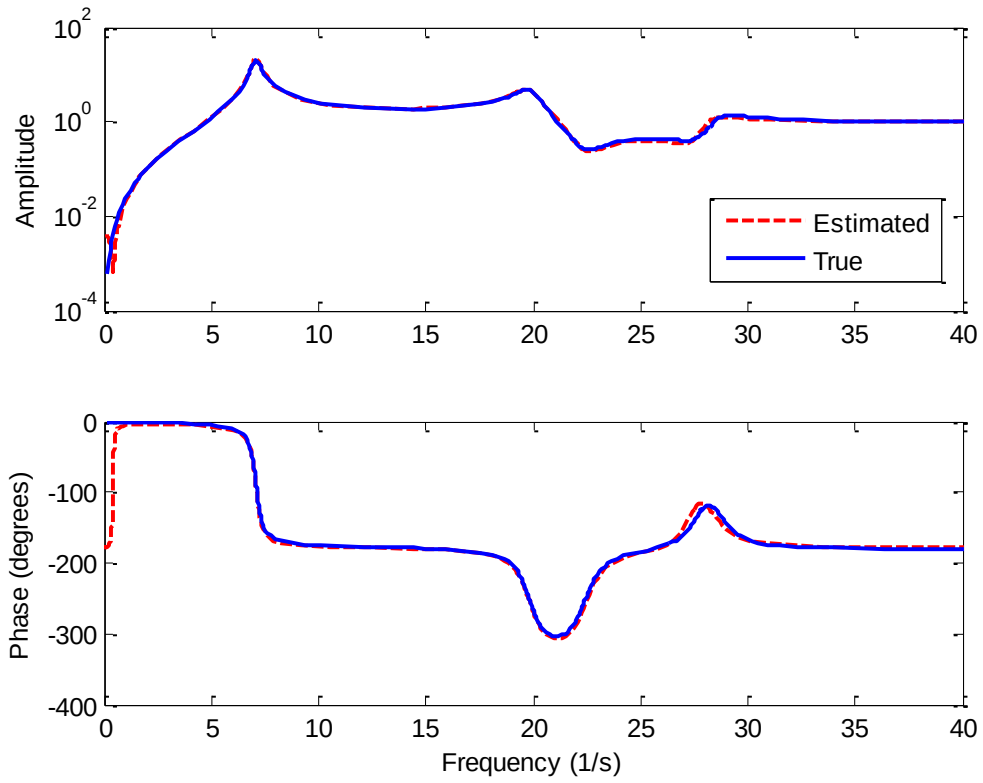


Figure 4.6. Parametric method for Substructure Type I with three DOFs (from 10th mass to 12th mass, $na=6, nb=8, nc=6$, and $nk=1$)

*Substructure Type I:* There is one external signal, which has the same dimension as the input signal and the output signal, i.e., $n_u = n_r = n_y = 1$, as shown in Figure 4.4 Here, only the results of Substructure Type I with three DOFs (Figure 4.5) are listed. The input of the ARMAX model is the absolute acceleration of the 9th mass ($\ddot{x}_9^a$), and the output is the acceleration of the 12th mass relative to the 9th mass ($\ddot{x}_{12}^r$). The orders of the ARMAX model are $na=6, nb=8, nc=6$, and $nk=1$. Figure 4.6 clearly shows that this substructure is identifiable. For this type of substructure, a substructure with any number of DOFs is identifiable if the number of independent external inputs is equal to the number of inputs to the substructure.

*Substructure Type II:* In this situation, the identifiability condition cannot be satisfied, which means that Substructure Type II is not identifiable since there is one external signal, two inputs, and one output of the plant, i.e., $n_u = 2, n_r = n_y = 1$. There are generally two methods to overcome this problem: adding different feedback laws or ensuring that the order of the regulator is higher than that of the plant. Here, the second method is more suitable, as it can be realized easily by ensuring the order of the rest of the structure higher than that of the substructure.

1) The Substructure Type II with four DOFs, including masses from the 2nd mass to the 5th mass (Figure 4.7) was studied. As this substructure includes the points from the 2nd mass to the 5th mass, the rest of the structure has a higher order than the substructure that can make the substructure system identifiable (SI). The absolute acceleration of the 1st ($\ddot{x}_1^a$) and the acceleration of the 6th mass relative to the 1st mass ($\ddot{x}_6^r$) are used as the inputs of the ARMAX model, and the acceleration of the 5th mass relative to the 1st mass ($\ddot{x}_5^r$) is used as the output of the ARMAX model. The orders of the ARMAX model are $na = 10$, $nb = [14,14]$, $nc = 8$, and $nk = [1,1]$. Table 4.3 lists the estimated modal frequencies of this substructure. Table 4.3 and Figure 4.8 show that this substructure is correctly identified.

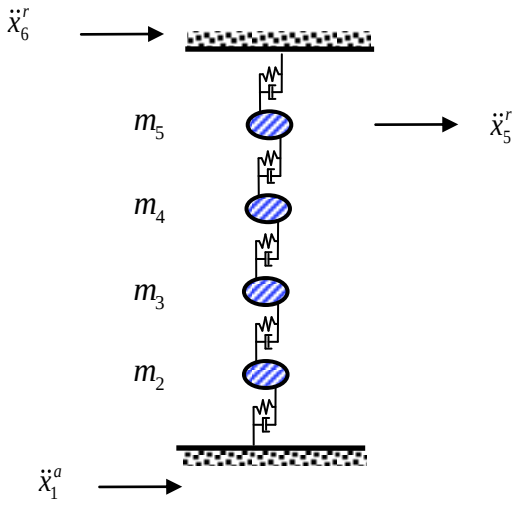


Figure 4.7. Substructure Type II with four DOFs (from 2nd mass to 5th mass)

Table 4.3. Estimated modal frequencies of Substructure Type II with four DOFs (from 2nd mass to 5th mass, $na = 10, nb = [14, 14], nc = 8$, and $nk = [1, 1]$)

| Mode | 1st | 2nd | 3rd | 4th |
|---|---|---|---|---|
| True Frequency (Hz) | 9.84 | 18.71 | 25.75 | 30.27 |
| Estimated Frequency (Hz) | 9.85 | 18.64 | 25.89 | 30.91 |

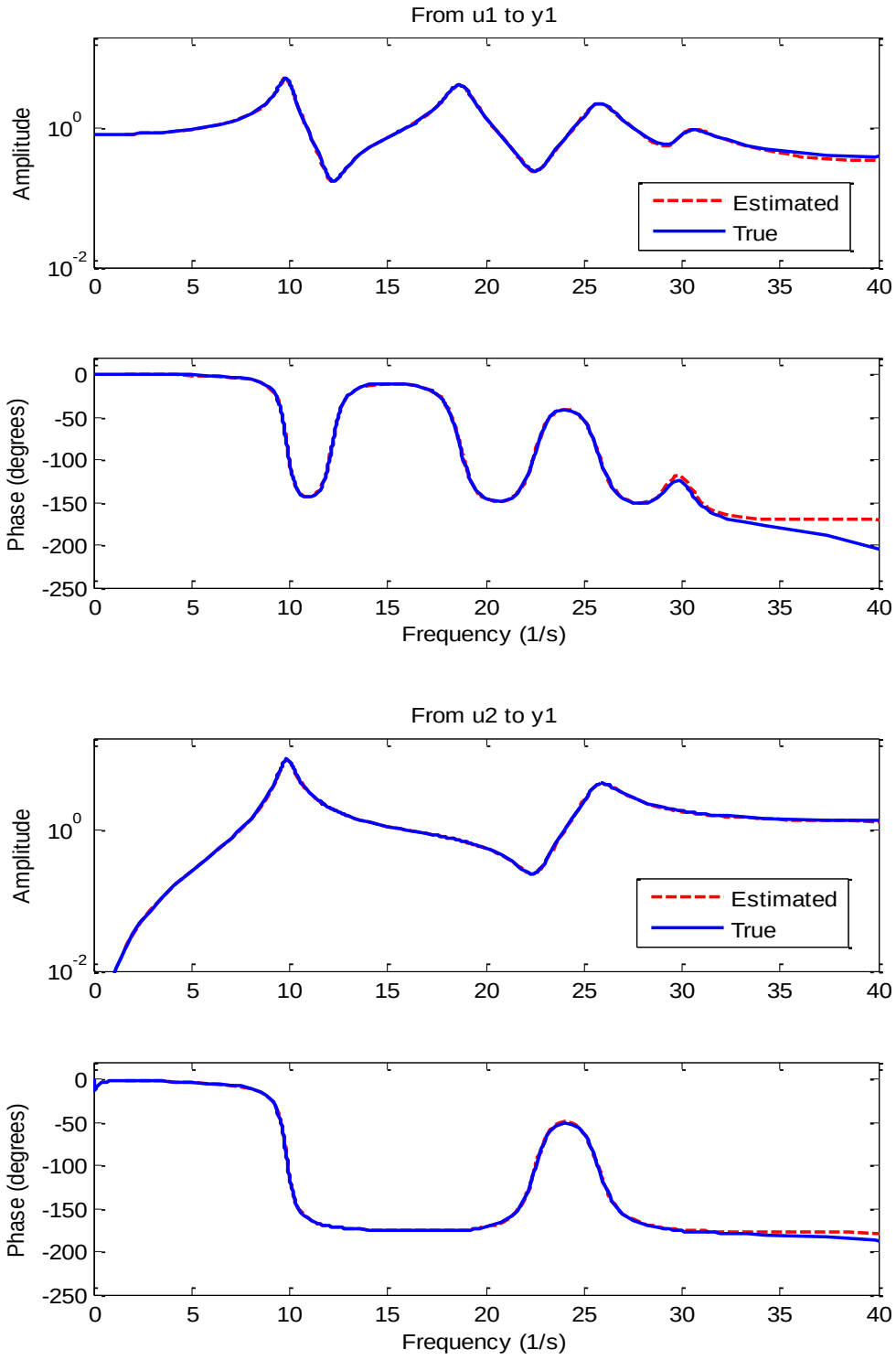


Figure 4.8. Parametric method for Substructure Type II with four DOFs (from 2nd mass to 5th mass, $na = 10, nb = [14, 14], nc = 8$, and $nk = [1, 1]$)

2) The Substructure Type II, which has five DOFs, as shown in Figure 4.9 was studied here. The rest of the structure has a lower order than the substructure since it has five DOFs (from 4th mass to 8th mass). The inputs are composed of the absolute acceleration of the 3rd mass ($\ddot{x}_3^a$) and the acceleration of the 9th mass relative to the 3rd mass ($\ddot{x}_9^r$). The acceleration of the 8th mass ($\ddot{x}_8^r$) is regarded as the output. The orders of the ARMAX model are $na = 10, nb = [14,14], nc = 8$, and $nk = [1,1]$. In Table 4.4, we can find that the identified second modal frequency has a big error and third, fourth and fifth modal frequencies cannot be identified. Table 4.4 and Figure 4.10 clearly show that the parametric method fails to identify this substructure.

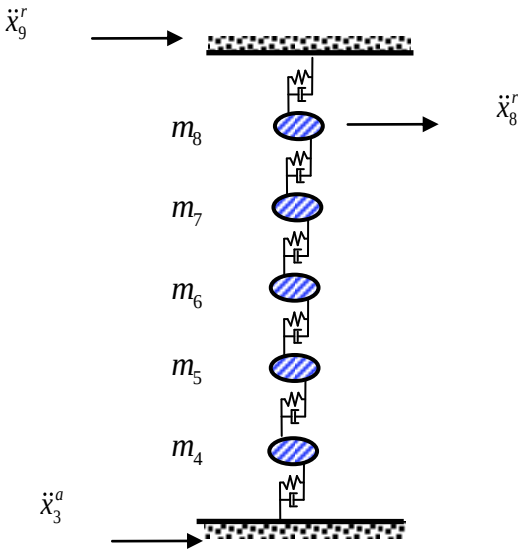


Figure 4.9. Substructure Type II with five DOFs (from 4th mass to 8th mass)

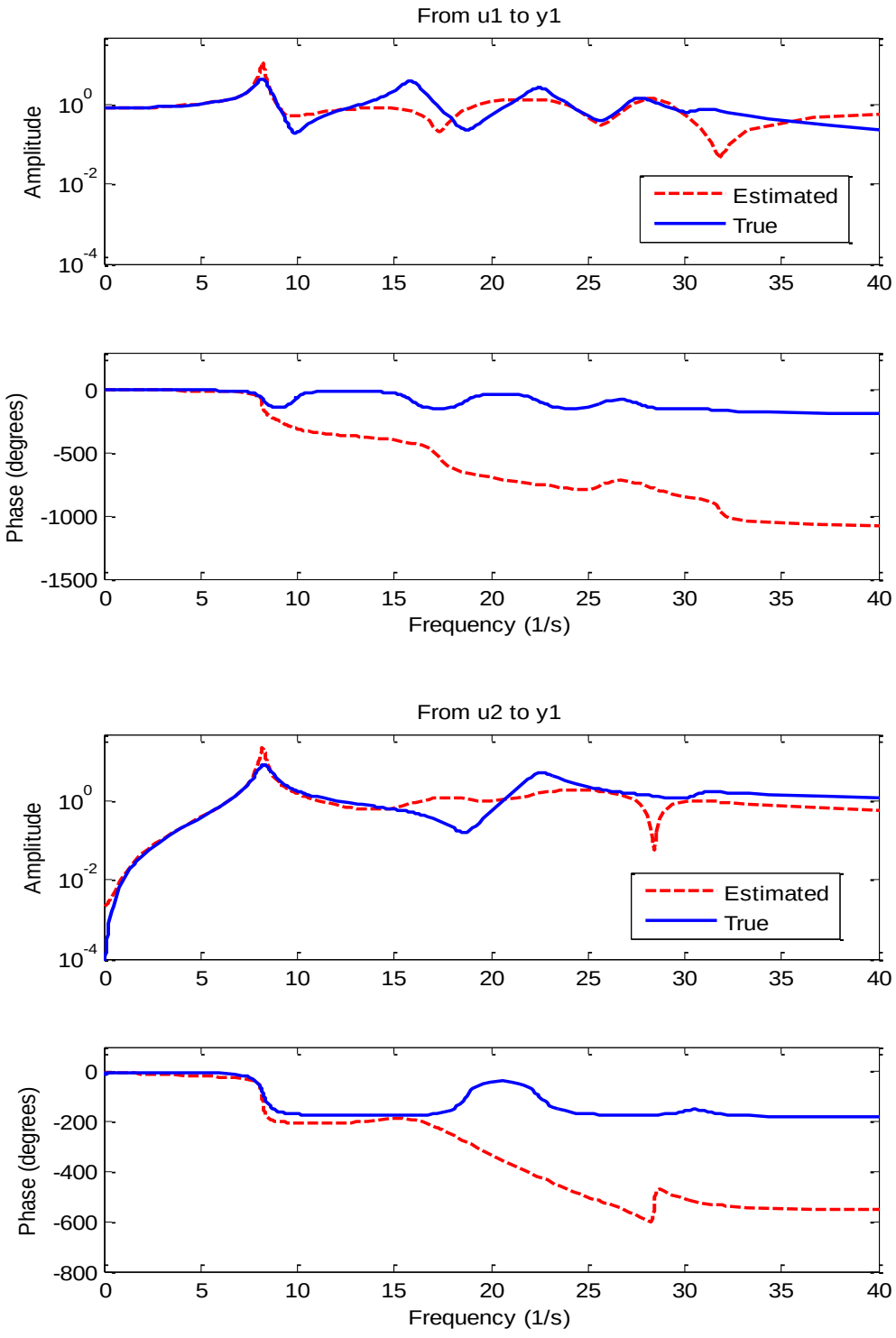


Figure 4.10. Parametric method for Substructure Type II with five DOFs (from 2nd mass to 5th mass, $na = 10, nb = [14, 14], nc = 8$, and $nk = [1, 1]$)

Table 4.4. Estimated modal frequencies of Substructure Type II (from 4th mass to 8th mass, $na = 10, nb = [14,14], nc = 8$, and $nk = [1,1]$)

| Mode | 1st | 2nd | 3rd | 4th | 5th |
|---|---|---|---|---|---|
| True Frequency (Hz) | 8.24 | 15.92 | 22.51 | 27.57 | 30.75 |
| Estimated Frequency (Hz) | 8.21 | 28.39 | | | |

It can be concluded that if the identifiability condition cannot be satisfied, the system is not SSI; however, it can be SI if the order of the regulator is higher than that of the plant.

*Substructure Type II':* In this situation, similar to Substructure Type II, Substructure Type II' cannot satisfy the identifiability condition.

1) The Substructure Type II' with four DOFs, from the 1st mass to the 4th mass (Figure 4.11) was studied. As this substructure includes the points from the 1st mass to the 4th mass, the rest of the structure has a higher order than the substructure that can make the substructure system identifiable (SI). The ground acceleration ($\ddot{x}_g$) and the acceleration of the 5th mass relative to the ground ($\ddot{x}_5^r$) are used as the inputs of the ARMAX model, and the acceleration of the 4th mass relative to the ground ($\ddot{x}_4^r$) is used as the output of the ARMAX model. The orders of the ARMAX model are $na = 10$, $nb = [12,12]$, $nc = 8$, and $nk = [1,1]$. Table 4.5 lists the estimated modal frequencies of this substructure and Figure 4.12 shows the result of parametric method for Substructure Type II' with four DOFs. From the results as shown in Table 4.3 and Figure 4.12, it is clear that this substructure is identifiable.

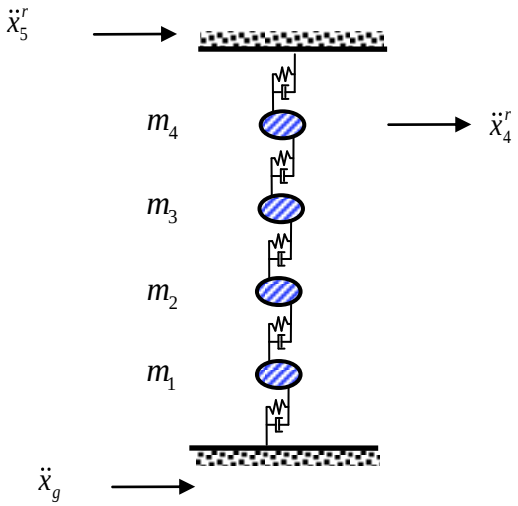


Figure 4.11. Substructure Type II' with four DOFs (from 1st mass to 4th mass)

Table 4.5. Estimated modal frequencies of Substructure Type II' with four DOFs (from 1st mass to 4th mass, $na = 10, nb = [12, 12], nc = 8$, and $nk = [1, 1]$)

| Mode | 1st | 2nd | 3rd | 4th |
|---|---|---|---|---|
| True Frequency (Hz) | 9.84 | 18.71 | 25.75 | 30.27 |
| Estimated Frequency (Hz) | 9.80 | 18.69 | 25.70 | 30.35 |

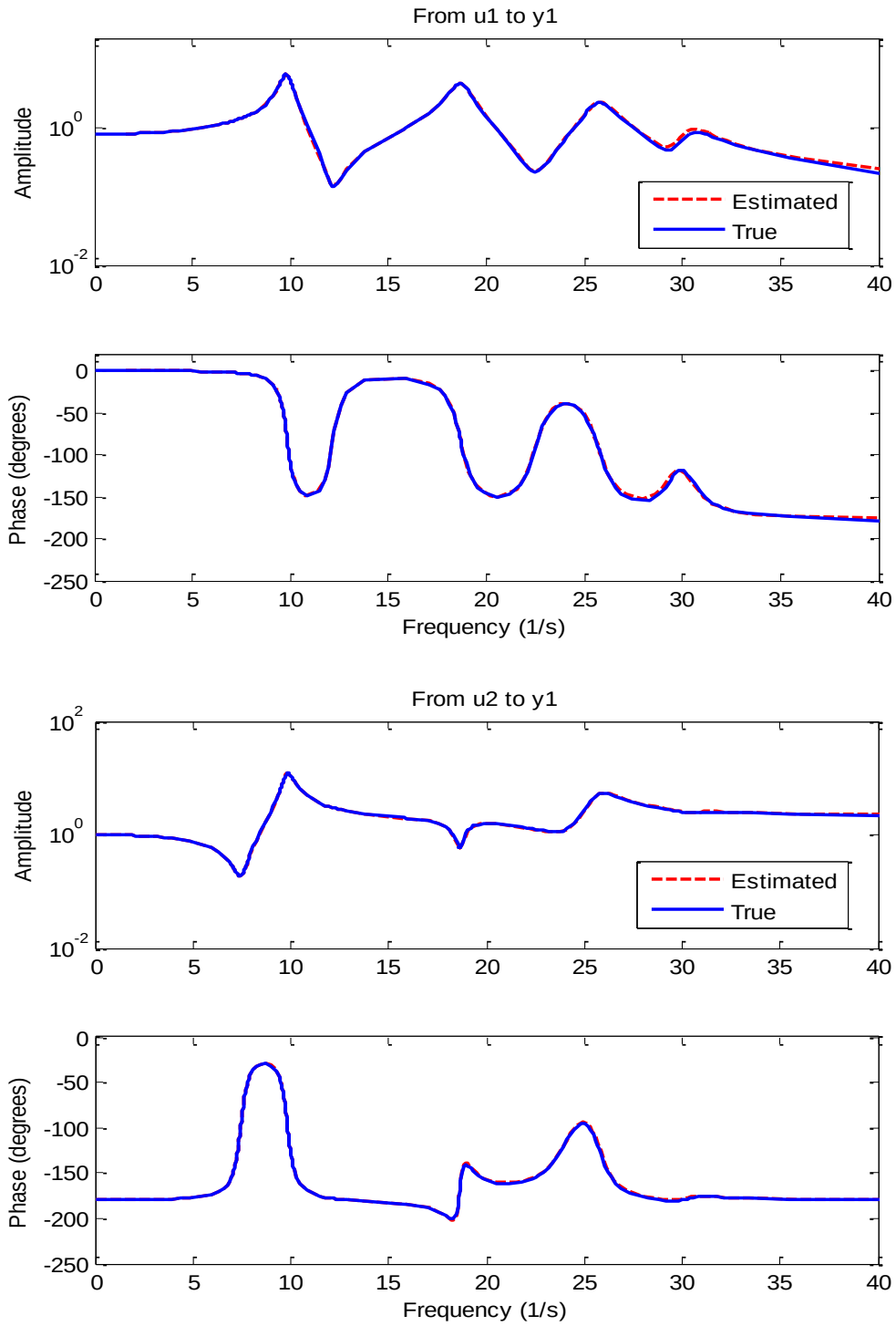


Figure 4.12. Parametric method for Substructure Type II' with four DOFs (from 1st mass to 4th mass, $na = 10, nb = [12, 12], nc = 8$, and $nk = [1, 1]$)

The Substructure Type II' with seven DOFs, from the 1st mass to the 7th mass (Figure 4.13) was studied. This substructure includes the points from the 1st mass to the 7th mass which means the rest of the structure has a lower order than the substructure. The ground acceleration ($\ddot{x}_g$) and the acceleration of the 8th mass relative to the ground ($\ddot{x}_8^r$) are used as the inputs of the ARMAX model, and the acceleration of the 7th mass relative to the ground ($\ddot{x}_7^r$) is used as the output of the ARMAX model. The orders of the ARMAX model are $na = 16$, $nb = [18, 18]$, $nc = 8$, and $nk = [1, 1]$. Table 4.6 lists the estimated modal frequencies of this substructure and Figure 4.14 shows the result of parametric method for Substructure Type II' with seven DOFs. In Table 4.6, the estimated modal frequencies have big errors when compared with the true value. From the results as shown in Table 4.6 and Figure 4.14, it is clear that this substructure is unidentifiable.

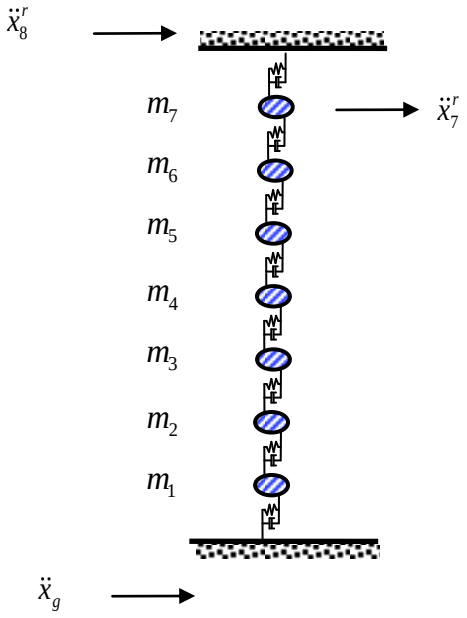


Figure 4.13. Substructure Type II' with seven DOFs (from 1st mass to 7th mass)

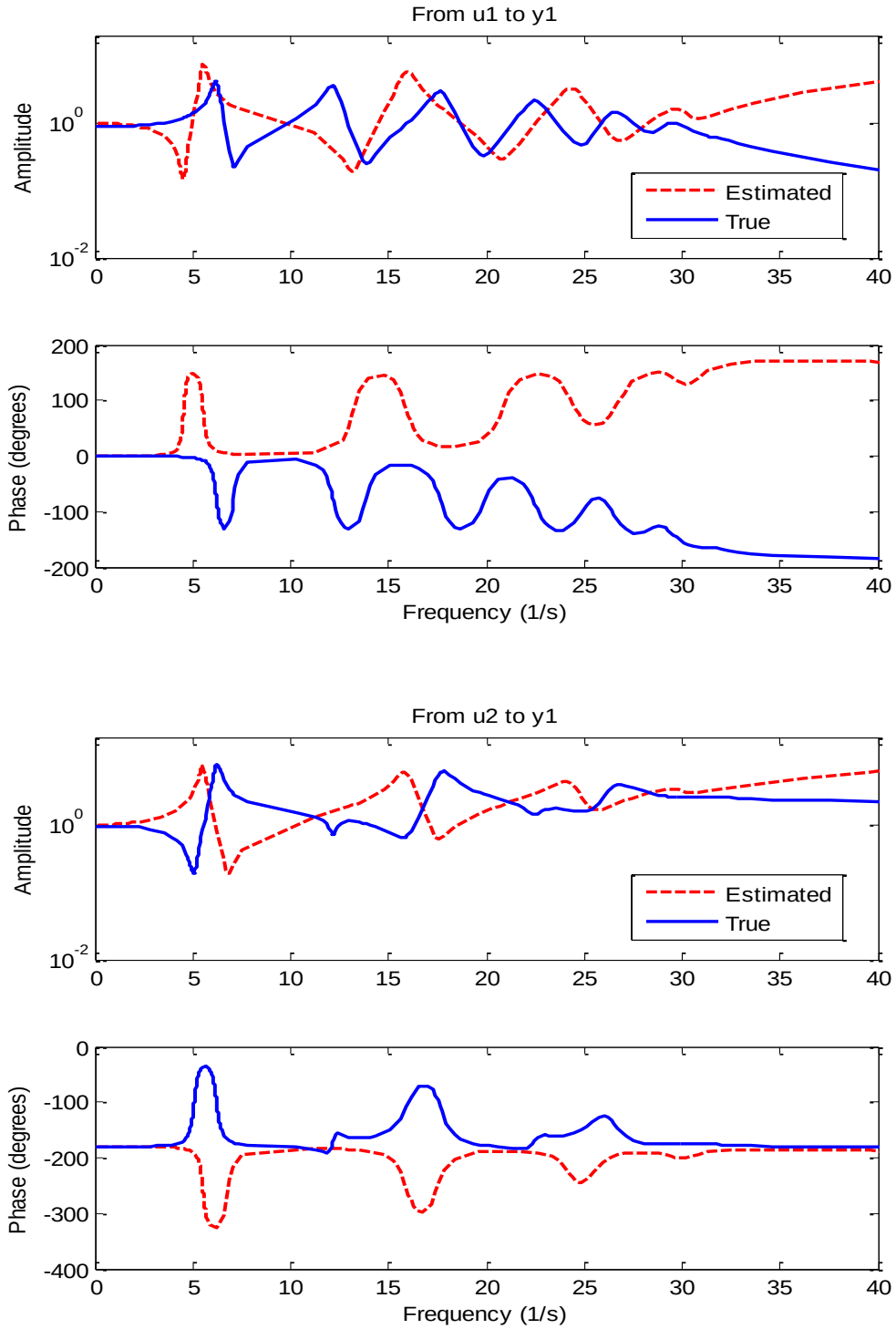


Figure 4.14. Parametric method for Substructure Type II' with seven DOFs (from 1st mass to 7th mass, $na = 16, nb = [18, 18], nc = 8$, and $nk = [1, 1]$)

Table 4.6. Estimated modal frequencies of Substructure Type II' with seven DOFs (from 1st mass to 7th mass, $na = 16, nb = [18, 18], nc = 8$, and $nk = [1, 1]$)

| Mode | 1st | 2nd | 3rd | 4th | 5th | 6th | 7th |
|---|---|---|---|---|---|---|---|
| True Frequency (Hz) | 6.21 | 12.18 | 17.68 | 22.51 | 26.47 | 29.41 | 31.22 |
| Estimated Frequency (Hz) | 5.53 | 15.91 | 24.39 | 29.91 | 49.31 | | |

If the identifiability condition cannot be satisfied, the system is not SSI; however, it can be SI if the order of the regulator is higher than that of the plant. This conclusion for Substructure Type II' is same as that for Substructure Type II, because Substructure Type II' is a special case of Substructure Type II.

### 4.5.2 System without External Input

Figure 4.15 shows the corresponding feedback system of the three types of substructures when there is no external signal. As there is no external signal $n_r = 0$, Equation (4.8) can be written as:

$$r \geq 1 + n_u / n_y \tag{4.10}$$

In this case, similar results to that of the case can be obtained when there is external input. The regulator with a higher order is used to guarantee the system identifiability of the substructure. For Substructure Type I, it is no longer true that Substructure Type I with any number of DOFs is identifiable. Table 4.7 and Table 4.8 list the estimated modal frequencies of Substructure Type I with three DOFs and six DOFs, respectively.

For Substructure Type I with three DOFs, the absolute acceleration of the 9th mass ($\ddot{x}_9^a$)

and the acceleration of the 12th mass relative to the 9th mass ($\ddot{x}_{12}^{r}$) are chosen as the input and output of the ARMAX model, respectively. The orders of the ARMAX model are $na = 8, nb = [12,12], nc = 8$, and $nk = [1,1]$. Table 4.7 and Figure 4.17 clearly show that the Substructure Type I with three DOFs is identifiable.

For Substructure Type I with six DOFs, the absolute acceleration of the 6th mass ($\ddot{x}_{6}^{a}$) and the acceleration of the 12th mass relative to the 6th mass ($\ddot{x}_{12}^{r}$) were chosen as the respective input and output of the ARMAX model. The orders of the ARMAX model are $na = 12$, $nb = [14,14]$, $nc = 8$, and $nk = [1,1]$. Table 4.8 indicates that the identified results have big errors and the 4th, 5th and 6th mode frequencies cannot be identified. Moreover, Figure 4.19 also shows that Substructure Type I with six DOFs is unidentifiable. The study indicated that Substructure Type I, with more than half of all the DOFs, is not identifiable when the system has no external input.

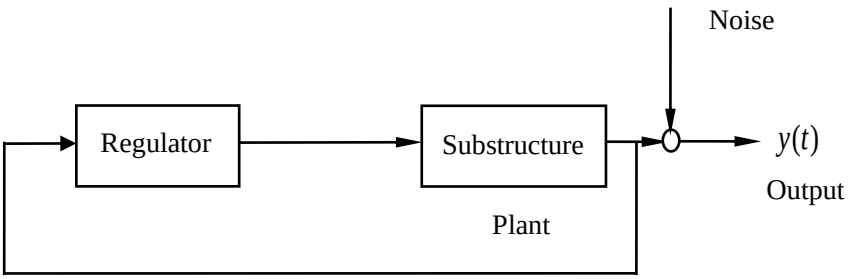


Figure 4.15. Feedback system without external signal

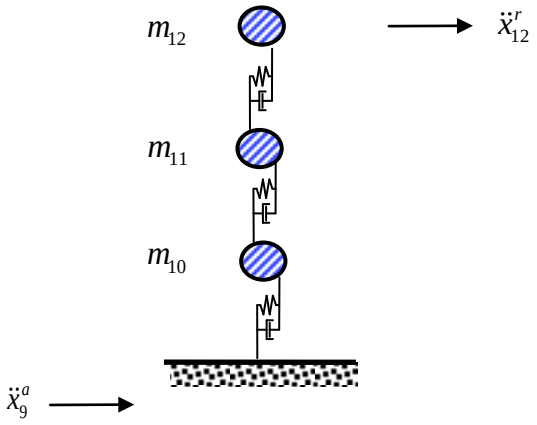


Figure 4.16. Substructure Type I with three DOFs (from 10th mass to 12th mass)

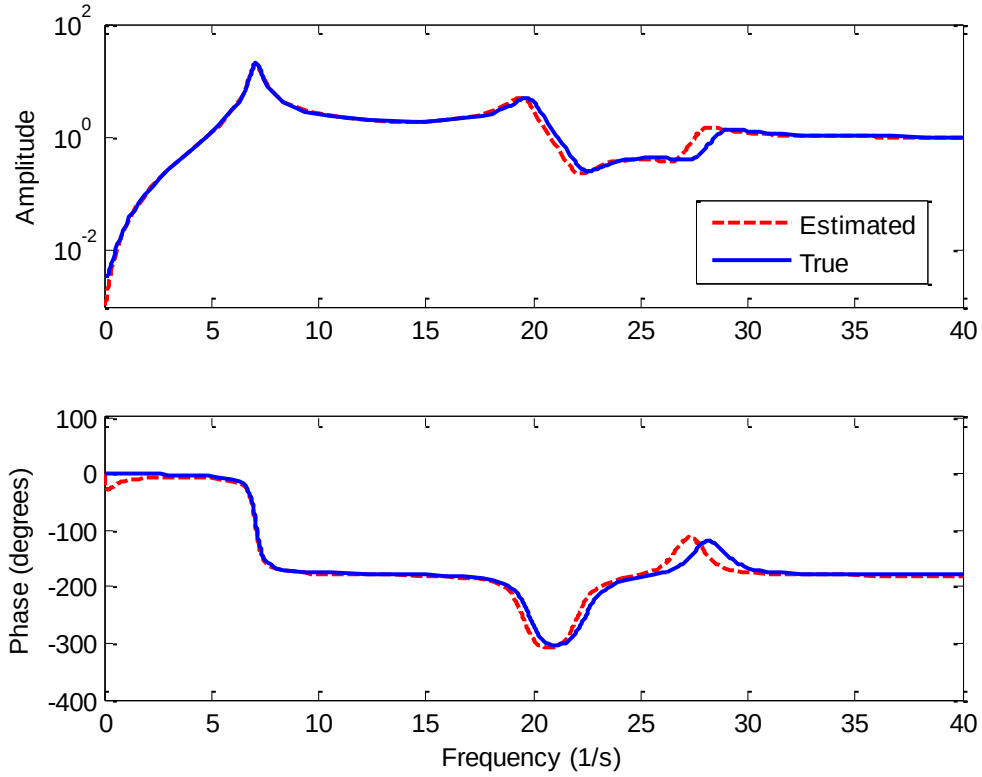


Figure 4.17. Parametric method for Substructure Type I with three DOFs (from 10th mass to 12th mass, $na = 8, nb = [12, 12], nc = 8$ and $nk = [1, 1]$)

Table 4.7. Estimated modal frequencies of Substructure Type I with three DOFs (from 10th mass to 12th mass, $na = 8, nb = [12, 12], nc = 8$, and $nk = [1, 1]$)

| Mode | 1st | 2nd | 3rd |
|---|---|---|---|
| True Frequency (Hz) | 7.08 | 19.85 | 28.68 |
| Estimated Frequency (Hz) | 7.07 | 19.53 | 27.75 |

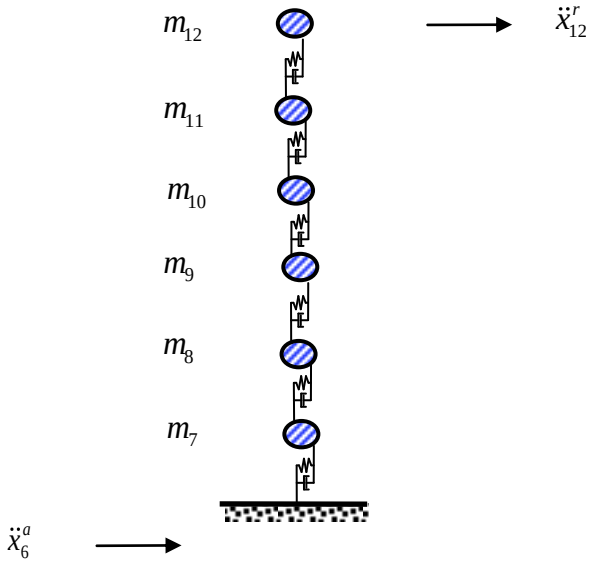


Figure 4.18. Substructure Type I with six DOFs (from 7th mass to 12th mass)

Table 4.8. Estimated modal frequencies of Substructure Type I with six DOFs (from 7th mass to 12th mass, $na = 12, nb = [14, 14], nc = 8$, and $nk = [1, 1]$)

| | 1st | 2nd | 3rd | 4th | 5th | 6th |
|---|---|---|---|---|---|---|
| True Frequency (Hz) | 3.84 | 11.29 | 18.08 | 23.83 | 28.18 | 30.91 |
| Estimated Frequency (Hz) | 11.24 | 21.42 | 29.78 | | | |

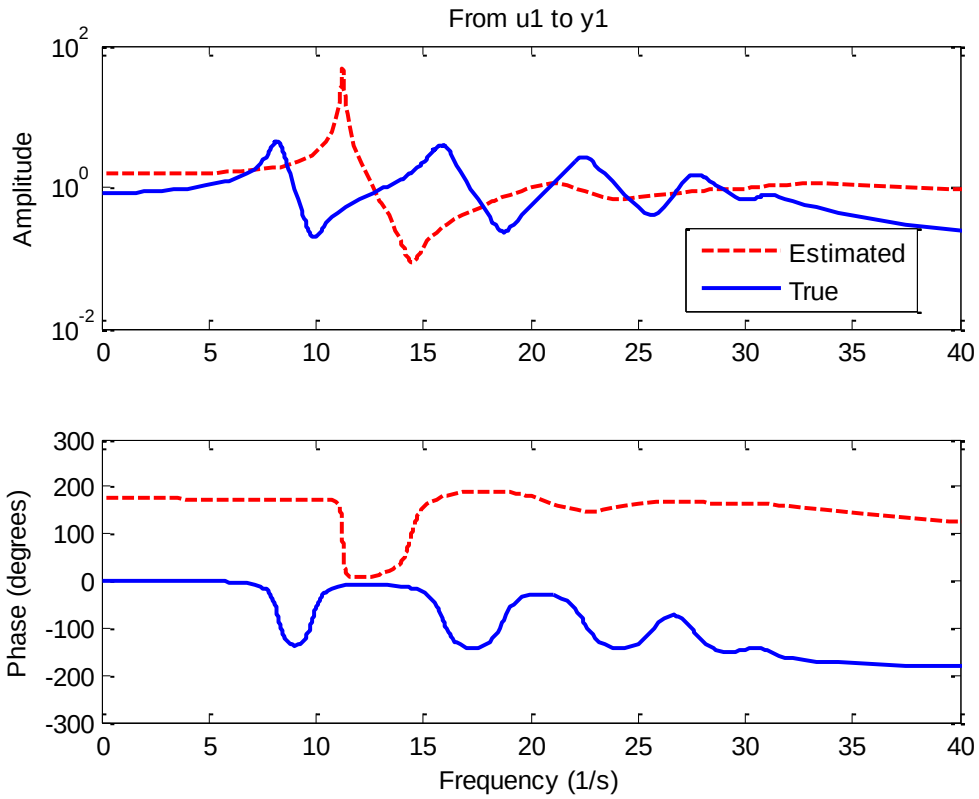


Figure 4.19. Parametric method for Substructure Type I with six DOFs (from 6th mass to 12th mass, $na = 12, nb = [14, 14], nc = 8$, and $nk = [1, 1]$)

## 4.6 Conclusions

In this chapter, the identifiability of substructures was carefully studied in cases of forced vibration and free vibration, and a structure division method was proposed to make the substructure identifiable when it is not strongly system identifiable (SSI). In the case of forced vibration, Substructure Type I is always identifiable if the number of independent external inputs is equal to the number of inputs to the system. As for the substructures type II and II', they are unidentifiable unless the order of the rest of the structure is higher than that of the substructure. In the case of free vibration, Substructure Type I, with more than half of all of the DOFs, is unidentifiable. The conclusions obtained from substructures type II and II' are similar in cases of forced

and free vibration. It must be noted that a regulator that has a higher order than the substructure can make the substructure system identifiable. Moreover, it was found that a substructure with more DOFs deteriorated the accuracy of the identification. If accuracy is a more important factor in identification, it is recommended that the substructures have as few DOFs as possible.

# *CHAPTER 5*

# Damage Detection Using Substructure Approach and Support Vector Machine

## 5.1 Introduction

In this chapter, a substructure algorithm is used to divide a complete structure into substructures to overcome the problems of data measurement and identification for large scale civil structure. As a substructure has a considerably smaller number of DOFs when compared with the entire structure, analyzing the substructure is quick and simple. Moreover, the structure division method proposed in Chapter 4 is used to ensure the identifiability of the substructures. As for substructures, a method using the support vector machine (SVM) to detect local damages in a shear structure with at most three sensors was proposed. The modal frequencies are used for forming feature vectors for pattern recognition.

## 5.2 Sensitivity of Modal Frequency Change to Damage

Existence of damage in a structure leads to changes of the vibration modes, which are

manifested as changes in the modal parameters (natural frequency, mode shape and damping value) (Stubbs, Kim et al. 1992; Salawu and Williams 1995; Sampaio, Maia et al. 1999; Ren and De Roeck 2002; Kim, Ryu et al. 2003; Maia, Silva et al. 2003). The use of changes in modal frequencies is feasible for damage detection because the modal frequencies can be quickly obtained and are often reliable. Moreover, it was shown that multiple modal frequency changes provide information on the location of damaged stories (Zhao and DeWolf 1999; Mita and Hagiwara 2003). For a multi-mass shear structure, the equilibrium equation for an undamped structure is given by

$$(-\omega_r^2[\mathbf{M}]+[\mathbf{K}])\{\phi\}_r = \{0\} \tag{5.1}$$

where $r$=1, 2, ⋯, $N$, **M** and **K** are mass and stiffness matrices, respectively. $\{\phi\}_r$ is the $r$-th mode shape corresponding to the modal frequency $\omega_r$ and is normalized to $\{\phi\}_r^T[\mathbf{M}]\{\phi\}_r = 1$. The sensitivity coefficient of the $r$-th modal frequency in terms of $k_{ij}$ can be obtained by the derivative of Equation (5.1) with respect to $k_{ij}$, where $k_{ij}$ is the element of the stiffness matrix.

$$\frac{\partial \omega_r}{\partial k_{ij}} = \frac{1}{2\omega_r}\{\phi\}_r^T \frac{\partial [K]}{\partial k_{ij}}\{\phi\}_r \tag{5.2}$$

If the symmetry of stiffness matrix is taken into consideration, the sensitivity coefficients can be rewritten as

$$\frac{\partial \omega_r}{\partial k_{ij}} = \begin{cases} \dfrac{1}{\omega_r}\phi_{ir}\phi_{jr}, & i \neq j \\ \dfrac{1}{2\omega_r}\phi_{ir}^2, & i = j \end{cases} \tag{5.3}$$

where $\phi_{ir}$ is $i$-th component of the $r$-th mode shape. This equation can be expanded using Taylor series and only the first order terms represents the change in modal

frequency is used, which can be written as

$$\Delta\omega_r = \sum_{i=1}^{N}\sum_{i=1}^{N}\frac{\partial\omega_r}{\partial k_{ij}}\Delta k_{ij} \tag{5.4}$$

When the $i^{\text{th}}$ story stiffness is reduced, only $k_{ii}$, $k_{(i-1)(i-1)}$, $k_{i(i-1)}$ and $k_{(i-1)i}$ are changed in the stiffness matrix. Hence Equation (5.4) can be simplified into

$$\frac{\Delta\omega_r}{\omega_r} = \frac{\Delta k_i}{2\omega_r^2}(\phi_{ir} - \phi_{(i-r)r})^2 \tag{5.5}$$

Equation (5.5) will be used for forming feature vectors for SVM based damage detection. More details can be found in Ref. (Mita and Hagiwara 2003)

## 5.3 Support Vector Machine

Support Vector Machine is a supervised learning method that analyzes data and recognizes patterns, used for classification and regression analysis (Mita and Hagiwara 2003). The SVM algorithm was invented by Vapnik (1995) and the current standard incarnation (soft margin) was proposed by Cortes and Vapnik (1995). A support vector machine constructs a hyperplane or set of hyperplanes in a high or infinite dimensional space, which can be used for classification, regression or other tasks. Intuitively, a good separation is achieved by the hyperplane that has the largest distance to the nearest training data points of any class, as in general the larger the margin the lower the generalization error of the classifier.

A training data $D$, a set of *n* points of the form

$$D = \left\{(x_i, y_i) \mid x_i \in R^n, y_i \in \{-1, 1\}\right\}_{i=1}^{n} \tag{5.6}$$

where the $y_i$ is either 1 or −1, indicating the class to which the point $x_i$ belongs.

Hyperplane can be written as

$$\mathbf{w}^T\mathbf{x} - b = 0 \tag{5.7}$$

where $\mathbf{w}$ is a normal vector, and it is perpendicular to the hyperplane.

Then, to find the maximum-margin hyperplane that divides the two classes. The example is shown in Figure 5.1. The proper $\mathbf{w}$ and $b$ can be chosen to maximize the margin, or distance between the parallel hyperplanes that are as far apart as possible and still separating the data. The optimization problem can be explained as

$$\begin{gathered}\min_{w}\left\{\frac{1}{2}\|\mathbf{w}\|^2\right\} \\ \text{subject to } y_i(\mathbf{w}^T\mathbf{x_i} - b) \geq 1, \quad i = 1, 2, \ldots, \text{n}\end{gathered} \tag{5.8}$$

This kind of SVM is called Hard Margin SVM because no error is allowed. However, such SVMs can be used only for a limited number of problems. In order to relax the situation, the Soft Margin method is used, which will choose a hyperplane that splits the examples as good as possible, and still maximizes the distance to the nearest split examples. The method introduces slack variables, $\xi_i$, which measure the degree of misclassification of the data $x_i$, and thus the optimization problem becomes

$$\begin{gathered}\min_{\mathbf{w},\xi}\left\{\frac{1}{2}\|\mathbf{w}\|^2 + C\sum_{i=1}^{n}\xi_i\right\} \\ \text{subject to } y_i(\mathbf{w}^T\mathbf{x_i} - b) \geq 1 - \xi_i, \quad i = 1, 2, \ldots, \text{n}, \xi_i \geq 0\end{gathered} \tag{5.9}$$

The purpose of the term $C\sum_{i=1}^{n}\xi_i$ is to keep the number of misclassified vectors under control.

The optimal hyperplane algorithm introduced above is a linear classifier. Whereas the original problem may be stated in a finite dimensional space, it often happens that in

that space the sets to be discriminated are not linearly separable. For this reason, the nonlinear classifiers are introduced by applying the kernel trick to maximum-margin hyperplanes. SVM schemes use a mapping into a larger space so that cross products may be computed easily in terms of the variables in the original space making the computational load reasonable. The cross products in the larger space are defined in terms of a kernel function which can be selected to suit the problem. In this study, the Gaussian kernel, Equation (5.10), was adopted.

$$K(x, x_i) = \exp(-\frac{\|x - x_i\|^2}{2\sigma}) \tag{5.10}$$

where $\sigma$ is the width parameter, which needs to be determined before the SVM is trained.

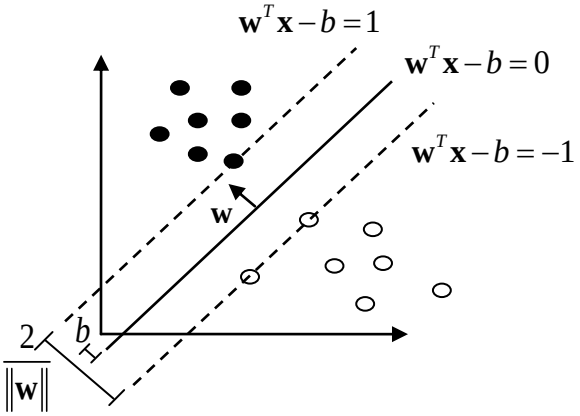


Figure 5.1. Maximum-margin hyperplane

## 5.4 Numerical Verification

A six-story shear structure was studied, and it was simplified into a 6-DOF lumped mass shear model. The mass of every floor and the lateral stiffness are 100 kg and 1

MN/m, respectively. The damping ratio for all modes is 3%. The data sampling frequency is 200 Hz. The noise level added into the acceleration is 3%. Gaussian white noise is used to simulate the ground acceleration. The story stiffness reduction was regarded as damage to the structure. Six cases of damage (damage in the 1st, 2nd, 3rd, 4th, 5th and 6th stories) with five different damage severities (10%, 20%, 30%, 40% and 50% lateral stiffness reduction) were studied. Therefore, there are 30 different damage scenarios totally. Table 5.1 and Table 5.2 list the basic information of the simulation and the modal frequencies of the overall structure.

Substructure approach was used to divide the structure into substructures, which have considerably smaller number of degrees of freedom (DOFs) when compared with the entire structure. By using the structure division method proposed in Chapter 4, the whole structure was divided into two substructures, Substructure I and Substructure II, with overlap, as shown in Figure 5.2 . According to the identifiability of substructure investigated in Chapter 4, Substructure I with any number of DOFs is identifiable if the number of independent external inputs is equal to the number of inputs to the substructure, and Substructure II can be identifiable on condition that the order of the regulator is higher than that of the plant. It is clear that the Substructure I, which consists of masses from 3rd to 6th, and Substructure II, which consists of masses from 1st to 2nd, are absolutely identifiable.

Equation (5.5) is used to construct the feature vectors. The frequency change vectors of different levels of damages in a single story are plotted in Figure 5.3 and Figure 5.4 for Substructure I and Substructure II, respectively. The damage severity varies in the way of story stiffness reduction from 10% to 50%. Figure 5.3 and Figure 5.4 show that the frequency change vectors can provide information on the location of damaged stories clearly. Frequency change vectors, which corresponding to 10%, 30% and 50% story stiffness reduction for each story, are used for training.

SVMs are defined:

*For Substructure I*, 3rd story damage (SVM3), 4th story damage (SVM4), 5th story damage (SVM5), 6th story damage (SVM6) and no story damage (SVM0I).

*For Substructure II*, 1st story damage (SVM1), 2nd story damage (SVM2) and no story damage (SVM0II).

The SVM0I and SVM0II can classify the frequency vectors for the undamaged substructure. This SVM can show whether the damage exists in the substructure. SVM*i* classifies the frequency change vectors for the substructure with damage in *i*-th story, where *i*=1, 2, ⋯, 6.

The tests were conducted by assuming five damage severities, 10%, 20%, 30%, 40% and 50% story stiffness reduction for each story. The damage cases from 1 to 5 are corresponding to 10%, 20%, 30%, 40% and 50% story stiffness reduction in the first story. Similarly, damage cases from 6 to 10 are corresponding to 10%, 20%, 30%, 40% and 50% story stiffness reduction in the second story. Figure 5.5 and Figure 5.6 plot the outputs from the SVM*i* (*i*=1, 2, ⋯, 6). The positive output from SVM*i* means the tested frequency change vectors is classified into *i*-th class and the negative outputs mean the tested frequency change vectors should be classified into other classes. From Figure 5.5 and Figure 5.6, the damage can be localized easily.

Table 5.1. Basic parameters of 6-DOF lumped mass shear model

| Mass of every floor | Lateral stiffness | Damping ratio | Sampling frequency | Noise level | Data length |
|---|---|---|---|---|---|
| 100 kg | 1 MN/m | 3% | 200 Hz | 3% | 2000 data |

Table 5.2. Modal information for 6-DOF lumped mass shear model

| Mode | 1st | 2nd | 3rd | 4th | 5th | 6th |
|---|---|---|---|---|---|---|
| Frequency (Hz) | 3.84 | 11.29 | 18.08 | 23.83 | 28.18 | 30.91 |

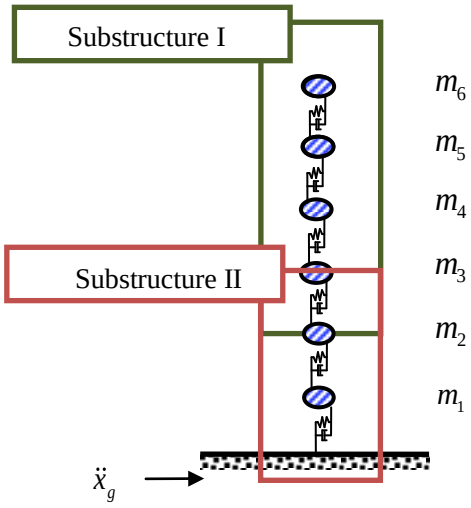


Figure 5.2. Structure division for 12-DOF structural system

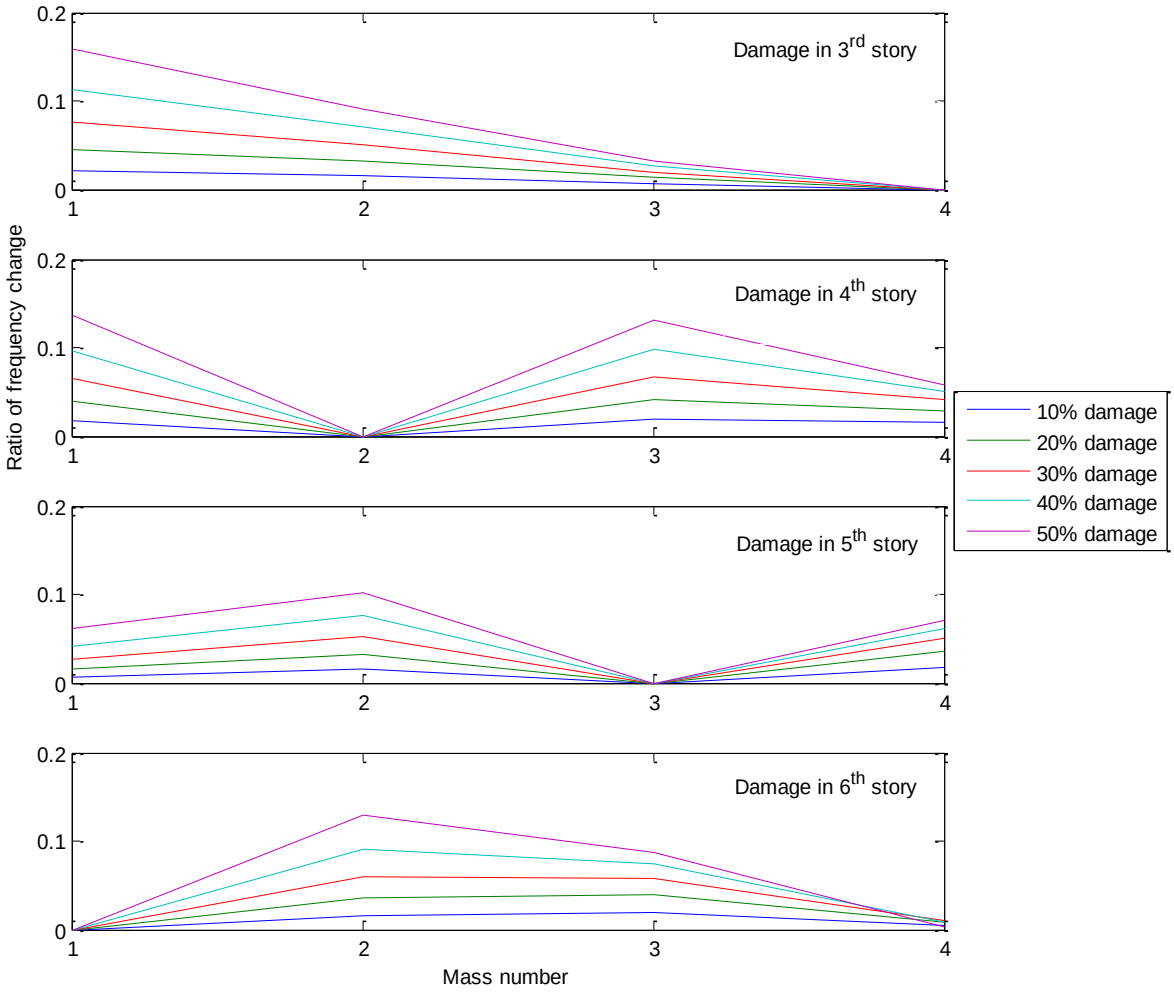


Figure 5.3. Frequency change vectors for Substructure I

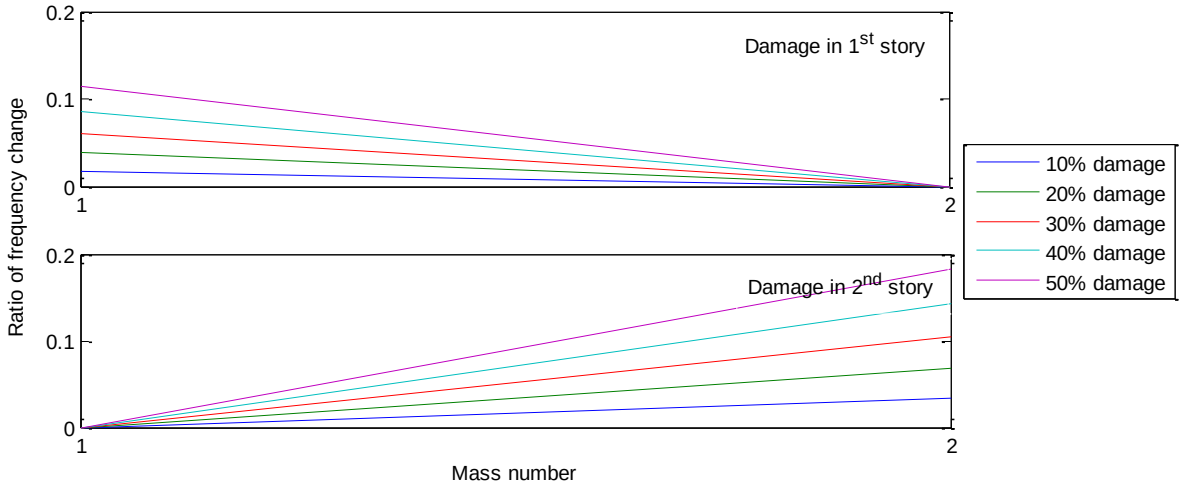


Figure 5.4. Frequency change vectors for Substructure II

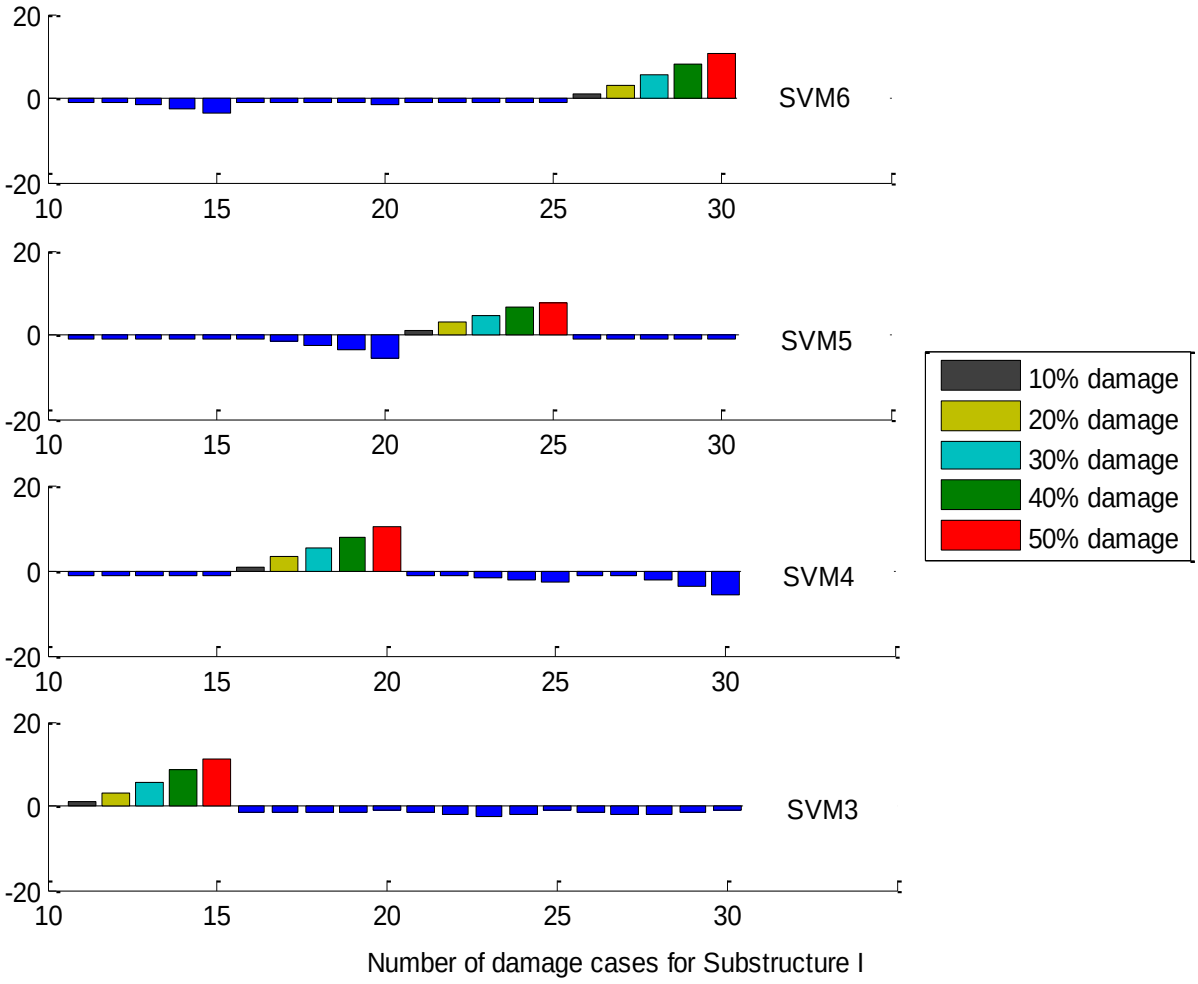


Figure 5.5. Output from SVM for Substructure I

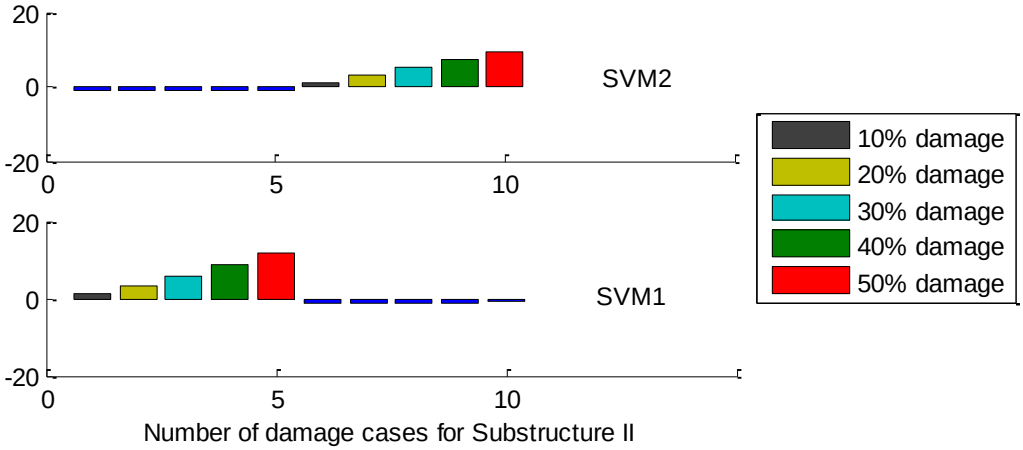


Figure 5.6. Output from SVM for Substructure II

## 5.5 Conclusions

In this chapter, substructure approach was applied to divide the structure into substructures, which have considerably smaller number of degrees of freedom (DOFs) when compared with the entire structure. The use of SVM simplifies the process of damage detection further. It was found that the frequency change vectors are very sensitive to the damage in stories, and the method combing the substructure approach and the SVM needs fewer sensors to localize the damage, meanwhile the accuracy of the identification results is satisfactory. As the use of SVM method, at most three sensors are needed to detect the damage for multiple-mass substructure, and only two sensors are needed for the top multiple-mass substructure. This can reduce the sensors needed to detect the damage of the whole structure significantly. Similar to the method proposed in the Chapter 3, this method needs to ensure the identifiability of the substructure. The identifiability of substructure must be paid more attention.

# *CHAPTER 6*
# Conclusions

The main contributions of this thesis are that it made improvements on the damage assessment based on autoregressive models and substructure approach. It introduced an effective damage detection method with fewer sensors. The proposed method is suitable for use in a parallel and distributed damage detection system and can work more efficiently for large scale structures. The identifiability of the substructure was also carefully studied. The identifiability has been rarely been considered in using substructure method. A structure division method to make the substructure identifiable was proposed when the substructure is not strongly system identifiable (SSI).

The damage assessment measures based on autoregressive (AR) model is very attractive in damage detection as the simplicity of AR model and the efficiency of the distance measures method. However, this method is susceptible to noise, and it is very difficult to decide the optimal AR order for distance measures. The improvements on this method aim at strengthening the noise immunity of the method and offer a feasible method to decide the optimal AR order. Thus, the cepstral distance based on the low-order AR models was adopted as the damage indicator, as the low-order AR models have advantages in terms of computational efficiency, emphasis of

high-energy frequency range, and less sensitivity to spectral peaks caused by noise. Moreover, the adaptive component weighting (ACW) was introduced to improve further the ability of this method in noise resistance, which is widely used in speaker identification to reduce the noise. It was found that the order determined by Akaike Information Criterion or Bayesian Information Criteria is not the optimum AR order for the distance measure. The method based on the ratios of the cepstral distance can be used to choose the optimum AR order for distance measures. The standard deviations of the AR coefficients have a significant effect on the accuracy of identification, especially when the standard deviations are not small enough relative to the damage indicators; on the contrary, the severity and location of the damage have little effect on the standard deviations of the AR coefficients. This problem can be overcome by reducing the standard deviations of AR coefficients in increasing the data length.

Most of the damage detection methods need complete information of the structure, which means many sensors are required to be installed into a building. It may be feasible for small systems. However, it is impossible for large-scale civil structures, as the large number of sensors results in long setup time, high equipment costs as well as enormous efforts needed for wiring and designing. Another problem for large civil structures is that data measurement and identification are not easy tasks. A new method, based on substructure approach, for the local damage detection of a shear structure was proposed for these problems. A substructure algorithm was used to divide a complete structure into substructures. Each substructure has a considerably smaller number of degrees of freedom (DOFs) when compared with the entire structure. It should be noted that a substructure is a feedback system as it has feedback forces from the remainder of the structure. This method confines each substructure one DOF and cuts substructure with overlaps, thus each substructure can satisfy the identifiability condition, and ARMAX models can be directly used to determine the

modal information of each substructure. Each substructure can be treated independently. Three sensors are enough for analyzing a substructure in this method, and for the top substructure, only two sensors are needed.

The study on identifiability of substructure showed that it was not true that the substructure can have as many DOFs as we want. To clarify the identifiability of the substructures, the substructures were classified into three types. Conclusions were obtained that in the case of forced vibration, the substructure with free end is always identifiable if the number of independent external inputs is equal to the number of inputs to the system. As for the other substructures, they are unidentifiable unless the order of the rest of the structure is higher than that of the substructure. In the case of free vibration, the substructure with free end with more than half of all of the DOFs is unidentifiable. The conclusions obtained from the other two substructures are similar in cases of forced and free vibration. To overcome this unidentifiability, a structure division method which ensures a higher order of regulator than that of the substructure was proposed. It was also found that a substructure with many DOFs deteriorated the accuracy of the identification. If accuracy is a primary object in identification, it is recommended that the substructures have as few DOFs as possible.

To reduce the sensors needed for damage detection, a method combing substructure approach and support vector machine (SVM) method was proposed. It was found that the frequency change vectors are very sensitive to the damage in story. The use of SVM simplified the process of damage detection further. As the use of SVM method, at most 3 sensors are needed to detect the damage for multiple-mass substructure, and only two sensors are needed for the top multiple-mass substructure. This can reduce the sensors needed to detect the damage of the whole structure significantly. One thing needs to be paid more attention is that similar to the method proposed in the Chapter 3, each substructure should be identifiable when dividing the structure.

Although much has been done for this damage assessment of shear structures based on autoregressive models and substructure approach, there are still several respects needs to be improved and extended.

*Distance measures of AR models:* In this thesis, the ratios of the cepstral distance are used as the indicators to choose the optimum AR order for distance measures. However it may not work if the structure to be detected is complicated. It will be attractive if a more general method on choosing the optimum AR order for distance measures is proposed. Another problem is that pre-whitening filter, which is very essential for this method, is needed to remove the strong mutual correlation in the acceleration data. Pre-whitening filter needs complete information of the structure. However, it is impossible for large-scale civil structures, since the large number of sensors results in long setup time, high equipment costs as well as enormous efforts needed for wiring and designing. Complicated and expensive SHM systems are by no means practical for most civil structures. If this problem can be overcome, it will be great improvement for this method.

*Substructure approach:* The improvements can be conducted on two respects: One is extending this method to a more general structure. The method proposed in this thesis is confined to detect the damage in a shear structure with conventional shape. However, the structure is more complicated in real application. Extending this method to a more complicated structure is urgently needed. Another task is making this method capable of detecting every element of a structure. A structure can be divided into much smaller elements. It will be extremely promising, if this method can detect the damage in any element of the structure. Moreover when these two improvements are conducted, the structure division method and the identifiability of substructure needs to be studied all over again, as structure division method and identifiability of substructure are also needed to be extended to the new structure and new requirements.

# References

Akaike, H. (1967). "Some problems in the application of the cross-spectral method." *Spectral analysis of time series*: 81-107.

Akaike, H. (1974). "A new look at the statistical model identification." *IEEE transactions on automatic control* **19**(6): 716-723.

Arikawa, S., H. Mitsuhashi, et al. (1996). "The investigation of Tibetan urban houses in U area of Tibet: A study on the shift from traditional materials to industiral ones (Part I)." *Journal of architecture,planning and environmental engineering. Transactions of AIJ*(487): 133-140.

Assaleh, K. and R. Mammone (1994). "New LP-derived features for speaker identification." *IEEE Transactions on Speech and Audio Processing* **2**(4): 630-638.

Aström, K. and T. Bohlin (1966). *Numerical identification of linear dynamic systems from normal operating records*. proceedings of the Second IFAC Symposium on the Theory of Self-adaptive Control Systems, National Physical Laboratory, Teddington, England, Plenum Press, New York.

Auweraer, H. V. d. and B. Peeters (2003). "Sensors and systems for structural health monitoring." *Journal of Structural Control* **10**(2): 117-125.

Basseville, M. (1989). "Distance measures for signal processing and pattern recognition." *Signal processing* **18**(4): 349-369.

Berman, A. and W. Flannelly (1971). "Theory of incomplete models of dynamic structures." *AIAA journal* **9**(8): 1481-1487.

Bernal, D. (2002). "Load vectors for damage localization." *Journal of Engineering Mechanics* **128**: 7-14.

Bogert, B., M. Healy, et al. (1963). "The quefrency alanysis of time series for echoes:

cepstrum, pseudo-autocovariance, cross-cepstrum, and saphe cracking, chapter 15." *Time Series Analysis. Wiley, New York*.

Cawley, P. and R. Adams (1979). "The location of defects in structures from measurements of natural frequencies." *The Journal of Strain Analysis for Engineering Design* **14**(2): 49-57.

Cempel, C. (1980). "Diagnostically oriented measures of vibroacoustical processes." *Journal of Sound and Vibration* **73**(4): 547-561.

Chance, J., G. R. Tomlinson, et al. (1994). *A Simplified Approach to the Numerical and Experimental Modelling of the Dynamics of a Cracked Beam*. Proceedings of the 12th International Modal Analysis Conference.

Cortes, C. and V. Vapnik (1995). "Support-vector networks." *Machine learning* **20**(3): 273-297.

Craig, R. and M. Bampton (1968). "Coupling of substructures for dynamic analysis." *AIAA journal* **6**(7): 1313-1319.

Dhiral, K., K. Kalpakis, et al. (2001). *Distance measures for effective clustering of ARIMA time series*. the 2001 IEEE International Conference on Data Mining, San Jose, CA, USA, Citeseer.

Farrar, C. and K. Worden (2007). "An introduction to structural health monitoring." *Philosophical Transactions of the Royal Society A: Mathematical, Physical and Engineering Sciences* **365**(1851): 303-315.

Fox, C. (1992). *The location of defects in structures-A comparison of the use of natural frequency and mode shape data*.

Gao, Y. and B. F. S. Jr (2006). "Online damage diagnosis for civil infrastructure employing a flexibility-based approach." *Smart Materials and Structures* **15**: 9-19.

Goldenfeld, N. and L. Kadanoff (1999). "Simple lessons from complexity." *Science* **284**(5411): 87.

Hayton, P., S. Utete, et al. (2007). "Static and dynamic novelty detection methods for jet engine health monitoring." *Philosophical Transactions of the Royal Society A: Mathematical, Physical and Engineering Sciences* **365**(1851): 493-514.

Hearn, G. and R. Testa (1991). "Modal analysis for damage detection in structures." *Journal of Structural Engineering* **117**(10): 3042-3063.

Hoshiya, M. and E. Saito (1984). "Structural identification by extended Kalman filter." *Journal of Engineering Mechanics* **110**: 1757.

Hou, J., L. Jankowski, et al. (2010) "A substructure isolation method for local structural health monitoring." *Structural Control and Health Monitoring* DOI: 10.1002/stc.389.

Hou, Z., M. Noori, et al. (2000). "Wavelet-based approach for structural damage detection." *Journal of Engineering Mechanics* **126**: 677-683.

Huang, H. and J. Yang (2008). "Damage identification of substructure for local health monitoring." *Smart Structures and Systems* **4**(6): 795-807.

Itakura, F. and T. Umezaki (1987). *Distance measure for speech recognition based on the smoothed group delay spectrum*. Acoustics, Speech, and Signal Processing, IEEE International Conference on ICASSP '87.

Kessler, S., S. Spearing, et al. (2002). "Damage detection in composite materials using frequency response methods." *Composites Part B: Engineering* **33**(1): 87-95.

Kim, J., Y. Ryu, et al. (2003). "Damage identification in beam-type structures: frequency-based method vs mode-shape-based method." *Engineering Structures* **25**(1): 57-67.

Koh, C., B. Hong, et al. (2003). "Substructural and progressive structural identification methods." *Engineering Structures* **25**(12): 1551-1563.

Koh, C., L. See, et al. (1991). "Estimation of structural parameters in time domain: a substructure approach." *Earthquake Engineering & Structural Dynamics* **20**(8): 787-801.

Lieven, N. and D. Ewins (1988). *Spatial correlation of mode shapes, the coordinate modal assurance criterion (COMAC)*. Proceedings of the 6th International Modal Analysis Conference, Bethel.

Ljung, L. (1999). *System identification : theory for the user*. Upper Saddle River, NJ, Prentice Hall PTR.

Ljung, L. (2002). "Asymptotic behavior of the extended Kalman filter as a parameter estimator for linear systems." *Automatic Control, IEEE Transactions on* **24**(1): 36-50.

Ljung, L. and T. Glad (1994). *Modeling of dynamic systems*. Englewood Cliffs, N.J., PTR Prentice Hall.

Ljung, L. and E. Ljung (1987). *System identification: theory for the user*, Prentice-Hall Englewood Cliffs, NJ.

Lynch, J. P. (2005). *Damage characterization of the IASC-ASCE structural health monitoring benchmark structure by transfer function pole Migration*, New

York, NY, United States, American Society of Civil Engineers, Reston, VA 20191-4400, United States.

Maia, N., J. Silva, et al. (2003). "Damage detection in structures: from mode shape to frequency response function methods." *Mechanical Systems and Signal Processing* **17**(3): 489-498.

Martin, R. (2000). "A metric for ARMA processes." *IEEE Transactions on Signal Processing* **48**(4): 1164-1170.

Mayes, R. (1991). *Error localization using mode shapes: An application to a two link robot arm*. Conference: 10. international modal analysis conference (IMAC), San Diego, CA (United States).

Mita, A. (2003). *Structural dynamics for health monitoring*, SANKEISHA Co Ltd.

Mita, A. and H. Hagiwara (2003). "Quantitative damage diagnosis of shear structures using support vector machine." *KSCE Journal of Civil Engineering* **7**(6): 683-689.

Oppenheim, A. and R. Schafer (1989). *Discrete-time signal processing*, Prentice-Hall, Inc. Upper Saddle River, NJ, USA.

Pandey, A., M. Biswas, et al. (1991). "Damage detection from changes in curvature mode shapes." *Journal of Sound and Vibration* **145**(2): 321-332.

Park, K., G. Reich, et al. (1998). "Structural damage detection using localized flexibilities." *Journal of Intelligent Material Systems and Structures* **9**(11): 911-919.

Peeters, B., J. Maeck, et al. (2001). "Vibration-based damage detection in civil engineering: excitation sources and temperature effects." *Smart Materials and Structures* **10**: 518-527.

Qian, Y. and A. Mita (2008). "Acceleration-based damage indicators for building structures using neural network emulators." *Structural Control and Health Monitoring* **15**(6): 901-920.

Qiao, P., K. Lu, et al. (2007). "Curvature mode shape-based damage detection in composite laminated plates." *Composite Structures* **80**(3): 409-428.

Ren, W. X. and G. De Roeck (2002). "Structural damage identification using modal data. II: Test verification." *Journal of Structural Engineering-Asce* **128**(1): 96-104.

Roeck, G. D. (2003). "The state-of-the-art of damage detection by vibration monitoring: the SIMCES experience." *Journal of Structural Control* **10**(2):

127-134.

Rytter, A. (1993). Vibration based inspection of civil engineering structures. *Department of Building Technology and Structural Engineering*. Denmark, Aalborg University. **Ph.D.**

Rytter, A. and P. Kirkegaard (1997). "Vibration based inspection using neural networks." *Structural Damage Assessment Using Advanced Signal Processing Procedures*: 97-108.

Söderström, T. and P. Stoica (1988). *System identification*, Prentice-Hall Englewood Cliffs, NJ.

Saito, T., S. Mase, et al. (2005). "A probabilistic approach to structural damage estimation." *Structural Control and Health Monitoring* **12**(3-4): 283-299.

Salawu, O. and C. Williams (1995). "Bridge assessment using forced-vibration testing." *Journal of Structural Engineering* **121**: 161-173.

Sampaio, R., N. Maia, et al. (1999). "Damage detection using the frequency-response-function curvature method." *Journal of Sound and Vibration* **226**(5): 1029-1042.

Schoen, P. (1992). "Delay structure conditions for identifiability of closed loop systems." *Automatica* **28**(5): 1047-1050.

Schwarz, G. (1978). "Estimating the dimension of a model." *The annals of statistics* **6**(2): 461-464.

Shi, Z., S. Law, et al. (1998). "Structural damage localization from modal strain energy change." *Journal of Sound and Vibration* **218**(5): 825-844.

Sohn, H. (2007). "Effects of environmental and operational variability on structural health monitoring." *Philosophical Transactions of the Royal Society A: Mathematical, Physical and Engineering Sciences* **365**(1851): 539-560.

Sohn, H. and L. A. N. Laboratory (2004). *A Review of Structural Health Monitoring Literature: 1996-2001*, Los Alamos National Laboratory.

Stubbs, N. and J. Kim (1996). "Damage localization in structures without baseline modal parameters." *AIAA journal* **34**(8): 1644-1649.

Stubbs, N., J. Kim, et al. (1992). *An efficient and robust algorithm for damage localization in offshore platforms*. Proceedings of the ASCE 10th Structures Congress.

Su, T. and J. Juang (1994). "Substructure system identification and synthesis." *Journal of Guidance, Control and Dynamics* **17**(5): 1087-1095.

Tohkura, Y. (1986). *A weighted cepstral distance measure for speech recognition*. Acoustics, Speech, and Signal Processing, IEEE International Conference on ICASSP '86.

Vapnik, V. N. (1995). *The nature of statistical learning theory*, Springer-Verlag New York, Inc.

Vestroni, F. and D. Capecchi (2000). "Damage detection in beam structures based on frequency measurements." *Journal of Engineering Mechanics* **126**: 761.

Wang, J., J. Ko, et al. (2000). *Modal sensitivity analysis of Tsing Ma Bridge for structural damage detection*. Proceedings of SPIE, Newport Beach, CA, USA.

West, W. (1986). *Illustration of the use of modal assurance criterion to detect structural changes in an orbiter test specimen*. Proceedings of the Air Force Conference on Aircraft Structural Integrity, Los Angles.

Williams, E. and A. Messina (1999). "Applications of the multiple damage location assurance criterion." *Key Engineering Materials* **167**: 256-264.

Wolff, T. and M. Richardson (1989). *Fault detection in structures from changes in their modal parameters*. Proceedings of the 7th International Modal Analysis Conference.

Xie, L., A. Mita, et al. (2010). "Identifiability of linear superstructures under feedback-Taking base-isolated structures as example." *Structural Control and Health Monitoring* **17**(4): 355-367.

Yoshimoto, R., A. Mita, et al. (2002). "Parallel identification of structural damages using vibration modes and sensor characteristics." *Journal of Structural Engineering* **48**: 487-492.

Yuen, K. and L. Katafygiotis (2006). "Substructure identification and health monitoring using noisy response measurements only." *Computer-aided civil and infrastructure engineering* **21**(4): 280-291.

Zhang, L., W. Quiong, et al. (1998). *A structural damage identification approach based on element modal strain energy*. Proceedings of ISMA23, Noise and Vibration Engineering, Leuven, Belgium.

Zhao, J. and J. DeWolf (1999). "Sensitivity study for vibrational parameters used in damage detection." *Journal of Structural Engineering* **125**: 410-416.

Zhao, Q., T. Sawada, et al. (1995). "Localized identification of MDOF structures in the frequency domain." *Earthquake Engineering & Structural Dynamics* **24**(3): 325-338.

Zheng, H. and A. Mita (2007). "Two-stage damage diagnosis based on the distance between ARMA models and pre-whitening filters." *Smart Materials and Structures* **16**: 1829-1836.

Zheng, H. and A. Mita (2008). "Damage indicator defined as the distance between ARMA models for structural health monitoring." *Structural Control and Health Monitoring* **15**(7): 992-1005.

Zheng, H. and A. Mita (2009). "Localized damage detection of structures subject to multiple ambient excitations using two distance measures for autoregressive models." *Structural Health Monitoring* **8**(3): 207-222.